NTNU
Norwegian University of
Science and Technology

Levels and Potential Immunotoxicity of Perfluoroalkyl and Polyfluoroalkyl Substances (PFASs) in White-Tailed Eagles (*Haliaeetus albicilla*), Norway

Jørgen Flo

Acknowledgements

Sammendrag

Grunnet sin høye trofiske posisjon i den marine næringskjeden er havørna eksponert for et stort omfang av miljøgifter. Perfluorerte og polyfluorerte alkylstoffer (PFASs) har persistente og bioakkumulative egenskaper og er nylig blitt funnet i høyere konsentrasjoner enn andre persistente organiske miljøgifter (POPs) i havørnunger. Gjennom eksperimentelle metoder har man funnet at PFASs påvirker immunologiske parametere ved relativt lave konsentrasjoner, men det gjenstår å påvise at stoffene har liknende effekt i ville fugler. I dette studiet ble nivåer av PFASs analysert i blod og fjær fra havørnunger på Steigen (n = 14, reder = 9) og Smøla (n = 13, reder = 10). Målet var å undersøke relasjonen mellom konsentrasjoner i fjær og plasma, samt å undersøke om variasjon kunne relateres til biologiske variabler og geografisk lokalitet. Videre ble det undersøkt om PFAS nivåer kunne assosieres med variasjon i to immunologiske indikatorer: differensialtelling av leukocytter og proteinfraksjoner.

Lineære nøstede modeller viste at nivåer av Σ_7PFASs i plasma øker med alder ($p < 0.01$) og masse ($p < 0.01$) ved begge lokasjoner, men at nivåer akkumulert gjennom dietten stiger raskere i havørnunger fra Steigen ($p < 0.01$). Det ble ikke funnet noen klar sammenheng mellom nivåer i fjær og plasma. Fjær hadde lavere konsentrasjoner og færre konsentrasjoner over deteksjonsgrensen. Kort oppsummert viser studiet at målte konsentrasjoner må sees i lys av variasjon forklart av variabler som alder, masse, kjønn og lokasjon der prøvene er tatt fra.

Det ble ikke funnet noen sammenheng mellom PFASs og proteinfraksjoner eller leukocytt prosentandeler. Nivåer av prealbumin ($p = 0.004$) og γ-globulin ($p = 0.054$) var forskjellige mellom de to populasjonene. Nivåer av prealbumin var også positivt assosiert med økende masse ($p < 0.01$). Havørnungene hadde høye prosentandeler av heterofile granulocytter, lymfocytter (31 %) og eosinofile granulocytter (16 %), sammenliknbare med nivåer i friske hvithodehavørn (*Haliaeetus leucocephalus*). Både nivåer av proteinfraksjoner og leukocytter antydet at havørnungene var friske. Det er mulig at de to biomarkørene anvendt ikke evner eller er sensitive nok til å detektere små immunologiske effekter av miljøgifter i ville dyr. I henhold til reproduserbarhet, viste proteinelektroforese seg å være den mest lovende biomarkøren. Nye teknologiske fremskritt vil med sikkerhet øke metodens sensitivitet og muligheten for å separere proteinfraksjoner ytterligere.

Abstract

The white-tailed eagle (WTE) is exposed to a wide range of contaminants due to its high trophic position in the marine ecosystem. Perfluoroalkyl and polyfluoroalkyl substances (PFASs) are persistent and bioaccumulative chemicals, which recently have been shown to exceed concentrations of other persistent organic pollutants (POPs) in WTE nestlings. Experimental studies suggest that immunomodulation by PFASs occurs at environmentally relevant levels, presenting the need for additional studies to determine if such effects are present in avian wildlife. The first aim of the current study was to investigate the levels of PFASs in plasma and feathers of WTE nestlings, assessing variation relating to differences in sampling location and biological variables. The second aim was to investigate the relationship between PFASs and two structural indicators of the immune system: leukocyte counts and protein fractions. Two WTE populations were sampled: Steigen (n = 14, nests = 9) and Smøla (n = 13, nests = 10).

Linear nested models showed that levels of Σ_7PFASs in plasma were significantly increasing with age ($p < 0.01$) and body mass ($p < 0.01$) in both populations, while suggesting a higher dietary accumulation in nestlings from Steigen ($p < 0.01$). The levels and detection frequency of PFASs were lower in feathers compared to plasma, and a clear connection between the two matrices could not be established. The current study emphasises the importance of variation explained by variables as age, mass, sex and sampling location when assessing environmental exposure to PFASs.

No associations were found between PFASs and protein fractions or leukocyte percentages. The prealbumin ($p = 0.004$) and γ-globulin ($p = 0.054$) concentrations differed between populations, and prealbumin levels were positively associated with mass ($p < 0.01$). WTE nestlings had high leukocyte percentages of heterophils (48 %), lymphocytes (31 %) and eosinophils (16 %), comparable with those of healthy bald eagles (*Haliaeetus leucocephalus*). Assessment of protein electrophoretic patterns and leukocyte percentages both suggested that all the nestlings in the current study were healthy. However, the sensitivity and ability of the two biomarkers to detect potentially small immunological effects of contaminants in wildlife may be insufficient. Protein electrophoresis showed to be the most promising biomarker in the current study, and further advances may aid sensitivity and identification of specific proteins.

List of abbreviations

A:G ratio	Albumin to globulin ratio	PFAS	Perfluoroalkyl substance
AICc WT	AICc Weight	PFCA	Perfluorocarboxylic acid
AICc	Akaike's information criteria	PFSA	Perfluorosulfonic acid
AM	Arithmetic mean	PFAA	Perfluoroalkyl acid
ANOVA	Analysis of variance	PFBA	Perfluorobutanoic acid
APP	Acute phase protein	PFPA	Perfluoropentanoic acids
BCCP	Blood clinical chemical parameters	PFHxA	Perfluorohexanoic acid
BFR	Brominated flame retardant	PFHpA	Perfluoroheptanoic acid
BSA	Bovine serum albumin (in cows)	PFOA	Perfluorooctanoic acid
CE	Capillary electrophoresis	PFNA	Perfluorononanoic acid
cm	Centimeters	PFDcA	Perfluorodecanoic acid
ctr	Contribution	PFUnDA	Perfluoroundecanoic acid
C_V	Coefficient of variation	PFDoDA	Perfluorododecanoic acid
DDE	Dichlorodiphenyltrichloroethylene	PFTrDA	Perfluorotridecanoic acid
DDT	Dichlorodiphenyltrichloroethane	PFTeDA	Perfluorotetradecanoic acid
DF	Degrees of freedom	PFBS	Perfluorobutane sulfonate
ECF	Electrochemical fluorination	PFHxS	Perfluorohexane sulfonate
EDC	Endocrine disrupting chemicals	PFHpS	Perfluoroheptane sulfonate
EDTA	Ethylenediaminetetraacetic acid	PFOS	Perfluorooctane sulfonate
EPA	US Environmental Protection Agency	linPFOS	linear Perfluorooctane sulfonate
g (kg)	Grams (kilograms)	brPFOS	branched Perfluorooctane sulfonate
GC	Glucocorticoid	PFDcS	Perfluorodecane sulfonate
GLM	Generalized linear model	PFOSA	Perfluorooctane sulfonamide
H:L ratio	Heterophil to lymphocyte ratio	Cl-PFHxPA	Chloro-Perfluorohexyl phosphonic acid
Ig	Immunoglobuling	6:2 FTS	6:2 Fluorotelomer sulfonate
ISTD	Internal standard solution	PFO	Perfluorooctanoate
IUCN	International Union for Conservation of Nature		
k	Overall depuration rate constant		
k_e	First-order elimination constant		
k_g	Growth rate constant		
KO	Knockout		
LC	Liquid chromatograph		
LD50	Median lethal dose		
LE	Lower estimate		
LMER	Linear mixed effect models, Nested linear models		
LOAEL	Lowest observable adverse effect level		
LOD	Limit of detection		
LOD	Limit of detection		
LOEL	Lowest observable effect level		
$\log_e$	natural logarithm		
LOQ	Limit of quantification		

LOQ	Limit of quantification	UPLC-MS/MS	Ultra-high pressure liquid chromatography triple-quadrupole mass-spectrometry
LRT	Long range transport	UV	Ultraviolet
MeOH	Methanol	W	Test parameter in Wilcoxon Rank-Sum Test = Mann-Whitney U Test
min	Minute	WBC	White blood cell
mL	Millilitre	wt (ww)	weight (wet weight)
mm	Millimetre	WTE	White-tailed eagle
n	Number of observations	μL	Microliters
ng	Nanogram	∑	Sum
NILU	Norwegian Institute for Air Research		
NINA	The Norwegian Institute for Nature Research		
NIST	National Institute of Standards and Technology		
NK	Natural killer cell		
nm	Nanometre		
OC	Organochlorine pesticide		
OHC	Organohalogen contaminants		
p	Probability of rejecting null hypothesis		
PCA	Principal Component Analysis		
PCB	Polychlorinated biphenyl		
PNEC	Predicted no effect concentration		
POP	Persistent organic pollutant		
PPAR	Peroxisome proliferator-activated receptors		
PV	Plasma volume		
QQ-plot	Quantile-quantile plot		
R2	Residual square		
RBC	Red blood cell (erythrocyte)		
RNA	Ribonucleic acid		
rs	Spearman's rho (p)		
RSTD	Recovery standard solution		
SE	Standard error		
SM	Smøla		
SMI	Scaled mass index		
SRM	Standard reference material control		
ST	Steigen		
TFE	Tetrafluoroethylene		
TP	Total protein		
TRV	Toxicity reference values		
UE	Upper estimate		
UNEP	United Nations Environment Programme		

Table of contents

1. Introduction

1.1. Perfluoroalkyl and polyfluoroalkyl substances

Perfluoroalkyl and polyfluoroalkyl substances (PFASs) are prone to long-range transport by air and oceanic currents, with a global distribution in both abiotic and biotic matrices (Butt et al., 2010). The unique properties and high biologic stability of some PFASs prevent metabolism and elimination in organisms, contributing to bioaccumulation in protein-rich tissues (Jones et al., 2003). PFASs have previously been shown to be capable of biomagnification in the marine food web (Tomy et al., 2004), potentially exposing marine birds of prey to high levels of PFASs. While the current literature suggests that immunomodulation occurs at environmentally relevant levels in experimental models, additional studies are needed to investigate the potential immunotoxic effects of PFASs in wild avian species (DeWitt et al., 2012).

1.1.1. Use and production

Perfluoroalkyl and polyfluoroalkyl substances (PFASs) are a large family of chemicals widely used in industrial and consumer product applications (Buck et al., 2011). Most PFASs consists of a fully fluorinated hydrophobic alkyl chain (perfluoroalkyl) and a hydrophilic functional group, illustrated in Table 1.1. This is although a very general description since PFASs includes more than 40 subfamilies, hundreds of different chemicals and isomers (Buck et al., 2011). Nonetheless, one of the reasons for its high commercial usage is the thermal stability of the perfluoroalkyl moiety, both hydrophobic and lipophobic in nature, combined with a varied functional group. Derived from this are properties unique to PFASs, as being non-sticky, non-wetting, slippery, and highly fire, temperature and weather resistant (Herzke et al., 2012). They are either used as raw material in surfactants or as components in numerous applications, such as inks, wax, varnishes, fire-fighting foam, coating, lubricants, water and stain repellents, cookware and textiles (Paul et al., 2009). Another property of PFASs is that they are chemically inert, initially considered nontoxic (Douvris and Ozerov, 2008; Herzke et al., 2012). Two major classes of PFASs are the perfluoroalkyl carboxylates (PFCAs), and the perfluoroalkyl sulfonates (PFSAs), sometimes referred to as perfluoroalkyl acids (PFAAs) (Buck et al., 2011).

Table 1.1

Examples of chemical structure and classification of poly- and perfluoroalkyl substances (PFASs). Name of compound is in italics.

Structure	Classification
	Perfluoroalkyl acid (PFAA) Perfluoroalkyl sulfonic acid (PFSA) *Perfluorooctanoic sulfonic acid (PFOS)*
	Perfluoroalkyl acid (PFAA) Perfluoroalkyl sulfonate (PFSA) *Perfluorooctane sulfonate (PFOS)*
	Perfluoroalkyl acid (PFAA) Perfluoroalkyl carboxylic acid (PFCA) *Perfluorooctanoic acid (PFOA)*
	Polyfluoroalkyl carboxylic acid *2,2,3,3,4,4,6,6,7,7,8,8,8- tridecafluorooctanoic acid*

In 1949, the 3M company started producing PFASs by electrochemical fluorination (ECF) (Paul et al., 2009). A method lacking isomeric purity was used, which resulted in a mixture of chain lengths, linear, branched and cyclic by-products in the process (Buck et al., 2011). Another method is telomerization of tetrafluoroethylene (TFE) units which yields straight-chain alcohols $(F(CF_2 CF_2)_nCH_2CH_2OH)$ for the conversion to final PFASs products (Buck et al., 2011). Therefore, a wide range of PFASs was produced, intentionally or as by-products. Estimation of production volume between 1970 and 2002 comprises 96 000 metric tons, considering perfluorooctane sulfonyl fluoride (POSF) alone. POSF-derived chemicals can degrade into perfluorooctanoic sulfonate (PFOS) over time, and is estimated to be the major source of PFOS in the environment. The corresponding estimated release of POSF to water and air over the same timespan was 45 250 metric tons (Paul et al., 2009). In 2002, 3M agreed upon a phase-out of PFOS and PFOA related compounds (Buck et al., 2011; Lau et al., 2007). Further concerns about the environmental impact of PFCAs and PFSAs have also led to the addition of PFOS in Annex B of the Stockholm Convention on Persistent Organic Pollutants (UNEP, 2009) and other regulatory and voluntary initiatives to reduce the emission of PFASs (Buck et al., 2011).

1.1.2. Distribution

Due to release during manufacture and through secondary products, PFASs are detected in environmental matrices around the globe (Giesy et al., 2001). These are all anthropogenic

2

chemicals, although some fluorinated compounds are naturally occurring. The difference is that the latter contain only one fluorine atom like the monofluoroacetic acid produced by plants in the genus *Dichapetalum* (Giesy and Kannan, 2002). Current evidence shows that fully fluorinated hydrocarbons are stable in air at high temperatures (in excess of 150 °C). They are non-flammable, not readily degraded by strong acids, alkalis, oxidizing agents, photolysis, irradiation or by persulfate (Chen et al., 2007; Lau et al., 2007). Properties that render these compounds practically non-biodegradable and persistent in the environment (Key et al., 1998). A wide range of PFASs are investigated, while the most efforts are concerned around PFOS and perfluorooctanoic acid (PFOA) (Kennedy et al., 2004; Lau et al., 2007). Several compounds act as precursor compounds of PFOS and PFOA through both abiotic and biotic transformation (Dinglasan et al., 2004). Models investigating the fate and transport of PFOS and its precursor compounds illuminate the effect of the 2002 phase-out (Armitage et al., 2009). Modelled surface ocean water concentration declines slowly overall, while increases in remote locations are expected until 2030 (Armitage et al., 2009). Two routes have been proposed and debated for the transport of PFCAs and PFSAs. One by indirect atmospheric transport of PFAAs precursors and subsequent degradation into PFCAs and PFSAs (Stock et al., 2007). The second by direct release and long-range transport by ocean currents (Yamashita et al., 2008, 2005). It was argued that negligible water pressure, high water solubility and moderate sorption to solids of perfluorooctanoate (PFO) suggests that transport to the Arctic is greater through oceanic currents than that of air-transport (Prevedouros et al., 2006). It was further estimated that 2 – 12 tonnes PFO are transported to the Arctic by oceanic transport, mainly by water through the West Spitzbergen Current, Barents Sea, Bering Strait, and the Norwegian Current.

1.1.3. Biomonitoring

Numerous studies have documented the widespread occurrence of PFASs. From the South Pacific to the North Pole, PFASs contamination is reported in many environmental compartments and trophic levels (Butt et al., 2010; Kannan et al., 2005; Loi et al., 2011). In environmental samples, the most common PFASs detected is PFOS followed by PFNA, PFUnDA (Perfluoroundecanoic acid), PFOSA (Perfluorooctane sulphonamide) and infrequently PFOA (Butt et al., 2010). Despite PFOA is frequently being the compound of highest concentration in ocean water samples (Butt et al., 2010; Yamashita et al., 2008, 2005). Biotic measurements extend to marine, freshwater and terrestrial ecosystems (Butt et al., 2010; Yamashita et al., 2008), stating both how ubiquitous these compounds are, and suggesting their bioaccumulative potential. Biomagnification through food chains is consistent with high levels of PFASs in the upper trophic levels, with some of the highest concentrations found in polar bears (Butt et al., 2010).

White-tailed eagles (WTE) and its relatives are extensively monitored (Bowerman et al., 2000; Leppert et al., 2004; Route et al., 2014). In a recent study of WTEs from Troms County, Northern Norway, organohalogenated compounds (OHCs) were measured in plasma. Of the OHCs, linear PFOS was the most abundant, averaging (± SE) 40.91 ± 5.75 ng/g ww (Sletten et al., 2016). In fish, liver of Arctic cod (*Arctogadus glacialis*) from the Barents Sea had concentrations (AM ± SE) of 2.02 ± 0.13 ng/g ww PFOS and 0.20 ± 0.02 ng/g ww PFNA (Haukås et al., 2007). In seabirds, PFASs were reported in plasma, eggs, liver and brain of glaucous gulls (*Larus hyperboreus*) from Svalbard and Bear Island (Bjørnøya). The predominant PFAS was PFOS with a mean of 134 ± 16.6 ng/g ww in plasma and 104 ± 13.2 ng/g ww in eggs. Of the PFCAs, the highest concentrations were detected in PFUnDA (plasma: 74 ± 8.0 ng/g ww, eggs: 21± 2.8 ng/g) > PFTrDA > PFDoDA ≈ PFDA (Verreault et al., 2005). In guillemot (*Uria Aalge*) eggs from Sklinna and Hjelmsøya (Norway), it was primarily detected PFOS, PFOSA, PFDA, PFUnDA, and PFDoDA. Egg samples from Sklinna had mean PFOS concentrations of 85 (range: 3.2-210) ng/g ww and a mean ∑PFCAs (PFDA, PFUnDA, and PFDoDA) concentration of 73 ng/g ww. In that study, it was found different spatial profiles of PFOS, PFOSA and PFCAs in eggs (Löfstrand et al., 2008), suggesting possible differences in exposure and composition of PFASs along the Norwegian coast.

The WTE (like many other birds of prey) is a protected species. Therefore, validating non-invasive biomonitoring tools like feathers and plasma is of both practical and ethical importance. In nestlings, the feathers are coupled to the blood stream during the moulting period (Jaspers et al., 2008). Through the blood, contaminants are deposited into the feather structure, linking feather concentrations to internal accumulation over time. The use of feathers as biomonitoring tool has many benefits; feathers are easily collected and less invasive than other sampling methods, they can be collected independent of sex, season and age, and they are easily stored (Jaspers et al., 2013). Feathers have previously been shown to be useful in detecting and monitoring metals (Bustnes et al., 2013a) and POPs (Eulaers et al., 2011a; Jaspers et al., 2006). However, the use of feathers for biomonitoring PFASs is still under investigation. In particular, the mechanisms relating to external deposition (through air, dust and water) or external (and internal) contamination via preen oil is not fully understood (Jaspers et al., 2013). Contaminant concentrations have also been shown to vary between feather types. Body feathers, compared to tail feathers and primary wing feathers, contain relatively high amounts of contaminants. They are also considered to be less invasive to sample, compared to tail and wing feathers (Jaspers et al., 2011). The feathers of large birds of prey are especially suited for biomonitoring, as they are relatively large compared to other species and few feathers are needed for analysis.

1.1.4. Toxicokinetics and toxicodynamics

The internal distribution of PFASs in an organism differs from the majority of POPs. Rather than accumulating in fat tissue, the high affinity for protein binding increases concentrations in liver, kidney and serum compared to other compartments (Andersen et al., 2008). The pharmacokinetic properties of each PFAS-compound are dependent on chain length and functional moiety, as well as biological parameters such as species, sex, age and health of the subject evaluated (Kudo et al., 2000; Lau, 2012). Elimination generally decreases with increasing length of the carbon chain (Andersen et al., 2008). Many PFASs are absorbed easily, and persistent to metabolism and elimination, consequently accumulated to high levels in biological systems (Lau et al., 2007). Current literature also suggests that PFASs undergo enterohepatic recycling (Jones et al., 2003; Lau et al., 2007), being reabsorbed from the intestine after biliary excretion (Roberts et al., 2002).

Due to their properties, PFASs can bind to various proteins in serum and in doing so interact with endocrine and immunological functions (Jones et al., 2003). Documented toxicological effects of PFASs range from reproductive and developmental toxicity (Ankley et al., 2005; Kato et al., 2014), endocrine disruption (Seacat et al., 2003; Thibodeaux et al., 2003) and immunotoxicity (reviewed by DeWitt et al., 2012). The extensive findings are both from experimental models and wildlife studies, dependent on species and type of PFASs compound. However, the acute toxicity of PFASs, such as PFOS are only considered to be moderate (EPA, 2000), and acute toxic effects are often observed in experimental studies with high dosage groups. For example, the LD_{50} of postnatal survival was estimated to be 3 mg/kg, in rats with a daily exposure of PFOS during the gestation period. Which corresponded to serum levels of approximately 70 µg/mL PFOS, measured in the neonatal rats (Lau et al., 2003).
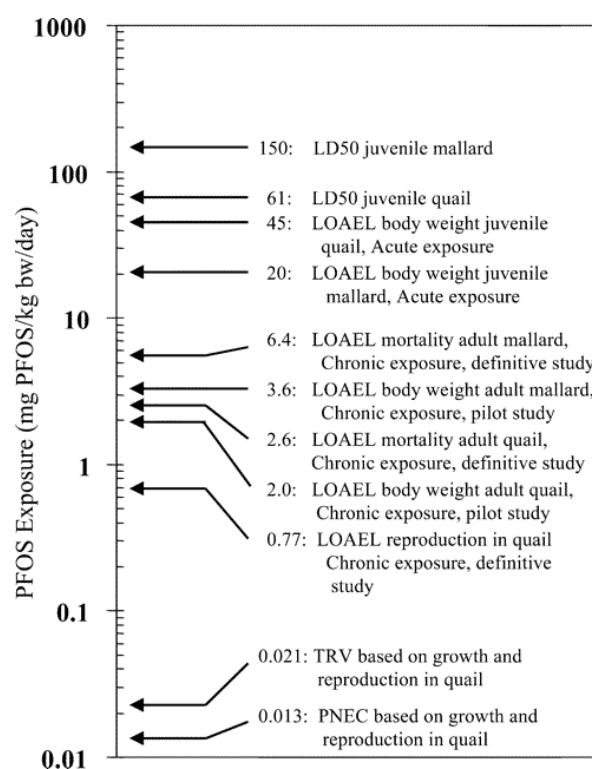
Figure 1.1: Toxicity thresholds for avian species expressed as daily intake of PFOS. PNEC: predicted no effect concentration, TRV: toxicity reference value, LOAEL: lowest observable adverse effect level, LD50: median lethal dose. From Newsted et al. (2005).

Figure 1.1 illustrate toxicity thresholds in birds. In that study, two avian species: mallard (*Anas platyrhynchos*) and northern bobwhite quail (*Colinus virginianus*), were exposed to PFOS through the diet. Toxicological endpoints included mortality, growth, histopathology and reproduction (egg production, fertility, hatchability and survival of offspring). The toxicity reference value (TRV) based on dietary PFOS concentrations, were 0.021 mg/kg consistent with a mean serum level of 1.7 µg/mL (Newsted et al., 2005). There is a limited amount of studies that report concentrations of this extent in avian wildlife. A study reported mean plasma concentrations of 941 ng/mL ∑PFASs (16 PFASs) in Bald eagle (*Haliaeetus leucocephalus*) nestlings from parts of the Mississippi river close to Minneapolis (Route et al., 2014). In that study, 5.1 % of the sampled nestlings were above the TRV estimated by Newsted et al., 2005. However, caution should be taken when comparing acute toxicity reference ranges with long-time exposure and accumulation of complex PFAS mixtures in wild birds.

1.2. Avian Immune system

To overcome the exposure to a wide range of pathogens in the environment, birds have evolved complex physiological defence mechanisms. These are similar to the mammalian immune system, hence divided into innate and acquired (adaptive) immunity (Davison, 2014; Demas and Nelson, 2012). Innate immunity is the first line of defence, including physical and chemical barriers, blood proteins and a wide range of cellular responses (Demas and Nelson, 2012). Adaptive immunity serves as an additional response, typically slower and pathogen-specific (Demas and Nelson, 2012). One branch of this is the memorization of antigens at first contact, presenting lifelong immunity through antibodies. The mechanisms of the immune system are complex, and interaction between the innate and adaptive branch occurs. Chickens (*Gallus gallus domesticus*) are extensively studied, but further studies also need to investigate wild bird populations to extend the knowledge of the immune system and possible species differences (Millet et al., 2007; Weber and Stilianakis, 2007).

1.2.1. White blood cells

There are various techniques to measure immunotoxicological effects of contaminants in avian species (Grasman, 2002). Some techniques assess the response to specific immunological challenges, while other focus on assessing the immunological structure. Structural assessment can be obtained through assessing cellularity and mass of immune organs, or by peripheral white blood cell counts and serum protein concentrations. Since blood cell counts only requires a small amount of blood this is a minimally invasive method and often applied in avian wildlife studies.

A decreased number of a specific cell type may suggest reduced immune function associated with these cells (Grasman, 2002). The blood of birds contains five types of leukocytes: heterophils, eosinophils, basophils, monocytes and lymphocytes (Clark et al., 2009). Heterophils are granulated leukocytes and the avian counterpart of the mammalian neutrophil. They form the first line of defence against invading microbial pathogens (Juul-Madsen et al., 2014). Dependent primarily on non-oxidative mechanisms, heterophils are phagocytic and show a wide range of antimicrobial activity (Harmon, 1998). Eosinophils are also part of the innate immune system. Upon activation, they secrete a range of toxic proteins and free radicals to kill pathogens, although there is evidence that the avian eosinophils differ from the mammalian eosinophils (Campbell, 1994). Basophils produce, store and release histamine, participating in acute inflammatory responses (Campbell, 1994). Monocytes can differentiate into macrophages and dendritic cells, and detect pathogens through a wide range of receptors. They are phagocytic cells of the innate immune system, but they also play a part in stimulating lymphocytes by cytokine production (Kaspers and Kaiser, 2014; Teh et al., 2000).

Lymphocyte progenitor cells develop into T-cells (in the thymus), B-cells (in the bursa of Fabricius) or natural killer- (NK) cells (Demas and Nelson, 2012). B-cells are constituents of the acquired immune system through antigen-antibody recognition and immunological memory. Through antibody production, B-cells neutralize pathogens and their products, block parasite binding to host cells, promote cellular mitigation and enhance phagocytosis, among other actions (Demas and Nelson, 2012). T-cells require direct contact with an infected cell to eliminate it. Cytotoxic T-cells serve through chemical or physical lysis. T helper cells do complementary actions by secreting cytokines and communicate with B-cells. The regulatory T cells work through downregulating or suppressing immune functions, to prevent excessive reactions (Demas and Nelson, 2012). In contrast to B- and T-cells, NK cells are part of the innate immune system, and attack and lyse infected cells (Demas and Nelson, 2012).

Several factors influence the avian immune system. These includes age and sex, environmental condition, social interactions, diet and toxicants (Koutsos and Klasing, 2014). Exposure to contaminants may increase the susceptibility to disease or cancer (Grasman, 2002). With a differential cell count, the relative proportions of specific cell types are obtained. It is also possible to estimate the relative amount of leukocytes to red blood cells. Since heterophils and lymphocytes are the most abundant leukocytes in avian species, many studies measure the heterophil to lymphocyte (H:L) ratio (Grasman, 2002). A study comparing haematological methods found relatively small measurement errors for the H:L ratio, suggesting its adequacy for ecological research purposes (Ots et al., 1998). Since heterophils are non-specific cells of the innate immune system and lymphocytes are highly specific cells of the adaptive immune

system, the H:L ratio is useful for interpretation (Ots et al., 1998). A higher H:L ratio may imply stress (Davis et al., 2008), disease (Davis et al., 2004), injury (Ots et al., 1998) or lower body condition (Pfaff et al., 2007). Contaminants that have been observed to elevate the heterophil to lymphocyte ratio in avian species are ethyl methanesulfonate and paraquat (Clark et al., 1988), selenium, arsenic and boron (Fairbrother and Fowles, 1990), and dioxin-like chemicals, including PCB (Grasman et al., 1996).

1.2.2. Serum protein electrophoresis and protein fractions

Protein electrophoresis is a widely used diagnostic technique used to detect a multiple of diseases in humans and animals (Cray and Tatum, 1998). Plasma proteins, largely synthesized in the liver (except immunoglobulins), have several different functions including the transport of molecules/hormones, blood clotting, and maintaining the osmotic pressure and pH. Many of these proteins are important in inflammatory responses, and for healing and tissue repair (Melillo, 2013). Protein electrophoresis proved a valuable diagnostic tool in humans and was soon included in avian species. First applied to chicken (Brandt et al., 1951), later linking changes in protein fractions and effects of stress, breeding, malnutrition and diseases (Cray and Tatum, 1998). The avian protein fractions are identified and ordered according to electrical charge and molecular weight (Melillo, 2013). The fraction that migrates the furthest is prealbumin, followed by albumin, α_1-globulins, α_2-globulins, β-globulins and γ-globulins (see Appendix J). The different protein fraction contains a range of proteins, shown in Table 2. The data from wild bird studies are although scarce, and protein fractions and patterns are highly variable between species (Cray et al., 2007). Literature describing protein fraction reference values and species-specific patterns in some raptors including bald eagles helped to determine the values in WTE nestlings (Cray and Tatum, 1998; Tatum et al., 2000).

The globulins contain acute phase proteins (APPs; most α- and β-globulins). The γ-globulins are not considered as APPs and increase during antibody responses (Fairbrother et al., 2004). APPs are part of the immune response to inflammation, infection or trauma (Melillo, 2013). The APPs that increases in response to inflammation are called positive APPs (such as antitrypsin, α-macroglobulin, Haptoglobin, fibrinogen, ferritin and Amyloid A), while albumin, prealbumin, and transferrin are sometimes referred to as a negative APPs since production decreases during inflammation (Fairbrother et al., 2004; Grasman, 2002; Melillo, 2013). Assessing protein concentrations can provide important information on immune and inflammation responses (Grasman, 2002). In prefledgling Herring gulls (*Larus argentatus*) and Caspian tern (*Sterna caspia*) from the Great Lakes, a positive association between PCBs and β-globulin were established, as well as a negative association between α-globulins and PCBs in Caspian terns (Grasman et al., 2000).

Table 1.2
Composition of the different protein fractions (Cray and Tatum, 1998; Fairbrother et al., 2004; Melillo, 2013).

Fraction	Proteins
Prealbumin	Transthyretin
Albumin	Albumin
α₁-globulin	α-1 antitrypsin
	α-1 acid glycoprotein
α₂-globulin	α-2 macroglobulin
	Haptoglobin
	Protein C
β-globulin	Fibrinogen
	β-lipoprotein
	Transferrin
	Complement
	C-reactive protein
	Ferritin
	Amyloid A
γ-globulin	Immunoglobulins (IgG, IgM, IgA and IgE)
	Complement degradation products

In a review article on avian immunotoxicology, it is underlined that further studies should elucidate toxic effects linking the immune system and the endocrine system (Fairbrother et al., 2004). In particular, the specific immune system is suppressed by corticosteroids, androgens, progesterone and adrenocorticotrophic hormone, whereas stimulated by prolactin, growth hormone, insulin, and thyroid hormone (Besedovsky and Del Rey, 1996; Fairbrother et al., 2004).

1.2.3. Immunotoxicity and PFASs

Immunomodulation by PFASs is reported from both experimental models and wildlife. From animal laboratory experiments, it is inferred that immune effects occur at serum levels below, within range or just above concentrations reported in highly exposed wildlife and humans (DeWitt et al., 2012). Several studies have found immunomodulation related to PFOS and PFOA exposure. These effects include inflammatory responses, production of cytokines, and adaptive and innate immune responses in rodent models, avian models and reptilian models (DeWitt et al., 2012). Knockout (KO) models found PFOS and PFOA activation of peroxisome proliferator-

activated receptors (PPARs), a ligand-activated transcription factor (DeWitt et al., 2009). Activation of PPAR *alpha* (PPARα) modulates lipid and glucose homeostasis, cell proliferation and differentiation, as well as inflammation. Other effects may occur independently of the receptor, including hepatic peroxisome proliferation, reduced lymphoid organ weights and altered antibody synthesis (DeWitt et al., 2009; Yang et al., 2001). Peden-Adams et al. (2008) suggested that PFOS targets humoral immune functions, B-cells or antigen-presenting cells in particular, at environmentally relevant levels. The same study also found a lowest observable effect level (LOEL) of 91.5 ng/g serum PFOS in male rats, multifold lower than reported in humans and in other literature. An *in ovo* exposure study found immune alterations in white leghorn chicken (*Gallus gallus*). Immunological effects included increased lysozome activity and suppressed the total immunoglobulin (IgM and IgY) levels, but also increased spleen mass and increased severity and frequency of brain asymmetry were observed at the lowest dose (1 mg/kg egg ww PFOS), suggesting that maternal transfer could pose risks in developing avian embryos (Peden-Adams et al., 2009).

Several studies have been conducted on blood clinical-chemical parameters (BCCPs) and haematological values in eagle species (Sonne et al. 2010; Bowerman et al. 2000; Jones et al. 2014). Assessment of baseline hematologic values in healthy birds is important for comparison between species of higher or lesser exposure to contaminants (Bowerman et al., 2000). In bald eagles, hematologic values were comparable to published ranges in birds, except from a higher ratio of eosinophils (Bowerman et al., 2000). In the same study, the absolute and relative numbers of lymphocytes in bald eagles varied with plasma concentrations of OCs and PCBs. Another study analysed relationships between organohalogen contaminants (OHCs) including PFASs, and BCCPs in white-tailed eagles and goshawks (Sonne et al., 2010). Although cautious with their conclusion, they suggest that impacts on kidney/liver functions by OHCs may have possible health impacts and infection risks. A repeated dose study of perfluorododecanoic acid (PFDoDA) in rats found the liver to be the main target for toxicity (Kato et al., 2014). The same authors also conducted a white blood cell (WBC) count which showed significant decreases in WBC, and lymphocyte, monocyte and eosinophil differential counts in the highest dosage group (2.5 mg PFDoDA/kg/day) (Kato et al., 2014). Although no study have yet associated chemical exposure with an avian epizootic, it is likely that immune suppression through chemical exposure and many low-level stresses (e.g., food reduction or climate stress) can cause increased morbidity in wild birds (Fairbrother et al., 2004).

1.3. Study species

The white-tailed eagle *(Haliaeetus albicilla)* also referred to as sea eagle, is a monotypic species and one of the world's largest eagles with a wingspan reaching 2.4 m (O'Rourke, 2014). Soaring high in the air, the adult is best recognized by its sheer size, broad wings, brown body, and contrasting white tail and head. The population is widely distributed throughout northern and central Eurasia, West Island and southwest of Greenland. Current population size ranges from 9000-12300 pairs in Europe with an increasing trend, which ranks the species as "Least Concern" on the IUCN Red List (BirdLife International, 2015). The dramatic population declines in the twentieth century were followed by conservation actions and the ban of DDT and other pollutants (Hailer et al., 2006). Through declines and recovery, Norway is described as a stronghold for the white-tailed eagle, current estimates counting 2800-4300 pairs (BirdLife International, 2015).

The white-tailed eagle (WTE) is a territorial, long-lived monogamous bird of prey. At an age of about 5 years, the WTE try to find a mate and a territory (Folkestad, 1994), residing sedentary through life that spans up to 30 years (Olsen, 2007). Successful breeding can result in 1-2 offspring(s) per year and the parenting is equally shared between male and female. The nestlings can fly after 11-12 weeks and are fed during a long period after that. Diet contains mostly of fish, seabirds and mammals dependent on the location of the territory (Folkestad, 1994). The species is well studied and has been monitored by The Norwegian Ornithological Society since 1974 (Gjershaug et al., 2008). The National Environment Monitoring Program included the white-tailed eagle as an indicator species in 1989, due to its position as an apex predator (Helander et al., 2008). The WTE, among other birds of prey, has been characterized as a useful environmental sentinel species to a range of environmental contaminants (Helander et al., 2008). Recent studies on WTEs have also shown higher PFASs concentrations than of other POPs (Bustnes et al., 2013b; Sletten et al., 2016).

The nestlings are especially suited for various reasons. They minimize confounding biological factors such as age and age-related metabolism, life-time bioaccumulation, reproductive state and migratory activity (Eulaers et al., 2014). They are easily accessible and feathers have less external contamination due to their shorter lifespan (Eulaers et al., 2011b). Nestlings may also be more sensitive to pathogens because of their rapid growth and partly immature immune system (Hanssen et al., 2013).

1.4. Aim

The aim of the present study is to (1) measure concentrations of PFASs in plasma and feathers of white-tailed eagle nestlings from Smøla and Steigen, and investigate factors affecting the PFAS levels, (2) explore the relationship between the concentration of PFASs in plasma and, the concentration of plasma protein fractions and the differential leukocyte counts.

1.1.   It is hypothesised that PFAS levels will increase with biological variables such as age and mass. PFAS levels are also dependent on trophic level and the concentrations in the local environment. It is therefore expected that the concentration will differ between the two populations. It is further hypothesised that the concentration in feathers will reflect accumulation over time and that the current study will give insight into the relevance of the use of feathers as a non-invasive biomonitoring tool for PFASs.

1.2.   PFASs have shown the potential for maternal transfer. It is hypothesised that concentrations deriving from maternal transfer are still present in the WTE nestlings. The relative importance of maternal transfer will be investigated by a theoretical approach. These aims and hypothesis (1.1 and 1.2) are visualised in Figure 1.2.

2.   Immunomodulation by PFASs is not well understood in avian wildlife. Thus, the current study will report leukocyte differential counts and concentration of protein fractions in plasma, and explore the relationship between these two immunological indicators and PFASs.
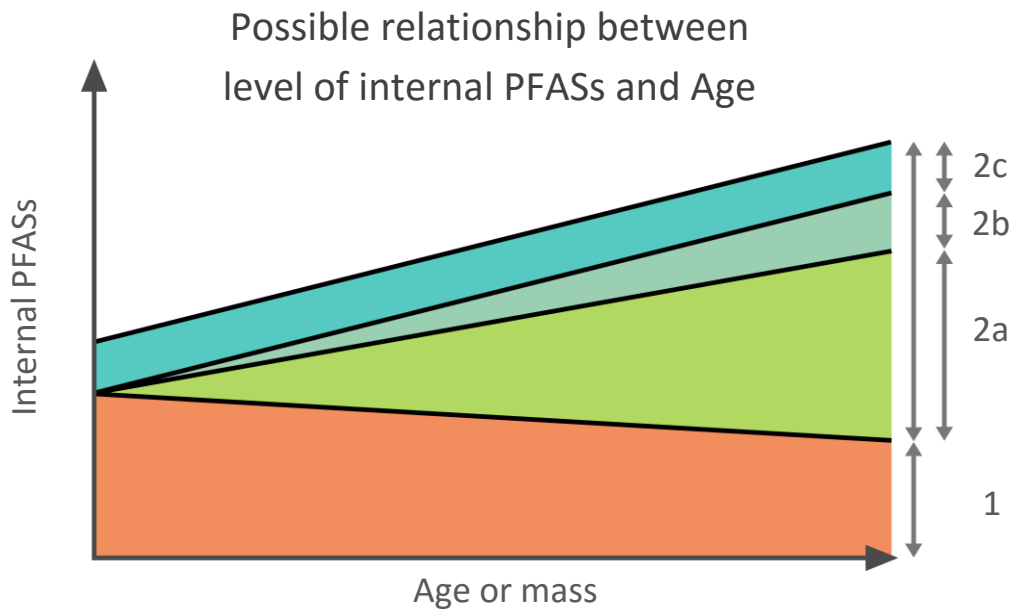
Figure 1.2: Hypothetical visualisation between age and internal PFASs of WTE nestlings. The figure is strictly simplified, and the difference between compartments and change in slope over time is not taken into account.

1. Maternal transfer to nestling

   PFASs are transferred from mother to egg, and it is also possible that there is a difference in contamination load between the first and second egg. The negative slope can be attributed to growth dilution, as well as elimination of PFASs. In a young nestling a higher proportion of the internal PFASs will be from maternal transfer than in a juvenile or adult bird.

2. Bioaccumulation from diet

   a. Bioaccumulation of PFASs over time through diet. It is assumed that this can be associated with mass and age, although this combines input and output.

   b. Difference in trophic level: these individuals have different dietary habits and feed on a higher trophic level than in 2a.

   c. Geographical difference in environmental contamination: the location is more contaminated and therefore internal PFASs reflects higher bioaccumulation through the food chain.

2. Materials and Methods

2.1. Study area

The sampling of nestlings was conducted June/July 2015 at two different locations in Norway, Steigen and Smøla (Figure 2.1). Steigen (67°N 15°E) is a municipality situated in Salten district, Nordland County. A total number of 14 birds were sampled from nine nests in this area, during three days (24.06 - 26.06). The nests were situated on small islands and skerries, distance ranging from 3-20 km west for Leinesfjorden. All nests were in close proximity to the sea. Smøla (63°N 7°E) is a municipality situated north in Møre og Romsdal county. A relative large island of approximate 270 km^2. During four days, 13 birds were sampled from ten nests, located both on mainland Smøla and smaller islands visited by boat (29.06 - 03.07).
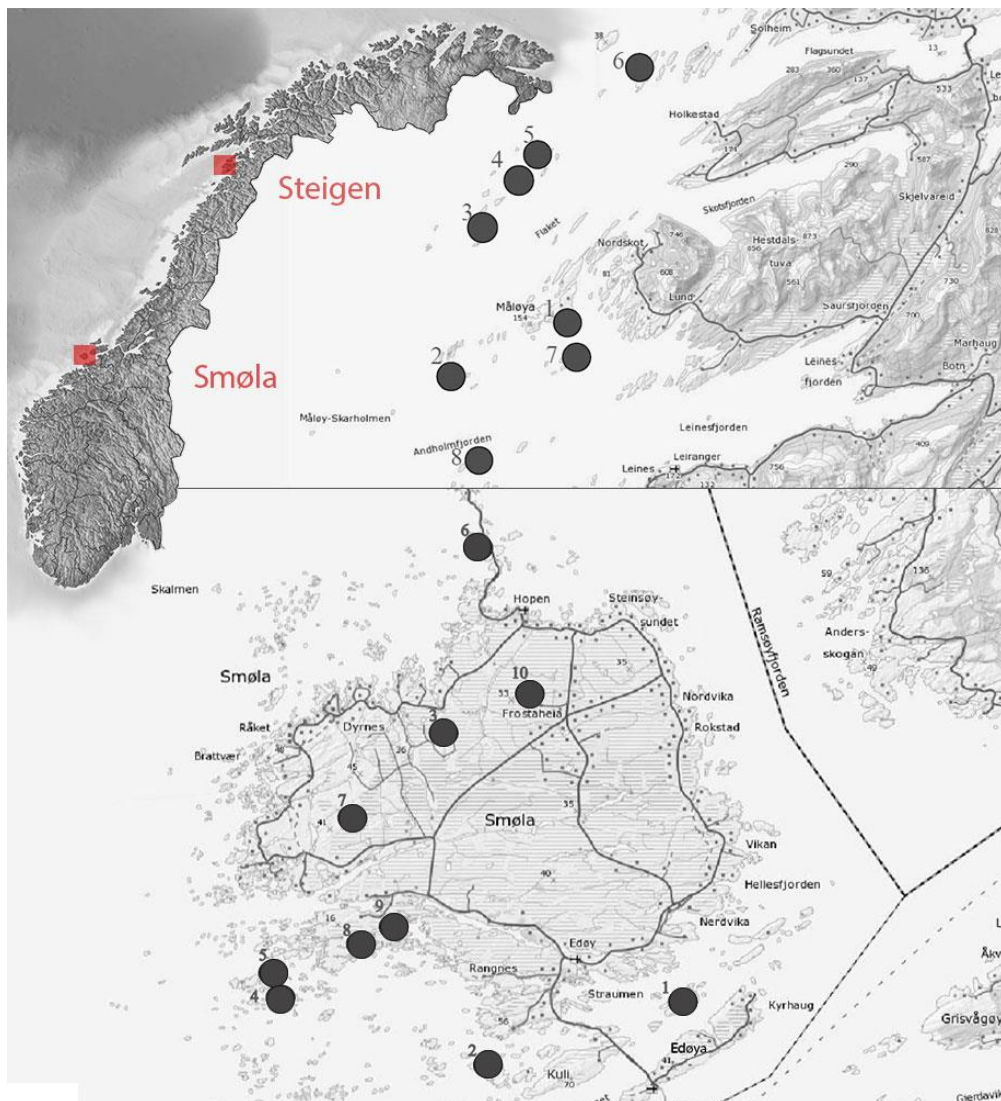
Fig. 2.1: Geographic locations of the two sampling sites in Norway. Steigen (upper part) and Smøla (lower part) are shown with nest locations (n = 27, nests = 19). Nest 9 in Steigen are not shown, but lies further south. Maps of Steigen and Smøla is made by Ingrid Engan Nøren.

2.2. Field sampling

Nestlings were caught in the nest or adjacent to it and sampled on the spot or carried to a more convenient site. The sampling was done immediately after approaching the nest and capture and capture of the nestlings (mean mm:ss = 06:47). Blood was taken from the right brachial vein with an heparinized vacutainer (Venosafe® BD, 9 mL) with a 23-gauge (0.6 mm) needle, before a small sample of 200 µL was collected in an EDTA capillary tube (Microvette®, Sarstedt) for blood smears. The biometrical data recorded included body mass (± 50 g), bill length (± 0.1 mm), bill height (± 0.1 mm), tarsus width (± 0.1 mm), tarsus depth (± 0.1 mm), hallux length (± 0.1 mm), tail length (± 0.1 mm), wing length (± 1 mm) and crop content (± 50 g). The sex was determined by comparing the tarsus depth and bill height with wing length. Subsequent conclusions were based on the relative thicker tarsus of females compared to males (Helander et al., 2008). Appendix E contains individual and sex-dependent biometrics. Ten feathers were pulled from the back of the nestling and stored in polyethylene bags. Samples were stored in cooling bags after sampling without direct contact with freezing elements. At the end of the day, the blood was centrifuged (6000 rpm, 10 min), in order to separate red blood cells and plasma. For the PFASs a volume of 200-300 µL plasma was stored in cryotubes. The plasma and feathers were stored in a freezer (-20 °C) until further processing.

Permission for sampling was given by the Norwegian Animal Research Authority and conducted after regulations by the Norwegian Animal Welfare Act.

2.3. Analysis of PFASs

All extraction and analysis of PFASs in plasma and feathers were conducted at the Norwegian Institute for Air Research (NILU) in Tromsø, Norway. The preparations of samples were carried out in August 2015 and stored for quantification in October at NILU using UHPLC-MS/MS.

The PFASs analysed in plasma and feathers were perfluorobutanoic acid (PFBA), perfluoroalkylpentanoic acid (PFPA), perfluorohexanoic acid (PFHxA), perfluoroheptanoic acid (PFHpA), perfluorooctanoic acid (PFOA), perfluorononanoic acid (PFNA), perfluorodecanoic acid (PFDA), perfluoroundecanoic acid (PFUnDA), perfluorododecanoic acid (PFDoDA), perfluorotridecanoic acid (PFTrDA), perfluorotetradecanoic acid (PFTeDA), perfluorooctane sulphonamide (PFOSA), perfluorohexane sulfonate (PFHxS), perfluoroheptane sulfonate (PFHpS), perfluorooctane sulfonate (PFOS), and perfluorodecanoic sulfonate (PFDS). Quantified PFASs in plasma are illustrated in Appendix B.

2.3.1. Plasma extraction

Analysis of PFASs in plasma was performed according to a modified version of the Powley method (Powley et al., 2005), further described by Herzke et al., (2009). Plasma was stored and transported in 1.5 mL cryotubes. Samples of 0.2 - 0.3 mL were thawed and spiked with a 20 µL internal standard solution (13C PFAS ISTD mix 0.1 ng/µL; Appendix F). For extraction, 1 mL of LiChrosolv Methanol (MeOH) was added, before the cryotubes were subject to three rounds of 10 min ultrasonic bath (Branson 2210) and vortexed (VWR International) before and in between. For sedimentation, the samples were centrifuged (Jouan S.A. Type A-14) at 2000 rpm for 5 min. The supernatant was transferred with Pasteur pipettes (150 mm glass) to Eppendorf centrifuge tubes (Polypropylene 1.5 mL fliptubes) containing approximately 25 mg ENVI-Carb (Sigma-Aldrich) absorbent and 50 µL glacial acetic acid. Tubes were vortexed (20 sec) and centrifuged at 10000 rpm for 10 min before 0.5 mL of supernatant were transferred to glass vials (2 mL). Finally, 20 µL of recovery standard solution (0.102 ng/µL 3,7-diMe-PFOA, 08.05.2015) was added, vials capped, vortexed and stored in a fridge until the analysis.

2.3.2. Feather extraction

Analysis of PFASs in feathers was performed according to a modified version of the Powley method (Jaspers et al., 2013; Powley et al., 2005). Feathers (2-3 per individual) were washed twice with distilled water in Petri dishes to remove most of the external contamination. In the washing process, the calamus and soft tissue were removed, and all the barbs were separated and cleaned. After drying, the feathers were cut into small pieces (<0.5 cm) in polypropylene tubes, weighted and spiked with 20 µL of internal standard (ISTD: Appendix F). The scissors and Petri dishes were cleaned in microsolv MeOH between each individual. Feather homogenates were then washed in 20 mL of Suprasolv hexane and put in an ultrasonic bath for 10 min and left to evaporate overnight. To denaturize the feathers, 2 mL of 200 mM NaOH in methanol was added and the samples were left for 60 min. Then 10 mL MeOH was added as an extraction medium. After three times of ultrasonic bath (10 min) and vortex (20 sec) in between, the feather-extract was set to soak overnight. To stabilize pH, 200 µL 2 M HCl in methanol was added followed by one round of vortex (2 sec) and ultrasonic bath (10 min). After centrifugation (2000 rpm, 5 min), the extracts were transferred into 15 mL centrifuge tubes. The tubes containing the feathers were rinsed once with MeOH and added to the supernatant. Then the extracts were evaporated to 2 mL (RapidVap) and 1 mL of the extracts was transferred to an Eppendorf tube containing 25 mg ENVI-Carb and 50 µL glacial acetic acid and vortexed (20 sec). The tubes were then centrifuged (10000 rpm, 10 min) and 0.5 mL of the supernatant were transferred to a 2 mL Clear vial before 20 µL recovery standard solution (0.102 ng/µL 3,7-diMe-PFOA, 08.05.2015) were added. The extract was then vortexed and stored in a fridge before the analysis by UPLC-MS/MS.

2.3.3. Quantification and quality assurance

Quantification of PFASs was conducted by NILU, with a 13C-labeled internal standard (Table F1). The chemicals of interest were quantified with linear regression. PFASs concentrations were analysed with an ultra-high pressure liquid chromatography triple-quadrupole mass-spectrometry (UHPLC-MS/MS, Thermo Scientific).

For quality control, one blank per 7th sample was included and the mean value was subtracted from the sample concentrations in the same batch. Plasma samples were further validated according to a standard reference material control (SRM 1957 05.02.2014) per 14th sample. The SRM was analysed human serum, provided by the National Institute of Standards and Technology (NIST). No reference material was available for feather extraction. Mean recovery of the internal standard was 83.0 % for plasma and 49.9 % for feathers (Table C3).

Calculations of the limit of detection (LOD) was set to three times the signal to noise. The limit of quantification was set to three times the LOD. The specific LOD and LOQ for each compound and amount of individuals above compound LOD and LOQ is listed in Table C1 and C2, Appendix C. Recovery standard (RSTD: 0.1 ng/μL 3,7-diMeo-PFOA in methanol) was provided by NILU. Measured recoveries in plasma and feathers are given in Table C3.

2.4. Blood smears

The blood smears were made according to the two slide "wedge" method described by Clark et al., (2009). A drop of blood (~25 μL) from a blood capillary tube was placed on a frosted glass slide and smeared with a second slider. This was repeated until at least two blood smears met the expected quality. Blood smears were then marked, air-dried and stored in screw-top vials and later in two box containers (capacity: 50 blood smears).

Staining of blood smears was done as soon as possible after field sampling (06.07 - 08.07). Before staining, the smears were fixated in methanol (99%) for 2 minutes and dried overnight. Smears were stained for 5 min in 50:50 May-Grünwald stain followed by 15 min in 1:10 Giemsa stain, diluted with Sørensen phosphate buffer (pH = 6.8). Between and after staining, smears were washed for 5 minutes in Sørensen phosphate buffer. Smears were mounted with Eukitt when they were completely dried.

2.4.1. Haematological cell counts

Blood smears were examined in a light-microscope (Eclipse 800) at 1000x. Leukocytes were identified and quantified in a monolayer-area along the x-axis of the blood film. Methods providing measurements of erythrocytes and leukocytes are described by Clark et al., (2009). Estimation of leukocyte concentration was obtained by counting 100 leukocytes. The cells were characterized as heterophils, eosinophils, basophils, monocytes or lymphocytes. In addition to the percentage of each leukocyte, a heterophil to lymphocyte (H:L) ratio was calculated. The total amount of counted red blood cells (RBCs) were estimated by counting three representative fields and multiply them with the total counted fields. The relative leukocyte levels (total leukocytes, lymphocytes and heterophils) were then calculated as leukocytes per 10 000 RBC.

2.4.2. Quality assurance

Blood smears were first assessed through a microscope for lysed cells and consistency in the monolayer (given a score between 1-10) and two smears from each individual were picked for further assessment. This was due to a trade-off between the sensitivity of the experiment and both workload for the assessor and quality of the leukocyte counts. The identification of each blood smear was then hidden by tape and instead given a random number calculated in R (1-54). This was done by a supervisor, so the identity of the numbers was kept from the assessor. This ensures a blind procedure to avoid experimental bias as observer-expectancy (Hurlbert, 1984).

Full randomization of sequencing prevents the time of measuring as a factor. To measure possible observer drift and repeatability, one of the samples was recounted five times. The coefficient of variation (C_V or $\widehat{C_V}$) is a measure of variability (Abdi, 2010), and calculations are given in Appendix G. To account for possible observer drift, the first five smears were recounted. Before counting the blood smears, definitions of the different cells were clarified. All definitions of cells were discussed with Hege Brun-Hansen at Oslo Veterinærhøgskole. By counting the same fields using a microscope with bridge (AxioCam ERc 5s), counting independently, the accuracy and definitions were further tested. The difference between myself and Hege Brun-Hansen was highest for lymphocytes (mean: ± 5% of 100 cells) and eosinophils (mean: ± 3.4%), and lower than ±1.5 % for the other cells. Definitions and pictures of cells encountered are given in Appendix G. For prevention of tired eyes, a limit of two hours without a break and four hours per day was set. During the blind procedure of leukocyte count further smears were excluded by quality assessments. The total number of smears included in the data analysed were 9 for Steigen (n = 7 nestlings) and 18 for Smøla (n = 12 nestlings).

2.5. Protein fractions

Plasma protein fractions were analysed by capillary electrophoresis (Sebia CAPYLLARYS 2 systems) at Sentrallabben, Veterinærhøgskolen. With the protein capillary electrophoresis (CE) and PHORESIS software, the concentrations of prealbumin, albumin, alpha 1 (α_1)-globulins, alpha 2 (α_2)-globulins, beta (β)-globulins and gamma (γ)-globulins were quantified in all plasma samples. To the knowledge of the author, no CE protein reference values for WTE are available. However, literature from its close relative, the bald eagle (*Haliaeetus leucocephalus*) and other raptors, were used for comparison and assessment of parting the different protein fractions (Cray and Tatum, 1998; Melillo, 2013; Tatum et al., 2000). Appendix J shows the raw data from protein CE. Two different graphs are included as these might be valuable as reference values for assessing protein fractions in WTEs and other raptors. Table D3 show all the individual protein levels in plasma samples (n = 27) from WTEs.

2.5.1. Quantification and quality assurance

Electrophoresis is based on separating components in silica capillaries by their electrophoretic mobility and electroosmotic flow at a specific pH in an alkaline buffer. Each sample is diluted with a dilution buffer and injected to the anodic end of the capillary. The capillaries were filled with a separation buffer and the protein fractions were separated by a high constant voltage. The protein fractions are then detected and quantified by UV absorbance. The protein patterns are interpreted and visualised as a graph. Quantification is relative to the total protein (g/dL), and each protein profile was assessed and each protein fraction was identified manually. For quality assurance, a set of eight controls were assessed before running the WTE samples.

2.6. Statistical analysis

Simple graphs and all tables were made in Excel (2016). Excel was also used for simple calculations as making the age variable (from wing length) and partly making the SMI (Scaled Mass Index). Principal component analysis (PCA), Analysis of Variance (ANOVA), Linear mixed effect regression (LMER), Spearman's rank-order correlation coefficient test (r_S), t-test, Shapiro-Wilcoxon test for normality, and homogeneity of variance was analysed in R (version 3.2.5).

Body mass (t = 2.78, p = 0.01) and age (t = 3.89, $p < 0.001$) differed significantly between the two populations. Body mass (Smøla: t = 4.82, p < 0.001, Steigen: t = 2.29, p = 0.049) also differed significantly between the sexes of each of the populations. Hence, most of the data are given for each population separately, although this was not chosen for all of the analyses. Correcting or controlling for covariates confounded to group factors is problematic, especially with a small sample size (Miller and Chapman, 2001). Separating the dataset might exclude

covariates as sex and differences between populations, but the number of individuals decreases. Therefore, rather than dividing the dataset, investigation of possible confounding factors was used when choosing best statistical solutions.

2.6.1. Treatment of samples under the limit of detection (LOD)

Compounds that were above the limit of quantification (LOQ) in more than 50 % of the samples (n = 27) was included in statistical analyses. Limit of detection (LOD) was set to three times the noise, and LOQ was set to three times the LOD. Samples that were under the LOD were given a random value between 0 - LOD. The LOD and LOQ for the compounds are given in Table C1-C2, Appendix C.

The following compounds met these criteria and were used in statistical analyses: In plasma: PFHpS, linPFOS, brPFOS, PFOA, PFNA, PFDA and PFUnDA. In feathers: PFUnDA.

2.6.2. Age, mass and scaled mass index (SMI)

The age variable was calculated from the tail length of the nestlings, according to equation 2.1. This equation was provided by Torgeir Nygård (NINA) and states that the tail feathers first start to grow after 30 days, and then grow 4.95 mm each day. A similar method is described by Helander, (1981), using the wing length to calculate the age. Wing length and tail length was significantly correlated for nestlings from Smøla and Steigen (r_s = 0.95, $p < 0.001$).

$$Age\ (days) = \frac{Tail\ lenght\ (mm)}{4.95} + 30 \qquad (eq.\ 2.1)$$

The mean mass of females and males were 5513 g and 4600 g, respectively. It was done a conscious choice to not center these, as this would have implication for any statistical interpretation. Instead, the mass difference between sexes was addressed through factorial variables and interaction models.

Scaled Mass Index (SMI) for all birds was calculated according to (Peig and Green, 2009). The SMI is computed as the individual mass (M_{ind}) times the mean length (L_μ) of the subpopulation (wing length used) divided by individual length (L_{ind}) (equation 2.2). b_{SMA} (constant) is called the scaling exponent and are calculated by the slope of the natural logarithm of both mass and length, divided by the Pearson's correlation coefficient (r) between mass and length. The theory behind SMI is that the mass is adjusted to the mass expected at L_μ (Peig and Green, 2009). Or simplified: an individual with a short length measure and a large mass (a "plump" bird) will get a high SMI.

$$SMI_{ind} = M_{ind}(\frac{L_{\mu}}{L_{ind}})^{b_{SMA}} \qquad (eq. 2.2)$$

The SMI was consistently higher for females, and since condition should not rely on sex, the SMI was centered according to equation 2.3, where SMI_C is the new centered individual SMI made of individual SMI, mean SMI of both populations, and mean SMI separated by sex.

$$SMI_C = \frac{\mu_{pop}}{\mu_{sex}} * SMI_{ind} \qquad (eq. 2.3)$$

2.6.3. Normal distribution

To assess the assumption of normal distribution for further statistical analysis, Shapiro-Wilcoxon test ($p < 0.05$) was applied to all parametric variables to assess normality. The non-normally distributed variables were $\log_e (x)$ transformed when statistical tests assumed a normal distribution. All PFASs were normally distributed, except PFHpS and brPFOS. Of the protein fractions α_1-globulins, β-globulins and γ-globulins did not meet the normal distribution requirements. Of the leukocytes: basophils and H:L ratio were not normally distributed. After $\log_e$ transformation, normal distribution was confirmed by Shapiro-Wilcoxon test and quantile-quantile (QQ)-plots.

2.6.4. Differences in contamination between categorical variables

To examine the relationship between numeric variables (cell fractions, PFASs and protein concentrations) and categorical variables (sex and population) a Mann-Whitney U test was applied. The independence between (sex) and inside (population) of these categories were not met, as 16 of 27 individuals sampled were siblings. In order to control for this, the factor nest (n = 19) was included in nested models. Significant level (p, two-way) of the Mann-Whitney U test was set to 0.05. At some instances a t-test ($p = 0.05$, two-way) was chosen; homogeneity of variance was investigated prior to the t-test.

2.6.4. Correlation

Correlation between variables was tested with Spearman's rank correlation coefficient (Spearman's rho | ρ) written as r_S. For variables that showed a normal distribution Pearson product-momentum correlation coefficient (Pearson's r) was used to confirm results, in the

case of big difference in output. Statistical significance for r_S was set to $p = 0.05$. Further correlation between variables is explored in the PCA.

2.6.5. Principal Component Analysis (PCA)

Two separate principal component analyses (PCAs) were performed to visualise patterns between PFASs, protein fractions and lymphocytes (package FactoMineR, R statistics version 3.2.5). The first PCA (PCA1) were made with data from all individuals (n = 27), and included the contributing variables PFASs and protein fractions. The second PCA (PCA2) were made of individuals (n = 19) successfully analysed for leukocytes, with the contributing variables PFASs and leukocyte fractions. For both PCAs; the variables age, mass, and SMI were set as supplementary quantitative variables, not contributing to the making of the PCA matrix, but visible in loading plots. In addition to age, mass, and SMI, variables calculated from other variables included in the PCAs were analysed as supplementary variables (not contributing to creating the PCA). Further, the categorical variables sex (M, F), population (ST, SM), location (Sea, Mixed, Inland), sibling (Yes, No) and firstSibling (1, 0: 1 means firstborn nestling) were included to analyse the relationship between individuals and quantitative variables. These do not contribute to the PCA, but patterns and relationship to different principal components/dimensions can elucidate the results.

The main result for PCA1 and PCA2 are given in the result part. A further description of eigenvalues, 3rd and 4th dimension (principal components) and statistical interpretation for individuals, quantitative and categorical variables are given in Appendix H. Both PCA1 and PCA2 were used descriptively to investigate relationships between PFASs and protein fractions and leukocyte percentages.

2.6.6. Linear mixed-effect regression

To accommodate for non-independency between nestlings, siblings from the same nests were given a numeric nest-factor (1 - 19). This was used as a random effect for further analysis of possible predictor variables that could explain the concentrations of PFASs and immunological parameters in plasma. Models were compared according to Akaike Information Criteria (AICc), and the most likely models are described. As response variable, the ∑PFASs was chosen, which was highly correlated with linPFOS ($r_S = 0.96$). The ∑PFASs was also investigated by nested analysis of variance (ANOVA) against different factors: sex (M, F), population (ST, SM), location (Sea, Seaboard, Inland) and sibling (Yes, No). The result of ANOVA is not presented but was used to choose regression models by investigating if predictor variables were confounded by groups.

2.6.7. Maternal transfer

The proportion of PFASs which can be attributed to maternal transfer was investigated by an exploratory approach. It is underlined that the estimates obtained by this method are only meant to point toward proportion size, and not measured in any way for any particular individual. For the calculations, weight and concentration of ∑PFASs from 23 WTE eggs (from Norway) analysed over the past two decades, were obtained from Torgeir Nygård (NINA). The dataset was used in an earlier report on contaminants in raptor eggs (Nygård et al., 2006). Concentrations of individual PFASs were not specified, and the eggshell is included in egg weight. A list of assumptions regarding the calculations is given in Table L1, Appendix L.

The two factors included estimating the proportion of maternal load were biological half-life and growth dilution. Elimination kinetics significantly differ between different PFASs and are also affected by species, compartment, exposure scheme, body size and physiological parameters. In a chicken exposure study, the biological half-life ($t_{1/2}$) of PFOS was determined to be 125 days (Yoo et al., 2009). To simplify, the half-life of PFOS was chosen to represent the half-life of ∑PFASs. When estimating the growth dilution constant, the slope of linear regression was taken from the natural logarithm of 1/mass (kg) between data of egg weight and mass of WTE nestlings from this study. The concentrations derived from maternal transfer in WTE nestlings was calculated from equation 2.3, while the overall depuration rate constant (k) from equation 2.4.

$$C_t = C_0 \times e^{-k \times t} \qquad (eq.\,2.3)$$

Where: C_t = Concentration at a given time (d^{-1}), C_0 = Concentration at a given time (d^{-1}), k = overall depuration rate constant and t = time (d^{-1}).

$$k = k_e + k_g \qquad (eq.\,2.4)$$

Where: k = overall depuration rate constant, k_e = first-order elimination constant and k_g = growth rate constant

A further description of the steps is given in Appendix L. From equation 2.3 rough estimates of mean ∑PFASs in WTE nestlings derived from maternal transfer was calculated. Mean age separated by sex and population was used as t (days). Since these are highly uncertain estimates, upper and lower limits were calculated by using mean age (separated by sex)

together with the lower and higher egg-concentrations. These are supposed to reflect rough estimates of range. Some of the eggs with a low weight was believed to have evaporated and was not used for calculations. The egg with the highest concentration and the two eggs with the lowest concentrations were also removed as these were considered outliers.

3. Results

3.1. Levels of PFASs in plasma

Plasma concentrations of PFASs quantified in more than 50 % of the samples from Smøla and Steigen are shown in Table 3.1. Of all the compounds, linear PFOS (linPFOS) was found at the highest concentrations, followed by brPFOS > PFUnDA ≥ PFNA > PFDA > PFOA > PFHpS. A significant difference in concentrations of brPFOS (W = 30, p = 0.002) and PFNA (W = 43, p = 0.019) was found between the two populations. No significant difference was found between sexes and levels of PFASs. However, the concentrations of ∑PFASs (ng/mL) were slightly higher for males compared to females within the two populations; Steigen (μ_M = 36.8 vs. μ_F = 29.3, p = 0.23) and Smøla (μ_M = 27.4 vs. μ_F = 23.1, p = 0.53). No significant difference was found between individuals with siblings and individuals without siblings. A high variation in concentration of ∑PFASs within nests was observed (see Figure D2, Appendix D), with a mean difference of 8.87 ng/mL (n = 8). The concentration of ∑PFASs within nests was not significantly higher in the older siblings (t = 0.91, p = 0.20, paired t-test), and the differences in concentration (older sibling − younger sibling) was not significantly correlated with the differences in age (r_s = 0.46, p = 0.24).

Table 3.1
Arithmetic mean ± standard error (AM ± SE), median and range of plasma concentrations (ng/mL) of detected compounds (>50%) from Steigen (n=14) and Smøla (n=13). < (under range) means that the compound was not detected in all plasma samples, and the value of the LOD is given. Compounds with significant differences between the two locations (p < 0.05) are denoted with * (Mann-Whitney U test).

Compound	p	Steigen (n=14)			Smøla (n=13)		
		AM ± SE	Median	Range	AM ± SE	Median	Range
PFHpS		0.08 ± 0.02	0.08	<0.08 - 0.31	0.06 ± 0.02	0.02	<0.02 - 0.26
brPFOS *		5.43 ± 0.80	5.38	1.85 - 11.7	2.36 ± 0.29	2.23	0.55 - 4.20
linPFOS		17.68 ± 1.67	16.54	9.55 - 27.07	15.40 ± 1.97	14.12	6.04 - 31.85
PFOA		0.51 ± 0.09	0.49	<0.14 - 1.27	0.35 ± 0.05	0.34	<0.12 - 0.57
PFNA *		3.68 ± 0.40	3.58	1.56 - 6.48	2.25 ± 0.32	1.82	0.57 - 4.86
PFDA		1.44 ± 0.13	1.44	0.91 - 2.52	1.27 ± 0.13	1.22	0.66 - 2.30
PFUnDA		3.66 ± 0.23	3.36	2.30 - 5.08	3.39 ± 0.19	3.59	2.43 - 4.36
∑PFASs		32.49 ± 2.95	30.98	17.21 - 51.37	25.09 ± 2.96	23.88	10.49 - 44.39

Comparing carbon chain lengths, the odd numbered PFCAs (PFNA and PFUnDA) have 2-7 fold higher concentrations than even numbered PFCAs (PFOA and PFNA), a pattern which is also evident in levels detected in the longer chained PFDoDA < PFTrDA (see Table C1, Appendix C). The recovery percentages of the plasma analysis are given in Table C3.

By composition, mean plasma levels of linPFOS constituted 60.1 % and 54.3 % in Steigen and Smøla, respectively. BrPFOS constituted 9.3 % and 15.8 % dependent on the population. Of the total PFASs, PFSAs constituted 69.6 % and 70.4 %, and PFCAs 30.4 % and 29.6 %, in nestlings from Steigen and Smøla (Figure 3.1). By comparing the two populations, nestlings from Steigen had a significantly higher contribution of linPFOS (p = 0.009) and a significantly lower contribution of brPFOS (p = 1.4e-05) and PFNA (p = 0.015) to the PFAS profiles, than nestlings from Smøla.
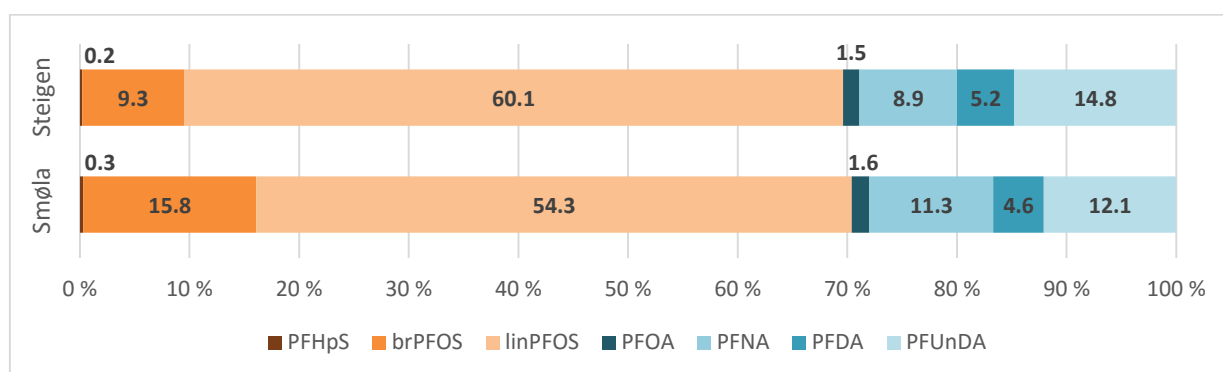
Figure 3.1: Mean percentage composition of PFASs concentrations in WTE nestlings, from Steigen (n = 14, top) and Smøla (n = 13, bottom).

3.1.1. Correlation analysis of PFASs

The compounds brPFOS, linPFOS, PFDA and PFUnDA had pairwise statistically significant correlations (r_S | rho) between 0.50 − 0.80 (Figure 3.2). Highest correlations were found between the individual compounds brPFOS - PFNA (r_S = 0.83, p < 0.001) and linPFOS - brPFOS (r_S = 0.79, p < 0.001). PFOA showed fewer significant correlations with the other PFASs, although significant with brPFOS (r_S = 0.47, p = 0.01), PFHpS (r_S = 0.42, p =0.01), and PFNA (r_S = 0.49, p = 0.03). PFHpS had 12 of 27 plasma samples below LOD (these were given a random value between 0 and LOD) and were less suited for comparison (not included in further remarks). There was no clear correlation pattern when investigating PFCAs (PFOA, PFNA, PFDA, and PFUnDA) or PFSAs (brPFOS and linPFOS) as groups, nor odd numbered PFASs (PFNA and PFUnDA) or even numbered PFASs (PFOA, brPFOS, linPFOS and PFDA).
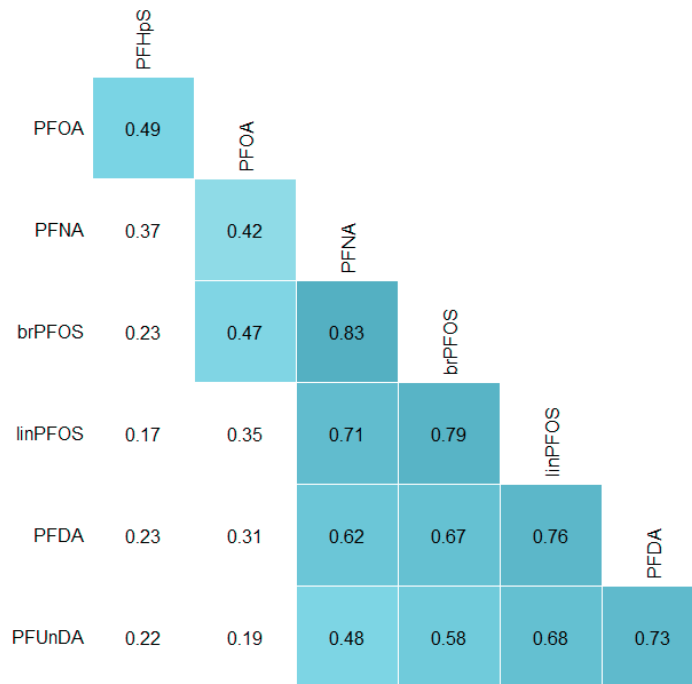
Figure 3.2: Plot of Spearman's rank correlation coefficient (r_S) between individual PFASs in plasma (n=27). Correlation coefficients (r_S) are given as a numeric value (between -1 and 1) and statistical significance (p <0.05) is shown as colour (white is not significant). The colour gradient relates to the correlation; darker colours equals higher correlation coefficients.

3.1.2. Association between PFASs, Age, and Mass

In Figure 3.3, ∑PFASs (ng/mL) are plotted against mass (g) of the nestlings and coloured by sex and population. ∑PFASs appears to be increasing with mass as hypothesised. Note that residual square (R^2) of the regression lines for Steigen is higher than for Smøla. Further, the concentration relative to mass is higher for Steigen compared to Smøla, but also for males compared to females. In theory, if the mass and ∑PFASs was a direct consequence of weight gain through the amount of food consumed, the lines of males and females would be expected to be parallel and overlap at some point.
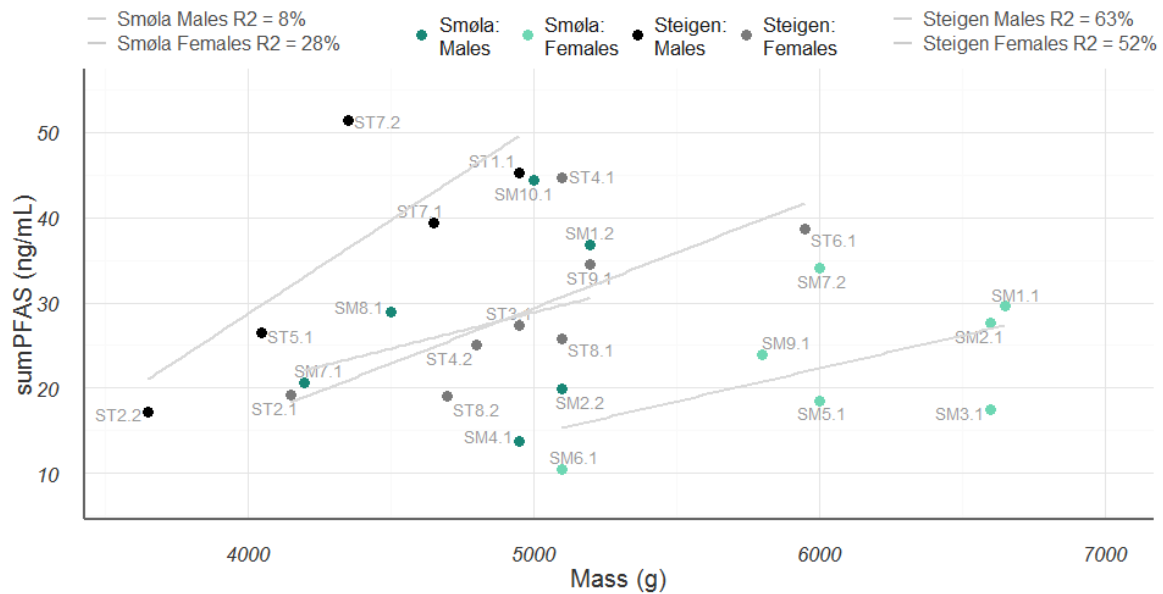
Figure 3.3: Relationship between mass (g) and ∑PFAS (ng/mL). The points are coloured after population (Smøla, Steigen) and sex (males, females). Linear regression is fitted for each of the groups, and square residuals are given as percentages.
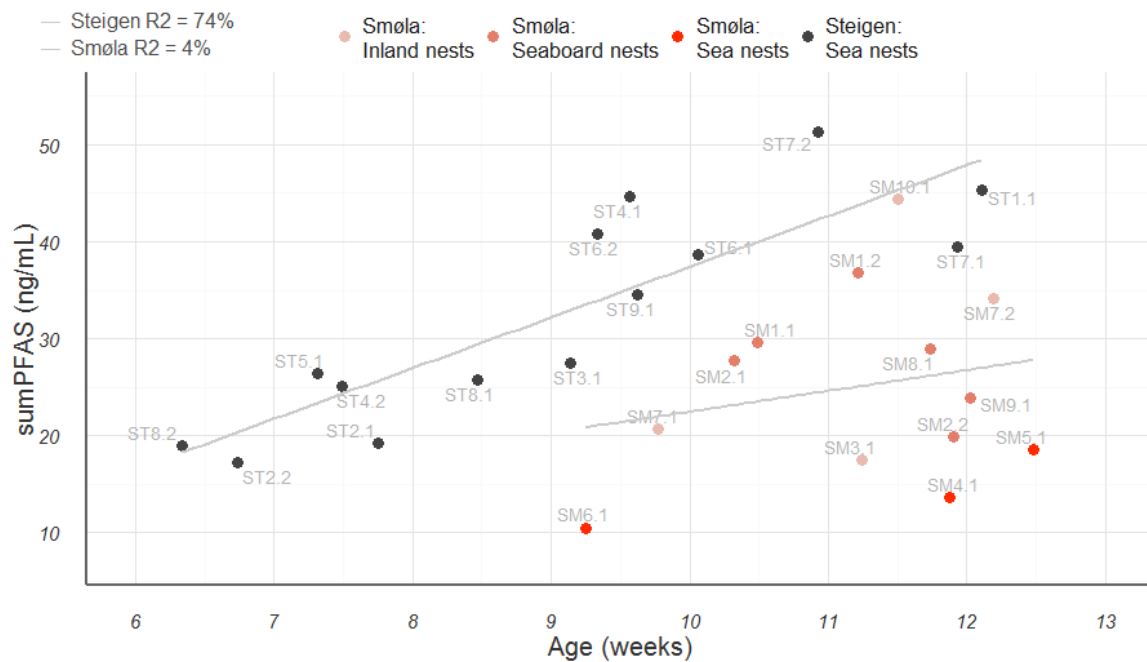
Figure 3.4: Relationship between age and ∑PFAS. The different nest locations were divided between inland, seaboard and sea, derived from Figure 2.1. All of the Steigen nests were located on small islands in the sea. At Smøla, some nests were located in the middle of the main island (inland), some at the edge/close to the main island (seaboard nests), and some further out towards the sea (sea nests). Linear regression is fitted for each of the groups, and square residuals are given as percentages.

Figure 3.4 shows ∑PFASs plotted against age (weeks), coloured by the location of the nest. It depicts that birds from Steigen have accumulated higher concentrations of PFASs relative to age. The age and ∑PFASs were significantly correlated (r_S = 0.88, p = 2.2e-16) for WTE nestlings from Steigen, but not for WTE nestlings from Smøla (r_S = 0.06, p = 0.86). The colour gradient of the Smøla nests represents different types of nest location (see Figure 2.1), which might contain information about diet fed to the nestling.

To further investigate the association between ∑PFASs, age and mass a set of nested linear models was investigated, based on Akaike's information criteria. The four best-ranked models are given in Table 3.2. Models 1 and 2 are similar to models 3 and 4, respectively. As an example, model 1 assumes a different slope between the males and females (shown as interaction) concerning the relationship between mass and ∑PFASs, while model 3 assumes the same slope, but different intercept. All models include a difference between Smøla and Steigen, while only model 1 and 3 include a difference between sexes.

Table 3.2

Model selection including the four best models predicting variation in plasma levels of ∑PFASs (ng/mL) in relation to mass (kg), age (days), sex and population (Pop). Model selection was done according to AICc. Four models had ΔAICc below 2 and are further described in Table 3.3. The two most likely models (Rank 1 and 2) assumes different regression slopes for mass between sexes, and age between population, respectively. The models were made from 19 nests and 26 (for mass) or 27 individuals. A full list is given in Appendix A.

	Models (n = 19)		Model selection			
Rank	Response	Predictor	AICc	ΔAICc	AICc WT	Sample size
1	∑PFASs ~	Mass:Sex[a] + Pop	197.03	0.00	0.27	26
2	∑PFASs ~	Age:Pop[b]	197.78	0.75	0.19	27
3	∑PFASs ~	Mass + Sex + Pop	198.07	1.04	0.16	26
4	∑PFASs ~	Age + Pop	198.92	1.89	0.11	27

a Interaction between the slope of mass (kg) and sex (different slopes for males and females
b Interaction between the slope of age (days) and population (different slopes for Steigen and Smøla)

Estimates of the best-ranked models predicting levels of ∑PFAS in plasma are given in Table 3.3. The ∑PFASs levels were predicted to be higher in the Steigen population relative to age or mass (Steigen ≈ + 17 ± 4 ng/mL). Model 2 also predicts a higher accumulation of ∑PFASs per day for nestlings from Steigen (0.69 ng/mL/day, p = 0.0005) in contrast to Smøla (0.46 ng/mL/day, p = 0.0035). By body mass, the ∑PFASs concentrations are expected to increase approximately with 11.3 ng/mL per kg weight gain, while males are expected to have 16.2 (± 5.0) ng/mL higher plasma concentrations than females (model 3). The alternative model (model 1) predicts a higher increase per kg weight gain for males (14.4 ng/mL, p = 0.0026) than females (10.9 ng/mL, p = 0.0043). Note that the intercept is negative for all models and that intercept of Steigen (model 1, 3, and 4) and males (model 3) is additive. Using model 3 as an example: if nestling is a male from Steigen the intercept equals -45.0 + 16.9 + 16.2. Further, the intercept refers to Smøla in model 1 and 4, Smøla and female in model 3, or both populations and sexes in model 2.

Table 3.3
The four most likely models explaining levels of ∑PFASs (ng/mL) in plasma. Contaminant variation is predicted by mass (kg), age (days), population and sex of WTE nestlings (n = 19 nests). The predictor variables Steigen and Male are additive to the intercept. The predictor variables Mass and Age are given as slopes. Significant t values for estimates are given as bold font, and p values were added as asterisks, where $p < 0.001$ is indicated by ***, $p < 0.01$ by **, and $p < 0.05$ by *.

Variable	Model 1			Model 2			Model 3			Model 4		
	Estimate	SE	t value	Estimate	SE	t value	Estimate	SE	t value	Estimate	SE	t value
Intercept	-42.832	20.147	**-2.126***	-11.3291	10.5549	-1.073	-45.001	21.44	**-2.099***	-24.3169	12.8131	-1.898
Steigen	17.205	4.538	**3.791**				16.846	4.603	**3.660**	17.2521	4.1513	**4.156***
Male							16.212	4.951	**3.274**			
Mass							11.339	3.557	**3.188**			
Mass:Female	10.901	3.338	**3.266**									
Mass:Male	14.365	4.102	**3.502**									
Age										0.6226	0.1598	**3.897**
Age:Smøla				0.4576	0.136	**3.364**						
Age:Steigen				0.6912	0.1634	**4.230***						

3.1.3. Maternal transfer

All estimates in this section are based on the assumptions and literature described in materials and methods 2.6.7 and Appendix L. By a first-order kinetic model the mean internal concentrations, derived from maternal transfer, was estimated to be between 1.1 − 3.1 ng/mL ∑PFASs (Table 3.4). The overall internal concentration decreased with 0.9 – 2.7 % of the initial egg concentrations. By proportion (internal/plasma ∑PFASs) this equals 4.5 − 10.6 % of the levels measured in plasma samples from nestlings in the current study. The lower and upper

estimates were based on the lowest and highest egg-concentrations considered, while age is set to the means of the different groups (separated by sex and population). The growth rate constant (k_g) was estimated to be higher for females than for males, meaning that females were expected to have a higher growth dilution than males. The elimination constant (k_e) was assumed equal between sexes. The rate constant (k) was calculated as $k_e + k_g$, and further description of these estimates are given in Appendix L.

Table 3.4

Estimates of internal concentrations (ng/mL) derived from maternal transfer in WTE nestlings. Calculations are based on mean age separated by population and sex, and mean (M), lower and upper range of ∑PFASs (ng/g ww) in eggs. Proportions[a] are calculated on estimated ∑PFASs (M., LE. and UE.) divided by plasma concentrations of ∑PFASs from WTE nestlings (n = 27).

Data from WTE nestlings (n = 27) from Smøla and Steigen					Data[d] from WTE eggs (n = 16)		Estimates of expected maternal load (∑PFASs) in WTE nestlings				
Pop.	Sex	M. age (days)	M. mass	M. ∑PFASs (ng/mL)	Rate constant k	M. egg ∑PFASs (range) (ng/g ww)		M.	LE.[b]	UE.[c] (ng/mL)	Proportion[a] of ∑PFASs (LE% - UE%) (%)	
SM	Males	79	4825	27.4	0.05385	115.5	(57.2 - 210.3)	1.6	0.8	3.0	6.0	(3.0 - 10.9)
SM	Females	78	6107	23.1	0.06026	115.5	(57.2 - 210.3)	1.1	0.5	1.9	4.5	(2.3 - 8.3)
ST	Males	69	4330	36.8	0.05385	115.5	(57.2 - 210.3)	2.8	1.4	5.1	7.6	(3.8 - 13.9)
ST	Females	60	4994	29.3	0.06026	115.5	(57.2 - 210.3)	3.1	1.5	5.7	10.6	(5.3 - 19.3)

Abbreviations: Pop. = population, SM = Smøla, ST = Steigen, M. = mean, ME. = mean estimate, LE. = lower estimate, UE. = upper estimate

a Proportions are calculated on estimated *internal* concentrations (ng/mL)/*plasma* concentrations (ng/mL), which assumes that the plasma concentration is equal to the mean internal concentrations

b Calculated with mean age and lower range of egg ∑PFASs

c Calculated with mean age and upper range of egg ∑PFASs

d Data were given by Torgeir Nygård (NINA), including concentrations of ∑PFASs and egg weight from 23 WTE eggs from Norway. Seven of the eggs were omitted for reasons described in Materials and Methods 2.7.6.

The one-compartment model made to estimate internal levels derived from maternal transfer is visualised in Figure 3.5. Concentrations of ∑PFASs derived from maternal transfer are shown as a function of age (days) of WTE nestlings. Note that the model growth dilution constant is based on the mass difference between eggs and WTE nestlings (Appendix L). The model does not take into account variation in growth with age.
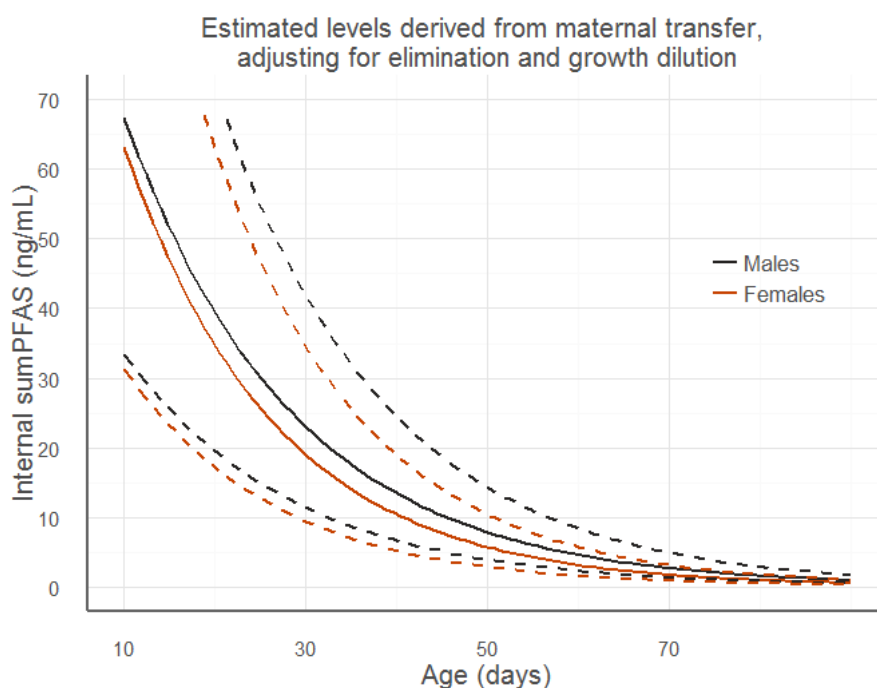
Figure 3.5: Estimated internal concentrations of ∑PFASs (ng/mL) derived from maternal transfer decreasing with age of nestling. The solid lines are based on mean egg-concentrations, and the stippled lines are based on the lowest and highest concentrations in eggs (not ± SE). The two sexes (colours) have the same elimination constant, while separate growth dilution constants.

3.2. Levels of PFASs in feathers

Ten different compounds were detected (>LOD) in feather samples (Table C2, Appendix C). These included PFOSA, PFHxS, linPFOS, PFHxA, PFOA, PFNA, PFDcDA, PFUnDA, PFDoDA, and PFTrDA. Only three compounds had concentrations above LOQ in more than 10/27 samples, these were PFUnDA (n = 16), PFOSA (n = 13) and PFTrDA (n = 11). PFUnDA was the only compound detected and quantified in more than 50% of the samples. Interestingly PFHxS had the highest mean concentration and highest concentration of any PFAS investigated in the feathers (μ = 2903.2 pg/g, upper concentration: 5168.7 pg/g), but could only be quantified in four samples. PFHxS was also detected in five plasma samples, but there was only one individual where it was both detected in plasma and feathers. The recovery percentages were between 48 – 55 % in the feather analysis (Table C3, Appendix C).

When comparing feather and plasma concentrations, a few observations stand out. Linear and branched PFOS were the compounds found to have the highest concentrations in plasma. In

feathers, linPFOS was detected in only four samples and brPFOS was not detected in any samples. On the other hand, PFOSA was quantified in 13 feather samples, while not detected in any of the plasma samples. Overall, the proportion of compounds above LOD is much lower in feathers, and concentrations are 3-20 times higher in plasma (except for PFHxS). The detection and concentration patterns of long chained PFCAs are similar, with higher concentrations in odd numbered PFCAs (PFNA, PFUnDA, and PFTrDA) in both feathers and plasma.

PFUnDA was the only PFAS with over 50% of the samples above LOQ. Feather samples from Steigen had a significantly higher concentration (t = - 3.4, p = 0.003) when excluding the samples below LOD from the data. PFUnDA levels in feather and plasma samples showed a significant correlation (r_S = 0.50, p = 0.008) with all individuals included (n = 27). Figure C1 (Appendix C) shows the linear relationship between plasma and feather PFUnDA concentrations plotted for all individuals above LOQ (R^2 = 0.24).

3.3. Levels of protein fractions

Protein fractions were analysed by protein electrophoresis, and examples of the electrophoretic pattern are given in Appendix J. Individual protein fractions are given in Appendix D, Table D3. None of the individuals showed a particularly abnormal electrophoretic pattern by visual inspection, compared to the others. The WTE nestling protein levels (Table 3.5) were compared to reference values from healthy adults of Bald eagle (*Haliaeetus leucocephalus,* n = 46) and healthy adults of Stellar's sea eagle (*Haliaeetus pelagicus,* n = 9) (Tatum et al., 2000). Levels were slightly lower in WTE nestlings for the total protein (x (multiplier): 0.9 - 0.8), albumin (x: 0.9 - 1.0), α_1-globulins (x: 0.2 - 0.1), α_2-globulins (x: 0.7 – 0.6), β-globulins (x: 0.9 – 0.8) and similar for γ-globulins (x: 1.0 – 1.1), compared to bald eagle and Stellar's sea eagle, respectively (Tatum et al., 2000). In contrast, WTE nestlings had 2.5 - 3.9 times higher prealbumin than Bald eagles and Stellar's sea eagle.

Table 3.5

Arithmetic mean ± standard error (AM ± SE), median and range of protein fractions (g/L), total protein (g/L) and albumin to globulin ratio from Steigen (n=14) and Smøla (n=13). Significant *p* values for estimates are given as asterisks, where p < 0.001 is indicated by ***, p < 0.01 by **, and p < 0.05 by * (Mann-Whitney U test).

Analyte		Steigen AM±SE	Median	Range	Smøla AM±SE	Median	Range	*p*	
Prealbumin	(g/L)	3.46±0.33	3.83	1.24-4.96	5.23±0.42	4.93	2.70-7.89	0.004	**
Albumin	(g/L)	14.34±0.45	14.53	10.60-16.55	14.55±0.49	14.20	11.87-17.27	0.943	
α_1-globulin	(g/L)	0.87±0.07	0.76	0.45-1.39	0.69±0.05	0.65	0.43-1.02	0.014	*
α_2-globulin	(g/L)	3.60±0.10	3.58	2.95-4.22	3.48±0.12	3.54	2.79-4.03	0.544	
β-globulin	(g/L)	4.84±0.13	4.83	4.05-5.71	5.17±0.26	4.93	4.12-7.68	0.297	
γ-globulin	(g/L)	3.32±0.21	3.17	2.21-5.25	2.80±0.12	2.75	2.21-3.53	0.058	
Total protein (g/L)		30.43±0.68	31.00	25.00-34.00	31.92±0.55	31.00	28.00-35.00	0.134	
A:G[a] ratio		1.42±0.03	1.42	1.16-1.68	1.64±0.05	1.65	1.39-2.07	0.003	**

[a] Albumin to globulin ratio: (albumin + prealbumin)/(α_1 + α_2+ γ globulins).

By population, prealbumin was significantly higher in the Smøla samples compared to Steigen (μ_{SM} = 5.23, μ_{ST} = 3.46, *p* = 0.004). Prealbumin also showed the highest percentage range and standard deviation relative to its mean. The A:G ratio (Figure 3.6) was consequently higher for Smøla (*p* = 0.003), due to the difference in prealbumin, but also because WTEs from Smøla had slightly to significantly lower concentrations of the globulins (α_1, α_2, and γ), except β-globulins.
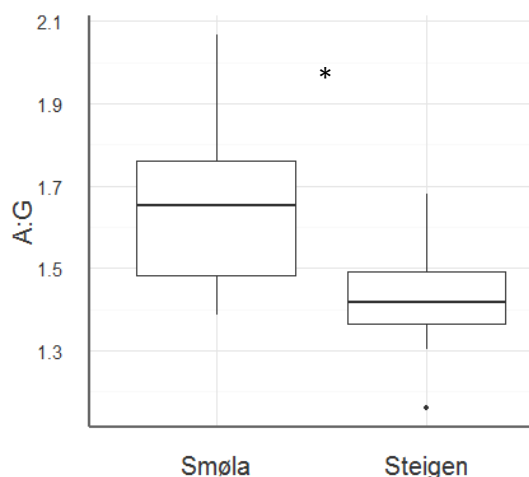
Figure 3.6: The albumin:globulin ratio (A:G) were significantly higher in nestlings from Smøla (*p* = 0.003). The box represents the median (bold line) and the 25th and 75th percentage quartiles. Potential outliers are shown when outside the 1.5 interquartile range (upper and lower whiskers).

3.3.1. PFASs and protein fractions

Figure 3.7 shows the first two dimensions of PCA1, which included primary variables as protein fractions and PFASs in plasma (n = 27). The first two dimensions describe 54.0 % of the variation (Dim1: 32.1 %, Dim2: 21.9 %). Further description of PCA1 is given in Appendix H. Visualisation of PCA1 dimensions 3 and 4 are shown in Figure H1, eigenvalues of PCA1 are given in Table H1

and Figure H2, and values of variation in each dimension (individuals and variables), ctr (contribution to dimension) and cos2 (quality of representation) are given in Tables H2-H5 for the first five dimensions (cumulative variation = 82.8 %).
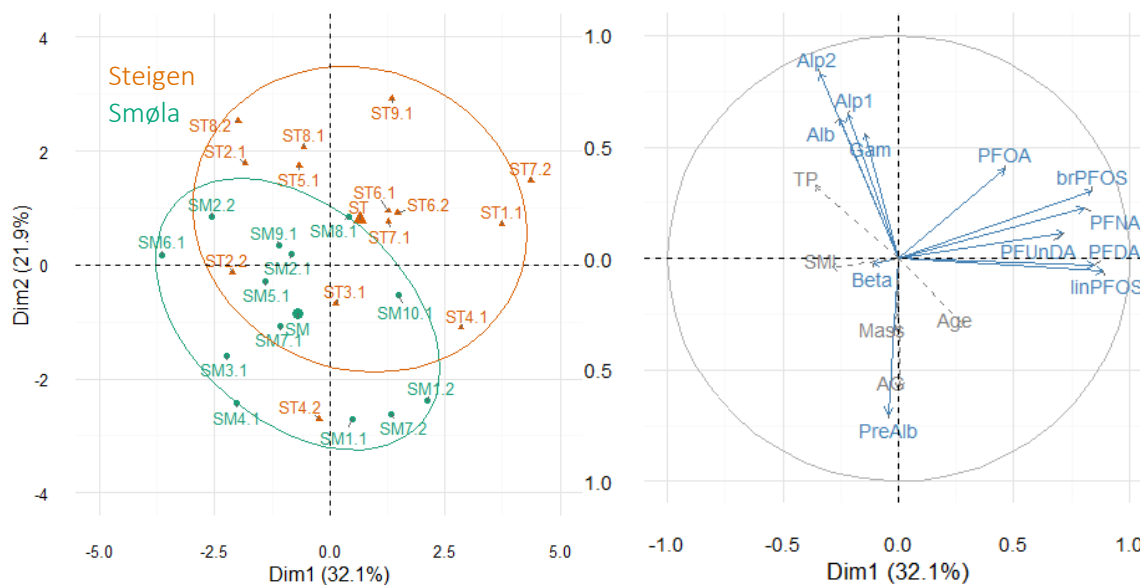
Figure 3.7: Principal Component Analysis of contaminants and proteins (PCA1). Dimension 1 explains 32.1 % of the total variation, while dimension 2 explains 21.9 %. Individuals in the score plot (left) are coloured after population (Steigen/Smøla), while the loading-plot (right) show contributing variables in blue and supplementary variables in grey. SMI = scaled mass index, TP = Total protein, AG = Albumin: Globulin ratio, PreAlb = Prealbumin, Alb = albumin, Alp1 = α_1-globulins, Alp2 = α_2-globulins, Beta = β-globulins, Gam = γ-globulins

Figure 3.7 shows a clear grouping pattern of the PFASs as shown in dim1 (loading score: positive 0.7 - 0.9). The compounds linPFOS, brPFOS, PFNA, PFDA and PFUnDA are relatively well projected (cos2: $0.5 - 0.8$) in this dimension, while PFOA was less correlated (loading: 0.46) to dim1 (Appendix H, Table H3). Protein fractions albumin, α_1-, α_2-, and γ-globulins are relatively well projected in dim2 and positively correlated, as well as negatively correlated to prealbumin.

SMI, age, and mass are not well projected (Table H4) in any of the four first dimensions (cos2: $0 - 0.15$). Therefore, it is hard to interpret if these variables are correlated to any of the primary variables. The score plot was visualised by colouring the two populations, Steigen and Smøla. The nestlings from Steigen had a higher mean concentration of PFASs and therefore score higher in dim1. Many of the individuals are well projected in dim1, as ST7.2 and ST1.1 which have the highest ∑PFASs concentrations, in contrast to SM6.1 which has the lowest (Table D1, Appendix D). From the PCA1 dimension 2, it also shows that plasma prealbumin concentrations are higher in the Smøla population. Factors as Sex (M/F), Sibling (Y/N),

firstSibling (1/0) and location (sea/mixed/inland) were also added as supplementary variables to PCA1 (Table H5). None of these factors correlated to a high degree to any of the dimensions interpreted. Note that these variables are portioned between Steigen and Smøla, which are differently projected in dim1, dim2, and dim4 (Figure 3.7 and H1, and Table H5).

3.3.2. Factors affecting protein fractions

Protein fractions are known to be associated with health condition, nutritional and physiological status, and contaminants (Grasman et al., 2000), which was further investigated by correlation and regression models (Figure 3.8, Appendix I, Tables I1, I2, and I3).

Figure 3.8 shows that body mass significantly affected prealbumin levels (t = 4.67: $p < 0.001$, DF= 18), with an increase of 1.12 g/L in prealbumin levels per kg weight gain (Figure 3.8 and Appendix I). All models with ΔAICc below 2 predicted a significant increase in prealbumin with an increase in mass. A:G ratio was significantly correlated to age (r_s = 0.48 , p = 0.011), and model 2 and 3 (Table I2) predicts an increase in A:G ratio relative to age. Only model 3 (Table I2) predicted a significant increase in A:G ratio with increasing age, but only for the Smøla population. The highest ranked model predicted population to be the best predictor of A:G ratio (Figure 3.8).
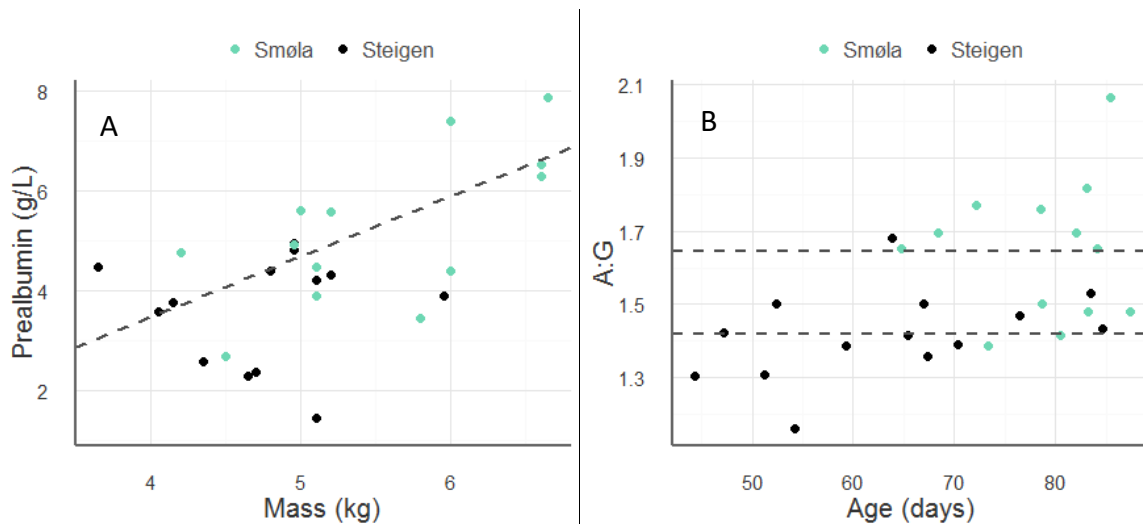
Figure 3.8: Visualisation of linear mixed-effect regression of the relationship between (A) plasma levels of prealbumin (g/L) and mass (kg), and (B) plasma albumin/globulin ratio (A:G) and age (days) in WTE nestlings (n = 19 nests) from Smøla (green dots) and Steigen (black dots). Linear regression models were ranked by AICc, and the most plausible models were visualised with dotted lines. In B, the two lines represent model estimates of Smøla (upper line) and Steigen (lower line)

Neither correlation nor models showed any strong association between PFASs and protein fractions. PFASs were generally negatively correlated with the different protein fractions, and only branched PFOS was significantly correlated (r_s = -0.42, p = 0.027) to total protein.

3.4. Levels of leukocytes

Leukocyte data are presented in Table 3.5, together with reference data from other birds. Heterophils were the most abundant cells followed by lymphocytes and eosinophils. Monocytes were rare and basophils were detected in less than half of the individuals. No significant differences in cell proportions (%) were detected between the two populations (Appendix K, Table K1), or between male and female WTEs. Although females had slightly a higher H:L ratio (μ_F = 1.90, μ_M = 1.35, p = 0.11).

Table 3.5

Differential leukocyte counts of nestling white-tailed eagles (n[a] = 19) from Steigen and Smøla, Norway. Values are given as arithmetic mean (AM), standard error (SE), median and range in percentages (%) of total leukocyte count and as cell type/10 000 erythrocyte (rel). Reference values from four different studies[b-e] were added for comparison. All reference values are from healthy birds.

	WTE			BE[b]	CB[c]	PF[d]	BP[e]
Parameter	AM ± SE	Median	Range	AM ± SE	AM ± SE	AM ± SE	AM ± SE
Lymphocytes (%)	31.4 ± 7.1	33	19 - 42	38 ± 2.2	20 ± 2.0	34.9 ± 0.5	27.1 ± 1.2
rel	31.7 ± 13.3	32.8	11.7 - 64.1				58.4 ± 4.3
Heterophils (%)	48.3 ± 7.0	48	36 - 62	44 ± 2.4	63 ± 2.7	61.1 ± 0.4	71.3 ± 1.2
rel	48.2 ± 17.2	46.2	22.1 - 89				187 ± 15.2
Eosinophils (%)	16.3 ± 6.0	15.5	8 - 28	13 ± 1.3	16 ± 2.9	2.2 ± 0.05	0.7 ± 0.1
Basophils (%)	0.4 ± 0.5	0	0 - 1.5		0 ± 0.1	0.1 ± 0.01	
Monocytes (%)	3.6 ± 1.7	4	1 - 6.5	4 ± 0.4	0 ± 0.2	1.5 ± 0.05	0.9 ± 0.1
Leukocytes rel	99.7 ± 31.6	102.8	46.9 - 169				249 ± 17.1
H:L ratio	1.7 ± 0.7	1.5	1 - 3.1				3.7 ± 0.3

a Two smears were analysed for each individual, while some of the smears were excluded during the blind procedure (described in Materials and Methods 2.4.2). A total of 19 of 27 birds, Steigen (n = 7) and Smøla (n = 12), met the quality assessment.

b Nestling Bald eagle (*Haliaeetus leucocephalus*) from Michigan (USA). Method: Wright stain. n=21 (Bowerman et al., 2000).

c Adult Common buzzard (*Buteo buteo*) from Madrid (Spain). Method: May-Grünwald Giemsa stain. n=23. (Hernandez and Fores, 1990).

d Nestling Peregrine falcon (*Falco peregrinus*) from central Spain. Method: Diff-Quick stain. n = 32. (Lanzarot et al., 2001).

e Nestling Burrowing Parrot (*Cyanoliseus patagonus*) from North-eastern Patagonia (Argentina). Method: Giemsa stain. n = 103 (Masello et al., 2009).

3.4.1. Morphology and clinical remarks

Characteristics and morphology of cells are given in Appendix G. The grade of haemolysis was varying between individual slides, which affected the amount of individuals investigated.

Various stages of polychromatic erythrocytes were observed but did not exceed 5 % of the total erythrocyte count. Reticulocytes (erythrocytes with cytoplasmic aggregation of RNA) were detected (<1 - 2 % of erythrocytes) in less than 50 % of the individuals. No hemoparasites were observed. The thrombocytes had a wide range of size and colour intensity between different individuals, from small cells with dense chromatin to larger, round and less dense cells, in contrast to descriptions of "typical" thrombocytes (Clark et al., 2009). Thrombocytes did not aggregate particularly as reported by many other studies (Hernandez and Fores, 1990; Masello et al., 2009). Small amounts of granular lymphocytes were observed in some individuals, which is assessed as "normal" for some bird species (Clark et al., 2009). No clinical difference was observed between the two populations.

3.4.2. PFASs and leukocyte profiles

Figure 3.10 shows the first two dimensions of PCA2, which included primary variables as leukocyte profiles (percentages) and PFASs levels in plasma (n = 19). The first two dimensions describe 58.5 % of the variation (Dim1: 37.9 % and Dim2: 20.6 %). Eigenvalues of PCA2 are given in Table H6 and Figure H4, in Appendix H. PCA2 3rd and 4th dimensions are shown in Figure H3, and values of variation in each dimension (individuals and variables), ctr (contribution to
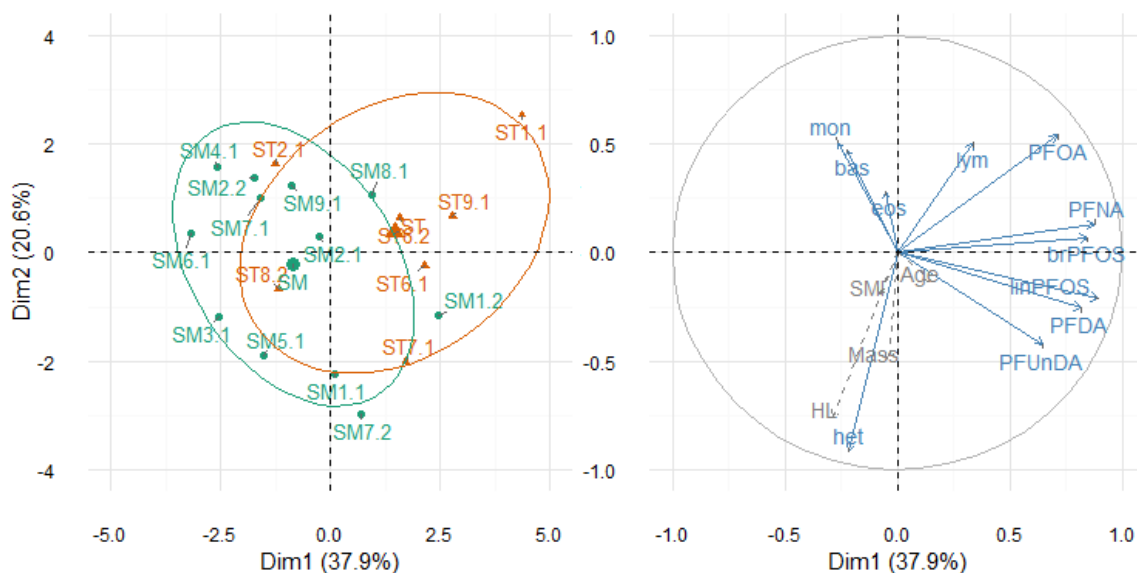
Figure 3.10: Principal Component Analysis of contaminants and leucocyte profiles (PCA2). Dimension 1 explains 37.9 % of the total variation, while dimension 2 explains 20.6 %. Individuals in the score-plot (left) are coloured after population (Steigen/Smøla), while the loading-plot (right) shows contributing variables in blue and supplementary variables in grey. SMI = scaled mass index, HL = heterophil/lymphocyte ratio, het = heterophils, lym = lymphocytes, eos = eosinophils, mon = monocytes and bas = basophils.

dimension) and cos2 (quality of representation) are given in Tables H7 – H10 for the first four dimensions (cumulative variation = 82.9 %).

Dim1 is related to the variation of contaminants (which are already presented). None of the leukocyte fractions shows high correlations with dim1, and therefore seem less associated with the PFAS variables. Heterophils are very well projected in dim2 (cos2: 0.84) with a negative correlation of -0.92. Heterophils are related to H:L ratio and consequently closely projected. Combining the score plot and loading plot, it gives the impression of a possible connection between Smøla and high leukocyte count for monocytes, basophils, and heterophils. But since these variables were best projected in dim2, and population difference is more evident in dim1, it is better to analyse these variables in connection to individuals and not population. By individuals, SM1.1, SM7.2, SM5.1, and SM3.1 have the highest heterophil counts, while ST1.1 has the lowest (Table D3, Appendix D). Note that also leukocytes with lower percentages (monocytes and basophils) had a high contribution to the construction of PCA2. By example, the basophil variable has the highest contribution to the construction of dim2 and second highest for dim4 (Table H8). This is visible in SM4.1, which has the highest basophil count of 1.5 (Table C3, Appendix C: mean between two blood smears).

3.4.3. Factors and leukocyte levels

A significant correlation was found between heterophils and chick mass (r_S = 0.55, p = 0.018) and between eosinophils and SMI (r_S = -0.57, p = 0.013). The relationships were further investigated with binomial generalized linear models (the response variable is expressed as proportions), but also with LMER. These models did not yield any significant effect of SMI on eosinophils, or mass on heterophils. No other significant correlations between leukocyte fractions and factors analysed for (age, mass, and SMI) were detected.

No significant correlations were found between H:L ratio and age, mass or SMI. Since lymphocytes produce immunoglobulins, lymphocytes and the γ-globulin fraction was expected to be related. However, no correlation was found between the two (r_S = 0.08, p = 0.73). The leukocyte proportions were not correlated with ∑PFASs (r_S = -0.21 – 0.24) or any individual PFAS. Through linear mixed effect models and generalized linear models (GLM), it was not found any effect of ∑PFASs on H:L ratio or any of the leukocyte percentages.

4. Discussion

The present study confirms that WTE nestlings are exposed to several PFASs. The results indicate that age, mass and population are important factors affecting levels of PFASs in plasma. Several PFASs were detected in feathers, although an association with plasma concentrations could not be established. Further, the effect of PFASs on parameters of the immune system was investigated. No indications of immunotoxic effect by PFASs were established. The data from this study can be used as reference values for wild WTE nestlings.

4.1. Levels of PFASs in plasma

The pollutant load of PFASs has been shown to be higher than that of other POPs in white-tailed eagles (Bustnes et al., 2013b; Sletten et al., 2016; Sonne et al., 2010). In the present study, the plasma concentrations of PFASs were lower than levels reported by others. By comparison, mean plasma PFOS levels were 2.3 – 2.5 lower than in WTE nestlings in two studies from Troms County. These nestlings were approximately 8 – 11 weeks old (Bustnes et al., 2013b; Sletten et al., 2016). Compared to Bald eagle (*Haliaeetus leucocephalus*) nestlings from parts of the Mississippi river close to Minneapolis, the WTE nestlings in the current study had 28 times lower PFOS levels (Route et al., 2014). In the same study, levels of PFASs in urban and industrialized areas were greatly decreased towards more remote locations. Smøla and Steigen are located relatively remote from larger cities, and local sources are not expected to be the main source of PFASs. However, the levels seen in this study compared to the levels from other studies from Norway were lower than expected.

As shown in PCA1 and PCA2 and by correlations, most of the 7 PFASs analysed were highly related, except PFOA and PFHpS. The low concentrations of PFOA do not correspond with the general trend of PFOA being one of the major PFASs in seawater (Butt et al., 2010), but are in agreement with other studies of PFASs in birds (Leat et al., 2013; Verreault et al., 2005). Verreault et al., (2005) argues that PFOA has a higher depuration and excretion rate, and possibly a lower bioavailability and bioaccumulation potential. This is further supported by Yoo et al., (2009), investigating elimination kinetics of PFOA in white leghorn chicken (*Gallus gallus*), obtaining a depuration half-life of 4.6 days, in contrast to 125 days determined for PFOS. The same logic can be applied to shorter-chained PFCAs like PFBA, PFPA, PFHxA and PFHpA. These were not detected in the present study. Another possible reason for this might also be general low concentrations of these PFCAs (4C-7C) in the environment. Plasma profiles of PFCAs were characterized by high proportions of longer- and odd-numbered carbon chain lengths compounds such as PFNA (9C) and PFUnDA (11C). A study of PFASs in samples from adult Glaucous gulls (*Larus hyperboreus*) from Svalbard and Bear Island (Norway) shows a similar

pattern (Verreault et al., 2005). The authors found high proportions of PFUnDA and PFTrDA, while PFNA was not found to the same extent. In the current study, PFDoDA and PFTrDA were also detected in the majority of plasma samples, but due to a large proportion below LOQ they were omitted from additional statistical analysis. Pharmacokinetic studies have found increasing half-life of PFASs with increasing chain length (Lau et al., 2007; Olsen et al., 2009). Studies have also found large differences in elimination and half-life of PFASs dependent on the species (Olsen et al., 2009, 2007).

Linear PFOS was the predominant compound in plasma, followed by branched PFOS, together making up 71 % of the detected PFASs. Even with the phase-out of PFOS in 2002 and addition to the Stockholm Convention on Persistent Organic Pollutants, PFOS is found consistently as the predominant PFASs in birds of prey (Jaspers et al., 2013; Leat et al., 2013; Sletten et al., 2016). There is no doubt that these actions have greatly reduced the emission of PFOS. However, continued manufacturing of PFOS precursors may result in further accumulation of PFOS (Kelly et al., 2009). The trophic magnification factor (TMF) can be obtained from the slope of the regression between compound concentrations and trophic levels (δ^{15} N) (Borgå et al., 2012). A study investigating compound magnification in an arctic marine food web, found PFOS to exhibit the highest TMF value compared to PFOSA and PFCAs (C7 – C13) (Kelly et al., 2009). In that study, the generally high degree of biomagnification of PFOS was attributed to high dietary absorption, strong partitioning into the organic-phase, a high metabolic resistance, and a high gastrointestinal uptake and slow elimination rate. Absorption, distribution, metabolism and elimination might vary between PFAS compounds and patterns in plasma of WTEs might reflect biomagnification through a complex and long marine food-chain. The current study shows that PFOS still constitute the highest proportion of any PFASs in WTEs, followed by long-chained PFCAs (9-11 C).

4.1.1. Levels of PFASs are associated with age and body weight

It was found that levels of PFASs were affected by both age and mass. The effect of these two variables was however only seen by addressing population- and sex differences in linear mixed models. Within a population, the ∑PFASs plasma concentrations were increasing by 0.45 and 0.69 ng/mL per day, for Smøla and Steigen respectively. In close relation to age, the ∑PFASs increased with 10.9 and 14.4 ng/mL per kg body weight, for females and males respectively, with the Steigen population having a higher baseline contamination. The similar concentrations measured in plasma between the two populations (only brPFOS and PFNA were significantly higher in the Steigen population) can be attributed partly to age and mass differences at the time of sampling. Nestlings from Steigen had significantly lower mass (μ_{ST} = 4.738 kg, μ_{SM} = 5.515 kg, p = 0.01) and age (μ_{ST} = 63.4 days, μ_{SM} = 78.8 days, p < 0.001) compared to

nestlings from Smøla. The difference in sampling time between the two populations was therefore found to affect tests assessing statistical differences and multivariate analyses. Age and mass did not correlate with PFASs in the two PCAs, confounded by the population factor. In the current study the importance to account for variables such as age, mass, sex, and location when analysing environmental exposure to PFASs, is revealed. It is further suggested to do sampling at a similar time after hatching if differences between locations are the objective of the study. This should be of even higher priority when assessing toxicological endpoints in wildlife, as third variables can affect both response and explanatory variables.

4.1.1.1. Differences between populations

According to linear mixed models, nestlings from Steigen have a higher uptake of PFASs than nestlings from Smøla. The nests in Steigen were located out towards the sea, in contrast to the majority of the Smøla nests which were located on the main island or the seaboard (edge of the main island). Thus, the Steigen population is assumed to have a more homogenous diet (fish and seabirds) than the Smøla population (also terrestrial prey). Following the same logic, it is assumed that nestlings from Steigen feed at a higher trophic level compared to Smøla. Unexpectedly, the nests furthest out towards the sea from Smøla, expected to feed at a higher trophic level, had some of the lowest concentrations of ∑PFASs. To further understand differences between the two populations, it is suggested to apply stable isotopes of nitrogen (δ^{15}N) and carbon (δ^{13}N). This would clarify if the differences observed are related to trophic level and type of diet.

The alternative hypothesis would be that the contamination in Steigen is higher than in Smøla. In a previous study, spatial trends in the Baltic Sea, North Sea, and the Norwegian Sea were investigated. PFASs concentrations increased towards industrialized coastal areas, while four sample sites close to the Norwegian coast (outside Bergen - Kristiansand) had relatively low concentrations (0.55 – 1.1 ng/L) (Ahrens et al., 2010). The low concentrations were attributed to a low human population along the Norwegian coastline (Ahrens et al., 2010). Both Steigen- and Smøla county have 2100<2600 inhabitants (SSB, 2016) and are not in close proximity to any larger cities, which makes LRT a more important source of contamination. A broad survey detected 2 times higher ∑PFASs concentrations in cod liver from Ulsteinvik (approximately 155 km south of Smøla) compared to Svolvær (close to Steigen: distance approximately 30 km). However, the levels of PFOS were quite similar (1.1 and 0.7 ng/g, respectively) (Fjeld et al., 2005). This opposes the idea of a higher environmental contamination in Steigen. Without any deeper knowledge of PFASs input from direct/indirect, local/remote sources (atmospheric deposition and oceanic transport) it is difficult to assess the differences between the two

locations. To the knowledge of the author, nothing suggests that Steigen would be more contaminated than Smøla. The Gulf Stream - Norwegian Current is assumed to be the main source of contaminants and flows northward along the Norwegian coastline, passing both locations.

4.1.1.2. Differences between sexes

Both mass and age were analysed through regression, but there is a striking difference between the models obtained. The effect of mass on PFASs levels is different between the sexes, but the effect of age is not. This is probably due to the difference between the two measurements; age is time passed from hatching, while the mass is dependent on sex. However, the model estimates of the effect of age of ∑PFASs might not detect differences between sexes for another reason. The calculation of age was dependent on tail feather length, with the same equation for both sexes. Helander (1981) showed that the wing length was a relatively good measure of age in two populations of WTE nestlings in Sweden, while the estimated equations were dependent on the sexes. In the current study, it was assumed that the tail feather growth was equal between the two sexes. However, it is advised that the currently used age-equation for WTE nestlings should be assessed for possible sex differences.

In the present study, male nestlings were found to accumulate higher levels of PFASs in relation to weight gain. The model estimates should however not be taken out of context. Model 3 (Table 3.3) suggest that males will have 16.2 ng/mL higher levels of ∑PFASs than females at a given mass. However, if a male and female have the same mass, the male would also have had a longer time to accumulate PFASs through the diet. The model estimates should therefore not be taken out of the range they are based upon, which is just above 5 kg for males and 6.5 kg for females measured in the current study. However, the observed plasma concentrations of ∑PFASs were higher for males compared to females within both populations. With a mean higher concentrations of 7.5 ng/mL ($p = 0.23$) and 4.3 ng/mL ($p = 0.53$), in nestlings from Steigen and Smøla, respectively. Further, the regression models (Table 3.3: Model 1 and 3) can also be used to interpret possible sex differences. By using the mean mass of males (μ_{ST} = 4.33 kg, μ_{SM} = 4.83 kg) and the mean mass of females (μ_{SM} = 4.99 kg, μ_{ST} = 6.11 kg) separated by population, the estimated concentrations of ∑PFASs were higher in males compared to females (Smøla: 1.7 − 2.8 ng/mL, Steigen: 7.8 − 8.7 ng/mL), according to the obtained models.

Various studies have investigated/validated sex differences in absorption (Arbuckle, 2006), distribution (Morris et al., 2003) metabolism and elimination (Lau et al., 2007; Lee and Schultz, 2010). In a fish experiment, the plasma elimination half-life of PFOA in female Fathead minnows (*Pimephales promelas*) was 6.3 h while 68.5 h in males (Lee and Schultz, 2010). The literature

on pharmacokinetic differences between sexes in birds is limited, and an alternative explanation is argued for in the current study. Males have a significantly lower mass which would reflect a generally lower volume to distribute contaminants. Hence, males will accumulate higher internal concentrations. This assumes that males and females consume the same amount of food and that the same pharmacokinetic mechanisms apply to both sexes. In the current study, the higher mean PFASs concentrations observed in males within the two populations is therefore suggested to be related to size dimorphism in WTEs, possibly as a consequence of lower compartment volumes in male WTEs. It should be noted that the differences observed in both populations were not statistically significant, and further studies are needed to determine if the observed differences in the current study are in fact a result of sexual dimorphism in WTEs.

4.1.2. Dietary uptake versus maternal transfer

One of the aims of this thesis was related to whether the PFASs analysed in plasma are mainly derived from dietary uptake or from maternal transfer. Since the nestlings were only sampled one time close to the fledgling stage, a conclusive answer may not be obtainable in this study. A study by Bustnes et al., (2013) investigated whether PFOS in WTE nestlings originated through dietary uptake or maternal transfer, investigating the effect of growth dilution. They found a negative relationship between levels of PFOS and growth rate, indicating growth dilution. Further, they found a significant increase in PFOS concentration between first (1-3 weeks after hatching) and second (fledgling stage) sampling, consistent with a high dietary intake (Bustnes et al., 2013b). In contrast, previous reports on Great skua chicks (*Stercorarius skua*) and Great tit (*Parus major*) have found high proportions of maternally transferred compounds (Bourgeon et al., 2013; Dauwe et al., 2006). For some species, this may question the relevance of nestlings as good sentinels for local contamination. In the current study, it is not possible to estimate the effect of growth dilution and elimination on the individual level. A more theoretic approach was chosen, based on literature and data of known ∑PFASs concentrations and weight of eggs. A one-compartment model was made on mean body gain from egg to nestlings and a theoretical half-life of PFASs. Estimates of internal concentrations were calculated on the mean age of the two populations and sexes, giving mean internal concentrations of 1.6 - 2.8 ng/mL ∑PFASs for males (Smøla - Steigen) and 1.1 - 3.1 ng/mL for females (Smøla – Steigen). These constitute 0.9 - 2.7 % of the maternally transferred compounds left after growth dilution and elimination. The effect of growth dilution was found to be the main factor in the decrease of contaminants, with a 10 fold higher rate constant than elimination. The elimination of PFASs is of course very dependent on the compound as discussed earlier. Therefore, the elimination might be more relevant for understanding the PFAS profiles, than for the measured ∑PFASs levels in WTE nestlings. The long elimination half-life of PFOS (Yoo et al., 2009) was chosen as

the half-life of PFASs, justified by its large contribution (90 > x > 70 %) to the total PFASs in eggs previously reported in several bird species (Bustnes et al., 2015; Gebbink and Letcher, 2012; Verreault et al., 2005).

The model predictions are based on several assumptions, and caution should be taken when interpreting the results. It should be kept in mind that the estimates are heavily influenced by initial egg concentrations, and as age decreases the possible error of the estimate increases. It might also be argued that the main effect of growth dilution is likely to happen early in the growth phase (Bustnes et al., 2013b), which is only partly addressed by the model (visualised in Figure 3.5). A further simplification was made assuming a total uptake of PFASs from egg yolk and albumen. Yolk absorption (not concerning contaminant absorption) has previously been found at 75 – 85 % depending on egg size in chickens (Nangsuay et al., 2011).

As hypothesised, the current plasma concentrations in nestlings rely on both maternal transfer and accumulation through diet. It is assumed that some part of the concentration measured is from maternal transfer. The modelled mean internal ∑PFASs concentrations were 4.5 – 10.6 % (Table 3.4) of the plasma concentrations measured in the current study. Note that this is not an estimate of levels resulting from maternal transfer in plasma. The distribution between the theoretic internal compartment and the plasma compartment is not known. However, by theory, the plasma compartment will also be subject to growth dilution and elimination. Hence, the current increase of ∑PFASs with age and mass is a combined effect of output and input. The current results indicate that plasma PFASs levels were related to a high dietary input, while estimates only suggest a minor effect of maternal transfer.

4.2. Levels of PFASs in feathers

Feathers are coupled to the blood circulation in nestlings and are therefore assumed to accumulate contaminants from the start of feather growth until sampling (Burger, 1993). In the current study, ten PFASs were detected in WTE feathers, while nine of these (PFOSA, PFHxS, linPFOS, PFHxA, PFOA, PFNA, PFDcDA, PFDoDA, and PFTrDA) were detected in less than 50 % of the samples (Appendix C, Table C2). PFUnDA was the only PFAS detected (and above LOQ) in more than 50 % of the samples. PFHxS, and linPFOS had the highest concentrations (μ = 2903 pg/g, μ = 891 pg/g), but were only detected in 4 and 5 individuals, respectively. Mean concentrations in PFCAs ranged between 44 – 448 pg/g. Both PFCAs and PFSAs were consistently lower than in plasma (x3 – x15). Interestingly, PFOSA was quantified in 13 feather samples, while not detected in plasma. As feathers are considered metabolically inactive (Burger, 1993), it is possible that internal PFOSA has been metabolized, hence no detectable concentrations in blood. Degradation of PFOSA into PFOS in rat liver has previously been shown

in an *in vitro* study (Xu et al., 2004). If this is the case, the source could be exposure at an earlier time or maternal transfer. PFOSA has previously been detected in herring gull eggs (Gebbink et al., 2009). External contamination is also a possible source. The issue of external contamination of PFASs is not well understood, and a field that needs further attention. As indicated in a study on Barn owl (*Tyto alba*) feathers, PFOA originated possibly from wet and dry deposition, while PFOS was associated with internal concentrations (Jaspers et al., 2013).

PFUnDA levels in feathers were significantly correlated with plasma levels (r_S = 0.50, p = 0.008). This confirms a connection with plasma but does not exclude external sources as preen oil and aerial deposition. The overall low detection rate of PFASs in feathers may oppose the idea of feathers as a valuable monitoring tool for PFASs. At the same time, because of the low detection, the association between internal and feather levels could not be sufficiently investigated. It was previously found that PFOS levels in feather and liver strongly correlated in barn owls living close to a PFAS production site (Jaspers et al., 2013). In that study, the mean feather concentrations were 30 times higher than in the current study. Therefore, the practicality of feathers as a biomonitoring tool might also rely on the contamination level. Plasma levels in this study were also relatively low, and the low contamination level may be limiting the use of feathers to detect and quantify contamination. It should also be kept in mind that the recovery rate in this study was low (45 – 55 %), further reducing the measured concentration in the current feather samples. It is further suggested to be even more rigorous when cutting WTE feathers than described in the current procedure. The barbs of feathers of WTEs are thicker than in most bird species, and should be cut or milled in smaller pieces enhance the extraction. In the present study, it can be argued that feathers could be a valuable asset when determining the presence of PFASs exposure, although not necessarily in relation to internal levels.

4.3. Protein fractions and association with PFASs

The protein fractions analysed in plasma of WTE nestlings were highly comparable to levels in other adult raptors (Tatum et al., 2000). The only exception was prealbumin which was 2.5 – 3.5 times higher than in other eagle species. Prealbumin is a transporter protein of growth hormones (Melillo, 2013), which may be the cause for its high levels in nestlings compared to adult eagles. It was also the most distinctive fraction comparing the two populations, being significantly higher (p = 0.004) in birds from Smøla. The nestlings from Smøla had significantly higher mass, and the prealbumin levels might be connected to this in some way. Prealbumin is also called transthyretin and have a high binding affinity to thyroxine (T_4) and retinol (Melillo, 2013), which is essential for growth. Prealbumin constituted 23 % of the total albumin

(prealbumin + albumin) in WTE nestlings which is comparable with 19.5 % in wild nestlings of peregrine falcons (Lanzarot et al., 2001). However, the variation between species is large, from constituting between 10 – 75 % or being entirely absent (Cray and Tatum, 1998).

Plasma proteins are both involved in immunological (Grasman, 2002) and endocrine functions (Jones et al., 2003). Regarding the importance of these proteins on health and physiological homeostasis, the ability of PFASs to displace hormones through high-affinity binding to plasma proteins is debated (Chen and Guo, 2009; Jones et al., 2003). Previously the potential of PFOS to displace various hormones, including corticosteroids in birds, was investigated (Jones et al., 2003). The displacement of corticosteroid occurred only at high concentrations in bald eagles, with an estimated 10 % effect concentration (EC10) of 160 µg/L PFOS. This is in agreement with the current understanding that albumin works as a binding pool of PFOS (and other PFASs), protecting organisms from adverse toxic effects.

The association between protein fractions and PFASs was tested by PCA, correlation and regression models. Associations were also assessed within the populations. The PFASs and protein fractions were projected in different dimensions of the PCA, suggesting that they were not related. By further statistical analysis, a generally small negative correlation between most PFASs and the different protein fractions was observed. The total protein concentration and brPFOS had a significant negative correlation (r_s = -0.42, p = 0.027). The association was not found by linear regression. PFASs levels, body mass, age and some of the protein fractions were significantly different between the two populations. The problematic relationship between predictor variables is shown through regression models (Figure 3.8 and Tables I1 - I2), suggesting a strong significant effect of mass on prealbumin (p < 0.001) in all the highest ranked models, while both suggesting an effect of population and age on A:G ratio. All these variables are associated with differences between population, while age and mass, and prealbumin and A:G ratio is also strongly correlated. The covariation between predictor variables, response variables and third variables makes it difficult to make interpretations and determine effects, although highly significant associations were found. The relationship between protein fractions and physiological variables should be further investigated so that toxicological studies have a higher chance of controlling for these variables.

Based on current literature, the protein fractions are primarily affected by nutritional and physiological status, or by infections and inflammation, although few studies have assessed the effect of environmental contaminants (Grasman et al., 2000). Even though no significant effects were found of PFASs on protein levels, PFASs are biologically and mechanistically associated with plasma proteins (Bischel et al., 2011; Chen and Guo, 2009). Therefore, the effect of plasma proteins (primarily albumin) on PFASs levels should also be taken into account. The binding of

PFASs to albumin may reduce elimination and therefore increase bioaccumulation (Beesoon and Martin, 2015). In a study investigating the binding affinity between various PFASs and albumin, the fraction of PFOS with concentrations ranging from 0.010 – 0.57 µM bound to 200 µM bovine serum albumin (BSA) was estimated to be 99 ± 0.5 % (Bischel et al., 2011). For comparison, the mean plasma concentrations of PFOS and albumin in nestlings were 0.033 nM and 215.52 µM, respectively, giving a molecular ratio of $1:6.5 \times 10^6$ (PFOS:albumin). If assuming a 1:1 binding stoichiometry between PFOS and albumin as shown in bald eagles (Jones et al., 2003), it would take many times higher concentrations to saturate albumin. This could explain the lack of association between PFAS and albumin (and potentially other protein fractions) in the current study.

4.4. Leukocyte levels

A large effort is made to address leukocyte reference ranges in various avian species. For the first time, to the knowledge of the author, leukocyte levels in WTEs are described. The predominant leukocytes in WTE nestlings were heterophils (38 %), followed by lymphocytes (31 %), eosinophils (16 %), monocytes (3.6 %), and basophils (0.5 %). As expected, our values were closest to nestling Bald eagles when compared to other raptors (Table 3.5), but also similar to Peregrine falcon (*Falco peregrinus*) nestlings and Common buzzard (*Buteo buteo*) adult. No significant differences between populations were found, although the comparison might be statistically biased by the low number of individuals, as well as confounded by factors related to population. Correlation analysis suggested an association between heterophils and mass, and eosinophils and SMI. This was not confirmed by models, and the associations might be by chance.

4.4.1. Leukocyte levels and associations with PFASs

No association between PFASs and leukocyte levels was detected. Current literature on immunomodulation by PFASs in avian species is very limited (DeWitt et al., 2012). Through an *in ovo* exposure study of PFOS in leghorn chickens, significant immunological effects at all treatments (1, 2.5, and 5 mg/kg egg wt) were observed. Specifically, PFOS exposure caused increased spleen mass, increased lysosome activity and suppressed IgM and IgY levels. However, no difference in white blood cell counts was observed (Peden-Adams et al., 2009). For comparison, the lowest treatment is tenfold higher than the mean egg concentrations of ∑PFASs found over the last 20 years in WTE eggs (Nygård et al., 2006). This is also comparable to literature of mammals. In one study, PFASs were shown to cause immunomodulation with an estimated serum LOEL of 91.5 ng/g in mice (Peden-Adams et al., 2008), while alterations in leukocyte levels were not detected. Another study found a significant decrease in the total

number of WBCs, neutrophils and lymphocytes in mice exposed to PFOS and PFOA, while in that study the serum concentrations upon sampling were as high as 340 μg/mL and 152 μg/mL, respectively (Qazi et al., 2009). The present study is therefore in agreement with the current literature. There is little evidence for alterations of leukocyte numbers by PFASs at the current environmental levels. However, this can also be viewed in an alternative way. Leukocyte differential count is a subjective method and bound to a certain variation, and therefore might not be sensitive enough to measure small toxic effects. It is also problematic for reasons explained by Fairbrother et al., (2004): A multitude of factors influence the leukocyte numbers, which makes interpretation difficult. Leukocyte proportions can increase in response to infections, even in the presence of immunosuppression.

4.5. Discussion of protein fractions and leukocyte counts as biomarkers

The protein fractions and leukocyte counts are different structural parameters of the immune system, and the information they provide is often used in combination with other assessments of health and diseases. The two assays are commonly used in veterinary medicine, while rarely applied together in studies of wild birds (Fairbrother et al., 2004). However, the sensitivity and ability of the two biomarkers to detect small immunological effects of contaminants in wildlife has previously been questioned (Fairbrother et al., 2004; Grasman, 2002). A combination of the two biomarkers provides more information, but there is often a need to choose between analyses due to cost efficiency, workload, sensitivity of the biomarker etc. The current study was not designed to assess the suitability of the two biomarkers, but such observations might be useful for choosing which toxicological endpoints to investigate in further studies.

WTEs are protected birds and the use of non-invasive biomarkers is often a prerequisite because of restrictive laws and regulations. The assessment of protein fractions and leukocyte counts only requires a one-time blood sample, which provides important information on health and physiological status. Protein electrophoresis was a fairly quick and relatively cheap assay, while leukocyte counts were the single most time-consuming procedure during the current study.

To investigate the relationship between contaminant exposure and toxicity in wild animals, a high degree of statistical power is needed to counteract the many confounding factors in field studies. Leukocyte counts have previously been found to be relatively insensitive indicators of immune reduction in laboratory rodents, which might be less susceptible to variation related to chemical, nutritional, and environmental stressors, than wild animals (Fairbrother et al., 2004). In addition, leukocyte percentages are also dependent on the quality of blood smears (e.g. shape of the blood layer, amount of lysed cells and staining) and interpretation by the

assessor. Many of the blood smears in the currents study were lost due to quality assurance, mainly nestlings from Steigen, because some of the blood smears were not made immediately after blood sampling. The current study emphasises the importance of using fresh blood to optimize result, and a single interpreter to reduce intra-observer variability. An advantage of conducting manual leukocyte counts is the possibility to detect larger hemoparasites and assessment of cell morphology, during the examination of the blood smears. This might not be achieved otherwise, and provide important information on the current health status of the birds.

The protein fractions are quantified by separating each distinctive band manually based on the electrophoretic pattern (Figure J1), and some of the fractions contain more than one protein. It should also be kept in mind that the biomarker is currently more sensitive for well documented species in veterinary medicine, and for humans. However, further technological advances in protein capillary electrophoresis should increase sensitivity and aid in the identification of specific proteins. Protein capillary electrophoresis also has many characteristics of a good biomarker (e.g. requires a small amount of blood, fast and cheap quantification, sensitive to diseases and inflammation, important for physiological functions, specific and reproducible), and this should facilitate the use of protein fractions in further immunotoxicological avian studies.

5. Conclusion

The present study detected a wide range of PFASs in both plasma and feathers in white-tailed eagle nestlings, confirming their environmental exposure. Plasma concentrations increased significantly with age and mass, consistent with bioaccumulation through dietary uptake. Linear regression also revealed different uptake between the populations, possibly as a result of different trophic levels which should be further investigated. The significant effect of mass on PFASs levels was further dependent on sex. Using a theoretical model, maternal transfer decreased significantly with age, primarily through growth dilution. Elimination of PFOS is believed to be a slow process, but may influence the PFASs composition. Therefore, the levels of PFASs in older nestlings of WTEs reflect primarily local contamination through the diet, confirming their use as sentinel species.

No association was found between PFASs and immunological endpoints. Both protein fractions and leukocyte levels may provide important information on immunological, physiological, and infection status, but may not have sufficient sensitivity to detect small immunological changes in wildlife. Therefore, further studies should establish the relationship between protein fractions, leukocyte counts, and physiological and environmental variables. In the current study, prealbumin was positively associated with mass and also associated with variation between the two populations. Assessment of protein electrophoresis and leukocyte counts both suggested that all the nestlings in the current study were healthy and therefore provides new reference values for these two biomarkers in white-tailed eagle nestlings.

6. References

Abdi, H., 2010. Coefficient of variation. Encylopedia Res. Des. 169–171.

Ahrens, L., Gerwinski, W., Theobald, N., Ebinghaus, R., 2010. Sources of polyfluoroalkyl compounds in the North Sea, Baltic Sea and Norwegian Sea: Evidence from their spatial distribution in surface water. Mar. Pollut. Bull. 60, 255–260.

Andersen, M.E., Butenhoff, J.L., Chang, S.C., Farrar, D.G., Kennedy, G.L., Lau, C., Olsen, G.W., Seed, J., Wallace, K.B., 2008. Perfluoroalkyl acids and related chemistries - Toxicokinetics and modes of action. Toxicol. Sci. 102, 3–14.

Ankley, G.T., Kuehl, D.W., Kahl, M.D., Jensen, K.M., Linnum, A., Leino, R.L., Villeneuve, D.A., 2005. Reproductive and developmental toxicity and bioconcentration of perfluorooctanesulfonate in a partial life-cycle test with the fathead minnow (*Pimephales promelas*). Environ. Toxicol. Chem. 24, 2316–2324.

Arbuckle, T.E., 2006. Are there sex and gender differences in acute exposure to chemicals in the same setting? Environ. Res. 101, 195–204.

Armitage, J.M., Schenker, U., Scheringer, M., Martin, J.W., Macleod, M., Cousins, I.T., 2009. Modeling the Global Fate and Transport of Perfluorooctane Sulfonate (PFOS) and Precursor Compounds in Relation to Temporal Trends in Wildlife Exposure. Environ. Sci. Technol. 43, 9274–9280.

Beesoon, S., Martin, J.W., 2015. Isomer-specific binding affinity of perfluorooctanesulfonate (PFOS) and perfluorooctanoate (PFOA) to serum proteins. Environ. Sci. Technol. 49, 5722–5731.

Besedovsky, H.O., Del Rey, A., 1996. Immune-Neuro-Endocrine Interactions: Facts and Hypotheses. Endocr. Rev. 17, 64–102.

BirdLife International, 2015. *Haliaeetus albicilla. The IUCN Red List of Threatened Species 2015*: e.T22695137A80155303. Available from: http//dx.doi.org/10.2305/IUCN.UK.2015-4.RLTS.T22695137A80155303.en [Cited 26.10.15].

Bischel, H.N., Macmanus-Spencer, L.A., Zhang, C., Luthy, R.G., 2011. Strong associations of short-chain perfluoroalkyl acids with serum albumin and investigation of binding mechanisms. Environ. Toxicol. Chem. 30, 2423–2430.

Black, P.A., McRuer, D.L., Horne, L.-A., 2011. Hematologic parameters in raptor species in a rehabilitation setting before release. J. Avian Med. Surg. 25, 192–198.

Borgå, K., Kidd, K.A., Muir, D.C.G., Berglund, O., Conder, J.M., Gobas, F.A.P.C., Kucklick, J., Malm, O., Powell, D.E., 2012. Trophic magnification factors: Considerations of ecology, ecosystems, and study design. Integr. Environ. Assess. Manag. 8, 64–84.

Bourgeon, S., Leat, E.K.H., Furness, R.W., Borgå, K., Hanssen, S.A., Bustnes, J.O., 2013. Dietary versus maternal sources of organochlorines in top predator seabird chicks: An experimental approach. Environ. Sci. Technol. 47, 5963–5970.

Bowerman, W.W., Stickle, J.E., Sikarskie, J.G., Giesy, J.P., 2000. Hematology and serum chemistries of nestling bald eagles (*Haliaeetus leucocephalus*) in the lower peninsula of MI, USA. Chemosphere 41, 1575–1579.

Brandt, L., Clegg, R.E., Andrews, A., 1951. The effect of age and degree of maturity on the serum proteins of the chicken. J. Biol. Chem. 191, 105–111.

Buck, R.C., Franklin, J., Berger, U., Conder, J.M., Cousins, I.T., de Voogt, P., Jensen, A.A., Kannan, K., Mabury, S.A., van Leeuwen, S.P., 2011. Perfluoroalkyl and polyfluoroalkyl substances in the environment: Terminology, classification, and origins. Integr. Environ. Assess. Manag. 7, 513–541.

Burger, J., 1993. Metals in feathers of brown noddy (*Anous stolidus*): Evidence for bioaccumulation or exposure levels? Environ. Monit. Assess. 24, 181–187.

Bustnes, J.O., Bårdsen, B.J., Bangjord, G., Lierhagen, S., Yoccoz, N.G., 2013a. Temporal trends (1986-2005) of essential and non-essential elements in a terrestrial raptor in northern Europe. Sci. Total Environ. 458-460, 101–106.

Bustnes, J.O., Bårdsen, B.J., Herzke, D., Johnsen, T. V., Eulaers, I., Ballesteros, M., Hanssen, S.A., Covaci, A., Jaspers, V.L.B., Eens, M., Sonne, C., Halley, D., Moum, T., Nøst, T.H., Erikstad, K.E., Ims, R.A., 2013b. Plasma concentrations of organohalogenated pollutants in predatory bird nestlings: Associations to growth rate and dietary tracers. Environ. Toxicol. Chem. 32, 2520–2527.

Bustnes, J.O., Bangjord, G., Ahrens, L., Herzke, D., Yoccoz, N.G., 2015. Perfluoroalkyl substance concentrations in a terrestrial raptor: Relationships to environmental conditions and individual traits. Environ. Toxicol. Chem. 34, 184–191.

Butt, C.M., Berger, U., Bossi, R., Tomy, G.T., 2010. Levels and trends of poly- and perfluorinated compounds in the arctic environment. Sci. Total Environ. 408, 2936–2965.

Campbell, T.W., 1994. Hematology. In: Ritchie, B.W., Harrison, G.J., Harrison, L.R. (Eds.), Avian Medicine: Principles and Applications. Wingers Publishing, Lake Worth, Florida, pp. 176–199.

Chen, J., Zhang, P. yi, Liu, J., 2007. Photodegradation of perfluorooctanoic acid by 185 nm vacuum ultraviolet light. J. Environ. Sci. 19, 387–390.

Chen, Y.M., Guo, L.H., 2009. Fluorescence study on site-specific binding of perfluoroalkyl acids to human serum albumin. Arch. Toxicol. 83, 255–261.

Clark, M.W., Gildersleeve, R.P., Thaxton, J.P., Parkhurst, C.R., McRee, D.I., 1988. Hematological effects of ethyl methanesulfonate, paraquat and phenylhydrazine in Japanese quail. Comp. Biochem. Physiol. 89, 15–30.

Clark, P., Boardman, W., Raidal, S., 2009. Atlas of Clinical Avian Hematology, 1st ed. Wiley-Blackwell, Chichester.

Cray, C., Tatum, L.M., 1998. Applications of Protein Electrophoresis in Avian Diagnostics. J. Avian Med. Surg. 12, 4–10.

Cray, C., Rodriguez, M., Zaias, J., 2007. Protein electrophoresis of psittacine plasma. Vet. Clin. Pathol. 36, 64–72.

Crookes, M., Brooke, D., 2011. Estimation of fish bioconcentration factor (BCF) from depuration data. Environment Agency, Bristol.

Dauwe, T., Jaspers, V.L.B., Covaci, A., Eens, M., 2006. Accumulation of organochlorine and

brominated flame retardants in the eggs and nestlings of great tits (Parus major). Environ. Sci. Technol. 40, 5297–5303.

Davis, A.K., Cook, K.C., Altizer, S., 2004. Leukocyte profiles in wild House Finches with and without mycoplasmal conjunctivitis, a recently emerged bacterial disease. Ecohealth 1, 362–373.

Davis, A.K., Maney, D.L., Maerz, J.C., 2008. The use of leukocyte profiles to measure stress in vertebrates: A review for ecologists. Funct. Ecol. 22, 760–772.

Davison, F., 2014. The Importance of the Avian Immune System and its Unique Features. In: Schat, K.A., Kaspers, B., Kaiser, P. (Eds.), Avian Immunology. Elsevier Ltd, London, pp. 1–11.

Demas, G.E., Nelson, R.R., 2012. Ecoimmunology. Oxford University Press, New York.

DeWitt, J.C., Shnyra, A., Badr, M.Z., Loveless, S.E., Hoban, D., Frame, S.R., Cunard, R., Anderson, S.E., Meade, B.J., Peden-Adams, M.M., Luebke, R.W., Luster, M.I., 2009. Immunotoxicity of perfluorooctanoic acid and perfluorooctane sulfonate and the role of peroxisome proliferator-activated receptor alpha. Crit. Rev. Toxicol. 39, 76–94.

DeWitt, J.C., Peden-Adams, M.M., Keller, J.M., Germolec, D.R., 2012. Immunotoxicity of perfluorinated compounds: recent developments. Toxicol. Pathol. 40, 300–311.

Dinglasan, M.J.A., Ye, Y., Edwards, E.A., Mabury, S.A., 2004. Fluorotelomer alcohol biodegradation yields poly- and perfluorinated acids. Environ. Sci. Technol. 38, 2857–2864.

Douvris, C., Ozerov, O. V, 2008. Hydrodefluorination of perfluoroalkyl groups using silylium-carborane catalysts. Science. 321, 1188–1190.

EPA, 2000. Perfluorooctyl sulfonates; Proposed significant new use rule. Fed. Regist. 65, 62319–62333.

Eulaers, I., Covaci, A., Herzke, D., Eens, M., Sonne, C., Moum, T., Schnug, L., Hanssen, S.A., Johnsen, T.V., Bustnes, J.O., Jaspers, V.L.B., 2011a. A first evaluation of the usefulness of feathers of nestling predatory birds for non-destructive biomonitoring of persistent organic pollutants. Environ. Int. 37, 622–630.

Eulaers, I., Covaci, A., Hofman, J., Nygård, T., Halley, D.J., Pinxten, R., Eens, M., Jaspers, V.L.B., 2011b. A comparison of non-destructive sampling strategies to assess the exposure of white-tailed eagle nestlings (*Haliaeetus albicilla*) to persistent organic pollutants. Sci. Total Environ. 410-411, 258–265.

Eulaers, I., Jaspers, V.L.B., Halley, D.J., Lepoint, G., Nygård, T., Pinxten, R., Covaci, A., Eens, M., 2014. Brominated and phosphorus flame retardants in White-tailed Eagle *Haliaeetus albicilla* nestlings: Bioaccumulation and associations with dietary proxies (δ13C, δ15N and δ34S). Sci. Total Environ. 478, 48–57.

Fairbrother, A., Fowles, J., 1990. Subchronic effects of sodium selenite and selenomethionine on several immune-functions in mallards. Arch. Environ. Contam. Toxicol. 19, 836–844.

Fairbrother, A., Smits, J., Grasman, K.A., 2004. Avian Immunotoxicology. J. Toxicol. Environ. Heal. Part B 7, 105–137.

Fjeld, E., Schlabach, M., Berge, J.A., Green, N., Eggen, T., Snilsberg, P., Vogelsang, C., Rognerud, S., Kjellberg, G., Enge, E.K., Dye, C.A., Gundersen, H., 2005. Screening of selected new organic contaminants 2004. Brominated flame retardants, perfluorinated alkylated substances, irgarol, diuron, BHT and dicofol, Norwegian Institute for Water Research, Report TA-2096/2005. Oslo.

Folkestad, A.O., 1994. Havørn *Haliaeetus albicilla*. In: Gjershaug, J.O., Thingstad, P.G., Eldøy, S., Byrkjeland, S. (Eds.), Norsk Fugleatlas. Norsk Ornitologisk Forening, Klæbu, pp. 110–111.

Gebbink, W.A., Hebert, C.E., Letcher, R.J., 2009. Perfluorinated carboxylates and sulfonates and precursor compounds in herring gull eggs from colonies spanning the Laurentian Great Lakes of North America. Environ. Sci. Technol. 43, 7443–7449.

Gebbink, W.A., Letcher, R.J., 2012. Comparative tissue and body compartment accumulation and maternal transfer to eggs of perfluoroalkyl sulfonates and carboxylates in Great Lakes herring gulls. Environ. Pollut. 162, 40–47.

Giesy, J.P., Kannan, K., Jones, P.D., 2001. Global biomonitoring of perfluorinated organics. Sci. World J. 1, 627–629.

Giesy, J.P., Kannan, K., 2002. Perfluorochemical surfactants in the environment. Environ. Sci. Technol. 36, 146–152.

Gjershaug, J.O., Kålås, J.A., Nygård, T., Herzke, D., Folkestad, A.O., 2008. Monitoring of raptors and their contamination levels in Norway. Ambio A J. Hum. Environ. 37, 420–4.

Grasman, K.A., Fox, G.A., Scanlon, P.F., Ludwig, J.P., 1996. Organochlorine-associated immunosuppression in prefledgling Caspian terns and Herring gulls from the Great Lakes: An ecoepidemiological study. Environ. Health Perspect. 104, 829–842.

Grasman, K.A., Armstrong, M., Hammersley, D.L., Scanlon, P.F., Fox, G.A., 2000. Geographic variation in blood plasma protein concentrations of young herring gulls (*Larus argentatus*) and Caspian terns (*Sterna caspia*) from the Great Lakes and Lake Winnipeg. Comp. Biochem. Physiol. - C Toxicol. Pharmacol. 125, 365–375.

Grasman, K.A., 2002. Assessing immunological function in toxicological studies of avian wildlife. Integr. Comp. Biol. 42, 34–42.

Hailer, F., Helander, B., Folkestad, A.O., Ganusevich, S. a, Garstad, S., Hauff, P., Koren, C., Nygård, T., Volke, V., Vilà, C., Ellegren, H., 2006. Bottlenecked but long-lived: high genetic diversity retained in white-tailed eagles upon recovery from population decline. Biol. Lett. 2, 316–319.

Hanssen, S.A., Bustnes, J.O., Schnug, L., Bourgeon, S., Johnsen, T.V., Ballesteros, M., Sonne, C., Herzke, D., Eulaers, I., Jaspers, V.L.B., Covaci, A., Eens, M., Halley, D.J., Moum, T., Ims, R.A., Erikstad, K.E., 2013. Antiparasite treatments reduce humoral immunity and impact oxidative status in raptor nestlings. Ecol. Evol. 3, 5157–5166.

Harmon, B.G., 1998. Avian heterophils in inflammation and disease resistance. Poult. Sci. 77, 972–977.

Haukås, M., Berger, U., Hop, H., Gulliksen, B., Gabrielsen, G.W., 2007. Bioaccumulation of per- and polyfluorinated alkyl substances (PFAS) in selected species from the Barents Sea food web. Environ. Pollut. 148, 360–371.

Helander, B., 1981. Nestling measurements and weights from two White-tailed Eagle populations in Sweden. Bird Study 28, 235–241.

Helander, B., Bignert, A., Asplund, L., 2008. Using raptors as environmental sentinels: monitoring the white-tailed sea eagle *Haliaeetus albicilla* in Sweden. Ambio 37, 425–431.

Hernandez, M., Fores, P., 1990. Clinical hematology and blood chemistry values for the buzzard (*Buteo buteo*). J. Raptor Res. 24, 113–119.

Herzke, D., Nygård, T., Berger, U., Huber, S., Røv, N., 2009. Perfluorinated and other persistent halogenated organic compounds in European shag (*Phalacrocorax aristotelis*) and common eider (*Somateria mollissima*) from Norway: A suburban to remote pollutant gradient. Sci. Total Environ. 408, 340–348.

Herzke, D., Olsson, E., Posner, S., 2012. Perfluoroalkyl and polyfluoroalkyl substances (PFASs) in consumer products in Norway - a pilot study. Chemosphere 88, 980–7.

Hurlbert, S., 1984. Pseudoreplication and the design of ecological field experiments. Ecol. Monogr. 54, 187–211.

Jaspers, V.L.B., Oorspoels, S., Covaci, A., Eens, M., 2006. Can predatory bird feathers be used as a non-destructive biomonitoring tool of organic pollutants? Biol. Lett. 2, 283–285.

Jaspers, V.L.B., Covaci, A., Deleu, P., Neels, H., Eens, M., 2008. Preen oil as the main source of external contamination with organic pollutants onto feathers of the common magpie (Pica pica). Environ. Int. 34, 741–748.

Jaspers, V.L.B., Rodriguez, F.S., Boertmann, D., Sonne, C., Dietz, R., Rasmussen, L.M., Eens, M., Covaci, A., 2011. Body feathers as a potential new biomonitoring tool in raptors: A study on organohalogenated contaminants in different feather types and preen oil of West Greenland White-tailed eagles (*Haliaeetus albicilla*). Environ. Int. 37, 1349–1356.

Jaspers, V.L.B., Herzke, D., Eulaers, I., Gillespie, B.W., Eens, M., 2013. Perfluoroalkyl substances in soft tissues and tail feathers of Belgian barn owls (*Tyto alba*) using statistical methods for left-censored data to handle non-detects. Environ. Int. 52, 9–16.

Jones, M.P., Arheart, K.L., Cray, C., 2014. Reference intervals, longitudinal analyses, and index of individuality of commonly measured laboratory variables in captive Bald eagles (*Haliaeetus leucocephalus*). J. Avian Med. Surg. 28, 118–126.

Jones, P.D., Hu, W., De Coen, W., Newsted, J.L., Giesy, J.P., 2003. Binding of perfluorinated fatty acids to serum proteins. Environ. Toxicol. Chem. 22, 2639–2649.

Juul-Madsen, H.R., Viertlböeck, B., Härtle, S., Smith, A.L., Göbel, T.W., 2014. Innate immune responses. In: Davison, F., Kaspers, B., Schat, K.A. (Eds.), Avian Immunology. Elsevier Ltd, pp. 121–147.

Kannan, K., Tao, L., Sinclair, E., Pastva, S.D., Jude, D.J., Giesy, J.P., 2005. Perfluorinated compounds in aquatic organisms at various trophic levels in a Great Lakes food chain. Arch. Environ. Contam. Toxicol. 48, 559–566.

Kaspers, B., Kaiser, P., 2014. Avian antigen-presenting cells. In: Davison, F., Kaspers, B., Schat, K.A. (Eds.), Avian Immunology. Elsevier Ltd, pp. 169–188.

Kato, H., Fujii, S., Takahashi, M., Matsumoto, M., Hirata-Koizumi, M., Ono, A., Hirose, A., 2014.

Repeated dose and reproductive/developmental toxicity of perflurododecanoic acid in Rats. Environ. Toxicol. 30, 1244–1263.

Kelly, B.C., Ikonomou, M.G., Blair, J.D., Surridge, B., Hoover, D., Grace, R., Gobas, F.A.P.C., 2009. Perfluoroalkyl contaminants in an arctic marine food web: Trophic magnification and wildlife exposure. Environ. Sci. Technol. 43, 4037–4043.

Kennedy, G.L., Butenhoff, J.L., Olsen, G.W., O'Connor, J.C., Seacat, A.M., Perkins, R.G., Biegel, L.B., Murphy, S.R., Farrar, D.G., 2004. The toxicology of perfluorooctanoate. Crit. Rev. Toxicol. 34, 351–384.

Key, B.D., Howell, R.D., Criddle, C.S., 1998. Defluorination of organofluorine sulfur compounds by *Pseudomonas sp.* strain D2. Environ. Sci. Technol. 32, 2283–2287.

Koutsos, E.A., Klasing, K.C., 2014. Factors modulating the avian immune system. In: Davison, F., Kaspers, B., Schat, K.A. (Eds.), Avian Immunology. Elsevier Ltd, London, pp. 323–338.

Kudo, N., Bandai, N., Suzuki, E., Katakura, M., Kawashima, Y., 2000. Induction of triglyceride accumulation in the liver of rats by perfluorinated fatty acids with different carbon chain lengths: comparison with induction of peroxisomal beta-oxidation. Chem. Biol. Interact. 124, 119–132.

Lanzarot, M.P., Montesinos, A., San Andrés, M.I., Rodríguez, C., Barahona, M.V., 2001. Hematological, protein electrophoresis and cholinesterase values of free-living nestling Peregrine falcons in Spain. J. Wildl. Dis. 37, 172–177.

Lau, C., Thibodeaux, J.R., Hanson, R.G., Rogers, J.M., Grey, B.E., Stanton, M.E., Buttenhoff, J.L., Stevenson, L.A., 2003. Exposure to perfluorooctane sulfonate during pregnancy in rat and mouse. II: Postnatal evaluation. Toxicol. Sci. 74, 382–392.

Lau, C., Anitole, K., Hodes, C., Lai, D., Pfhales-Hutchens, A., Seed, J., 2007. Perfluoroalkyl acids: A review of monitoring and toxicological findings. Toxicol. Sci. 99, 366–394.

Lau, C., 2012. Perfluorinated compounds. In: Luch, A. (Ed.), Molecular, Clinical and Environmental Toxycology. Springer, London, pp. 47–86.

Leat, E.H.K., Bourgeon, S., Eze, J.I., Muir, D.C.G., Williamson, M., Bustnes, J.O., Furness, R.W., Borgå, K., 2013. Perfluoroalkyl substances in eggs and plasma of an avian top predator, great skua (*Stercorarius skua*), in the north Atlantic. Environ. Toxicol. Chem. 32, 569–576.

Lee, J.J., Schultz, I.R., 2010. Sex differences in the uptake and disposition of perfluorooctanoic acid in Fathead minnows after oral dosing. Environ. Sci. Technol. 44, 491–496.

Leppert, L.L., Layman, S., Bragin, E.A., Katzner, T., 2004. Survey for hemoparasites in imperial eagles (*Aquila heliaca*), steppe eagles (*Aquila nipalensis*), and white-tailed sea eagles (*Haliaeetus albicilla*) from Kazakhstan. J. Wildl. Dis. 40, 316–319.

Loi, E.I.H., Yeung, L.W.Y., Taniyasu, S., Lam, P.K.S., Kannan, K., Yamashita, N., 2011. Trophic magnification of poly- and perfluorinated compounds in a subtropical food web. Environ. Sci. Technol. 45, 5506–5513.

Löfstrand, K., Jörundsdóttir, H., Tomy, G., Svavarsson, J., Weihe, P., Nygård, T., Bergman, Å., 2008. Spatial trends of polyfluorinated compounds in guillemot (*Uria aalge*) eggs from North-Western Europe. Chemosphere 72, 1475–1480.

Masello, J.F., Choconi, R.G., Helmer, M., Kremberg, T., Lubjuhn, T., Quillfeldt, P., 2009. Do leucocytes reflect condition in nestling burrowing parrots *Cyanoliseus patagonus* in the wild? Comp. Biochem. Physiol. Part A Mol. Integr. Physiol. 152, 176–181.

Melillo, A., 2013. Applications of serum protein electrophoresis in exotic pet medicine. Vet. Clin. North Am. - Exot. Anim. Pract. 16, 211–225.

Miller, G.A., Chapman, J.P., 2001. Misunderstanding analysis of covariance. J. Abnorm. Psychol. 110, 40–48.

Millet, S., Bennett, J., Lee, K.A., Hau, M., Klasing, K.C., 2007. Quantifying and comparing constitutive immunity across avian species. Dev. Comp. Immunol. 31, 188–201.

Morris, M.E., Lee, H.J., Predko, L.M., 2003. Gender differences in the membrane transport of endogenous and exogenous compounds. Pharmacol. Rev. 55, 229–240.

Nangsuay, A., Ruangpanit, Y., Meijerhof, R., Attamangkune, S., 2011. Yolk absorption and embryo development of small and large eggs originating from young and old breeder hens. Poult. Sci. 90, 2648–2655.

Newsted, J.L., Jones, P.D., Coady, K., Giesy, J.P., 2005. Avian toxicity reference values for perfluorooctane sulfonate. Environ. Sci. Technol. 39, 9357–9362.

Nygård, T., Herzke, D., Polder, A., 2006. Miljøgifter i rovfuglegg i Norge. *NINA Rapport 213*. 42 pp. Trondheim.

O'Rourke, E., 2014. The reintroduction of the white-tailed sea eagle to Ireland: People and wildlife. Land use policy 38, 129–137.

Olsen, G.W., Burris, J.M., Ehresman, D.J., Froelich, J.W., Seacat, A.M., Butenhoff, J.L., Zobel, L.R., 2007. Half-life of serum elimination of perfluorooctanesulfonate, perfluorohexanesulfonate, and perfluorooctanoate in retired fluorochemical production workers. Environ. Health Perspect. 115, 1298–1305.

Olsen, G.W., Chang, S.C., Noker, P.E., Gorman, G.S., Ehresman, D.J., Lieder, P.H., Butenhoff, J.L., 2009. A comparison of the pharmacokinetics of perfluorobutanesulfonate (PFBS) in rats, monkeys, and humans. Toxicology 256, 65–74.

Olsen, S.F., 2007. Rovfugler og ugler i Nord-Europa. Wigestrand Forlag, Stavanger.

Ots, I., Murumägi, A., Hõrak, P., 1998. Haematological health state indices of reproducing Great Tits: methodology and sources of natural variation. Funct. Ecol. 12, 700–707.

Paul, A.G., Jones, K.C., Sweetman, A.J., 2009. A first global production, emission, and environmental inventory for perfluorooctane sulfonate. Environ. Sci. Technol. 43, 386–392.

Peden-Adams, M.M., Keller, J.M., Eudaly, J.G., Berger, J., Gilkeson, G.S., Keil, D.E., 2008. Suppression of humoral immunity in mice following exposure to perfluorooctane sulfonate. Toxicol. Sci. 104, 144–154.

Peden-Adams, M.M., Stuckey, J.E., Gaworecki, K.M., Berger-Ritchie, J., Bryant, K., Jodice, P.G., Scott, T.R., Ferrario, J.B., Guan, B., Vigo, C., Boone, J.S., McGuinn, W.D., DeWitt, J.C., Keil, D.E., 2009. Developmental toxicity in white leghorn chickens following in ovo exposure to perfluorooctane sulfonate (PFOS). Reprod. Toxicol. 27, 307–318.

Peig, J., Green, A.J., 2009. New perspectives for estimating body condition from mass/length data: The scaled mass index as an alternative method. Oikos 118, 1883–1891.

Pfaff, J.A., Zanette, L., MacDougall-Shackleton, S.A., MacDougall-Shackleton, E.A., 2007. Song repertoire size varies with HVC volume and is indicative of male quality in song sparrows (*Melospiza melodia*). Proc. R. Soc. London B Biol. Sci. 274, 2035–2040.

Powley, C.R., George, S.W., Ryan, T.W., Buck, R.C., 2005. Matrix effect-free analytical methods for determination of perfluorinated carboxylic acids in environmental matrixes. Anal. Chem. 77, 6353–6358.

Prevedouros, K., Cousins, I.T., Buck, R.C., Korzeniowski, S.H., 2006. Sources, fate and transport of perfluorocarboxylates. Environ. Sci. Technol. 40, 32–44.

Qazi, M.R., Bogdanska, J., Butenhoff, J.L., Nelson, B.D., DePierre, J.W., Abedi-Valugerdi, M., 2009. High-dose, short-term exposure of mice to perfluorooctanesulfonate (PFOS) or perfluorooctanoate (PFOA) affects the number of circulating neutrophils differently, but enhances the inflammatory responses of macrophages to lipopolysaccharide (LPS) in a simil. Toxicology 262, 207–214.

Roberts, M.S., Magnusson, B.M., Burczynski, F.J., Weiss, M., 2002. Enterohepatic circulation: physiological, pharmacokinetic and clinical implications. Clin. Pharmacokinet. 41, 751–790.

Route, W.T., Russell, R.E., Lindstrom, A.B., Strynar, M.J., Key, R.L., 2014. Spatial and temporal patterns in concentrations of perfluorinated compounds in bald eagle nestlings in the upper midwestern United States. Environ. Sci. Technol. 48, 6653–6660.

Seacat, A.M., Thomford, P.J., Hansen, K.J., Clemen, L.A., Eldridge, S.R., Elcombe, C.R., Butenhoff, J.L., 2003. Sub-chronic dietary toxicity of potassium perfluorooctanesulfonate in rats. Toxicology 183, 117–131.

Sletten, S., Bourgeon, S., Bårdsen, B.J., Herzke, D., Criscuolo, F., Massemin, S., Zahn, S., Johnsen, T.V., Bustnes, J.O., 2016. Organohalogenated contaminants in white-tailed eagle (*Haliaeetus albicilla*) nestlings: An assessment of relationships to immunoglobulin levels, telomeres and oxidative stress. Sci. Total Environ. 539, 337–349.

Sonne, C., Bustnes, J.O., Herzke, D., Jaspers, V.L.B., Covaci, A., Halley, D.J., Moum, T., Eulaers, I., Eens, M., Ims, R.A., Hanssen, S.A., Einar Erikstad, K., Johnsen, T., Schnug, L., Rigét, F.F., Jensen, A.L., 2010. Relationships between organohalogen contaminants and blood plasma clinical-chemical parameters in chicks of three raptor species from Northern Norway. Ecotoxicol. Environ. Saf. 73, 7–17.

SSB, 2016. *Population and population changes, Q2 2016.* Statistisk sentralbyrå (SSB) [Online]. Available from https//www.ssb.no/en/befolkning/statistikker/folkemengde/kvartal/2016-08-18 [Cited 19.08.2016].

Stock, N.L., Furdui, V.I., Muir, D.C.G., Mabury, S.A., 2007. Perfluoroalkyl contaminants in the Canadian arctic: Evidence of atmospheric transport and local contamination. Environ. Sci. Technol. 41, 3529–3536.

Tatum, L.M., Zaias, J., Mealey, B.K., Cray, C., Bossart, G.D., 2000. Protein Electrophoresis As a Diagnostic and Prognostic Tool in Raptor Medicine. J. Zoo Wildl. Med. 31, 497–502.

Teh, C., Le, Y., Lee, S.H., Lu, J., 2000. M-ficolin is expressed on monocytes and is a lectin binding to N-acetyl- D -glucosamine and mediates monocyte adhesion and phagocytosis of *Escherichia coli*. Immunology 101, 225–232.

Thibodeaux, J.R., Hanson, R.G., Rogers, J.M., Grey, B.E., Barbee, B.D., Richards, J.H., Butenhoff, J.L., Stevenson, L.A., Lau, C.A., 2003. Exposure to perfluorooctane sulfonate during pregnancy in rat and mouse. I: Maternal and prenatal evaluations. Toxicol. Sci. 74, 369–381.

Tomy, G.T., Budakowski, W., Halldorson, T., Helm, P.A., Stern, G.A., Friesen, K., Pepper, K., Tittlemier, S.A., Fisk, A.T., 2004. Fluorinated organic compounds in an eastern Arctic marine food web. Environ. Sci. Technol. 38, 6475–6481.

UNEP, 2009. *Governments unite to step-up reduction on global DDT reliance and add nine new chemicals under international treaty.* United Nations Environment Programme (UNEP) [Online]. Available from: http//chm.pops.int/Convention/Pressrelease/COP4Geneva8May2009/tabid/542/language/en-US/Default.aspx [Cited 01.03.2016].

Verreault, J., Houde, M., Gabrielsen, G.W., Berger, U., Haukås, M., Letcher, R.J., Muir, D.C.G., 2005. Perfluorinated alkyl substances in plasma, liver, brain, and eggs of glaucous gulls (*Larus hyperboreus*) from the Norwegian Arctic. Environ. Sci. Technol. 39, 7439–7445.

Weber, T.P., Stilianakis, N.I., 2007. Ecologic immunology of avian influenza (H5N1) in migratory birds. Emerg. Infect. Dis. 13, 1139–1143.

Xu, L., Krenitsky, D.M., Seacat, A.M., Butenhoff, J.L., Anders, M.W., 2004. Biotransformation of N-Ethyl-N-(2-hydroxyethyl)perfluorooctanesulfonamide by rat liver microsomes, cytosol, and slices and by expressed rat and human cytochromes P450. Chem. Res. Toxicol. 17, 767–775.

Yamashita, N., Kannan, K., Taniyasu, S., Horii, Y., Petrick, G., Gamo, T., 2005. A global survey of perfluorinated acids in oceans. Mar. Pollut. Bull. 51, 658–668.

Yamashita, N., Taniyasu, S., Petrick, G., Wei, S., Gamo, T., Lam, P.K.S., Kannan, K., 2008. Perfluorinated acids as novel chemical tracers of global circulation of ocean waters. Chemosphere 70, 1247–1255.

Yang, Q., Xie, Y., Eriksson, A.M., Nelson, B.D., DePierre, J.W., 2001. Further evidence for the involvement of inhibition of cell proliferation and development in thymic and splenic atrophy induced by the peroxisome proliferator perfluoroctanoic acid in mice. Biochem. Pharmacol. 62, 1133–1140.

Yoo, H., Guruge, K.S., Yamanaka, N., Sato, C., Mikami, O., Miyazaki, S., Yamashita, N., Giesy, J.P., 2009. Depuration kinetics and tissue disposition of PFOA and PFOS in white leghorn chickens (*Gallus gallus*) administered by subcutaneous implantation. Ecotoxicol. Environ. Saf. 72, 26–36.

Appendices

Appendix A

Model selection predicting ∑PFASs in plasma of WTE nestlings

Table 3.2

Model selection including all models predicting variation in plasma levels of ∑PFASs (ng/mL) in relation to mass (kg), age (days), SMI, sex and population (Pop). Model selection was done according to AICc. The models were made from 19 nests and 26 (for mass and SMI) or 27 WTE nestlings.

		Models (n = 17)		Model selection		
ID	Response	Predictor	AICc	ΔAICc	AICc WT	Individuals
1	∑PFAS	~ Mass:Sex[a] + Pop	197.03	0.00	0.27	26
2	∑PFAS	~ Age:Pop[a]	197.78	0.75	0.19	27
3	∑PFAS	~ Mass + Sex + Pop	198.07	1.04	0.16	26
4	∑PFAS	~ Age + Pop	198.92	1.89	0.11	27
5	∑PFAS	~ Mass:Pop[a] + Pop + Sex	199.79	2.76	0.07	26
6	∑PFAS	~ Mass*Sex[b] + Pop	200.53	3.49	0.05	26
7	∑PFAS	~ Age:Pop[a] + Pop	200.77	3.74	0.04	27
8	∑PFAS	~ Age + Sex + Pop	201.38	4.35	0.03	26
9	∑PFAS	~ SMI + Pop	202.64	5.61	0.02	26
10	∑PFAS	~ SMI	203.61	6.58	0.01	26
11	∑PFAS	~ Mass + Pop	204.15	7.12	0.01	26
12	∑PFAS	~ Mass	205.17	8.14	0	26
13	∑PFAS	~ Mass:Sex[a]	206.56	9.52	0	26
14	∑PFAS	~ Mass + Sex	206.81	9.77	0	26
15	∑PFAS	~ 1 (null model)	209.36	12.33	0	27

Pop = population (Steigen and Smøla), SMI = Scaled mass index
a Interaction, estimating different slopes dependent on variables (age and mass) and factors (sex and population)
b Interaction and additive effect: Mass:Sex + Sex + Mass
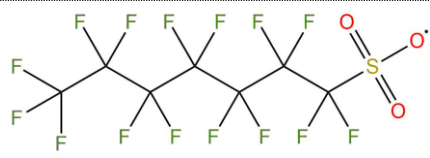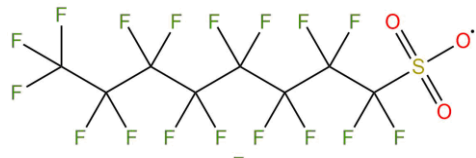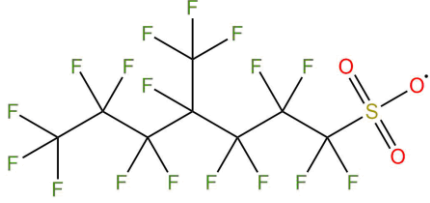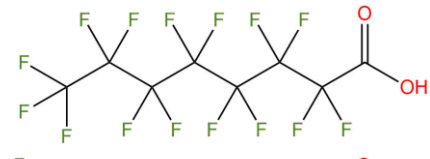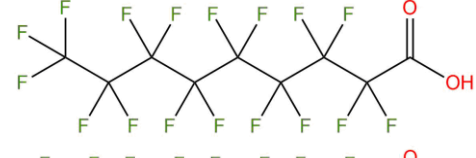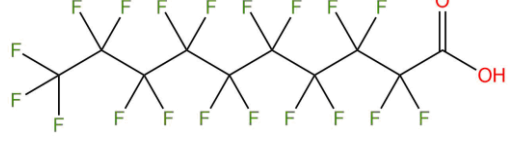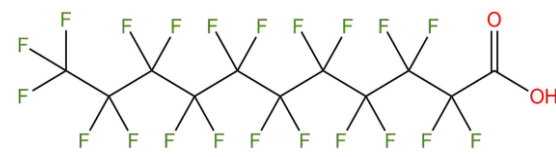
Appendix B

Perfluoroalkyl substances (PFASs), nomenclature and classification

Table B1.
Chemical structure and name of compounds quantified in over 50% of the plasma samples.

Structure	Compound name
Perfluoroalkyl sulfonates (PFSAs)	
	Perfluoroheptane sulfonate PFHpS
	Perfluorooctane sulfonate Linear PFOS/ PFOS linPFOS
	Perfluorooctane sulfonate Branched isomer brPFOS
Perfluoroalkyl carboxylic acids (PFCAs)	
	Perfluorooctanoic acid PFOA
	Perfluorononanoic acid PFNA
	Perfluorodecanoic acid PFDA
	Perfluoroundecanoic acid PFUnDA

Appendix C

Detection and quantification of PFASs in plasma and feather samples

Table C1:
Limit of detection (LOD), Limit of quantification (LOQ), samples (n) above LOD and LOQ, arithmetic mean (AM) and range of PFASs concentrations (ng/mL) in plasma samples of WTE nestlings from Smøla and Steigen. LOD was quantified as 3 times the signal/noise. LOQ was calculated as 3 times LOD. Concentration is calculated on samples above LOQ, thus slightly different from PFAS concentrations used in statistical analysis.

| Compounds | Plasma samples | | Concentrations (ng/mL)[a] | | Detected (n) | | LOD | LOQ |
	n>LOD	n>LOQ	AM	Range	Steigen	Smøla	(ng/mL)	(ng/mL)
PFOSA	0	0	-	-	-	-	23.35	70.05
PFBS	0	0	-	-	-	-	169.11	507.32
PFHxS	5	5	1.27	0.90-1.79	X (3)	X (2)	0.10	0.30
PFHpS	15	14	0.14	0.05-0.31	X (8)	X (7)	0.01	0.03
brPFOS	27	26	4.08	1.30-11.70	X (14)	X (13)	0.20	0.60
linPFOS	27	27	16.59	6.04-31.85	X (14)	X (13)	0.20	0.60
PFDcS	0	0	-	-	-	-	4.20	12.61
PFBA	0	0	-	-	-	-	169.11	507.32
PFPA	0	0	-	-	-	-	1.31	3.93
PFHxA	0	0	-	-	-	-	1.31	3.93
PFHpA	0	0	-	-	-	-	1.31	3.93
PFOA	25	19	0.56	0.31-1.27	X (13)	X (12)	0.10	0.30
PFNA	27	27	2.99	0.57-6.48	X (14)	X (13)	0.10	0.30
PFDcDA	27	27	1.36	0.66-2.52	X (14)	X (13)	0.10	0.30
PFUnDA	27	27	3.53	2.30-5.08	X (14)	X (13)	0.20	0.60
PFDoDA	25	6	0.79	0.65-0.94	X (14)	X (11)	0.20	0.60
PFTrDA	19	13	0.99	0.70-1.47	X (10)	X (9)	0.20	0.60
PFTeDA	0	0	-	-	-	-	0.20	0.60

a Calculations of concentrations above LOQ.

Table C2:
Limit of detection (LOD), Limit of quantification (LOQ), samples (n) above LOD and LOQ, arithmetic mean (AM) and range of PFASs concentrations (pg/g) in feather samples of WTE nestlings from Smøla and Steigen. LOD was quantified as 3 times the signal/noise. LOQ was calculated as 3 times LOD.

Compounds	Feather samples		Concentrations (pg/g)[a]		Detected in (n)		LOD	LOQ
	n>LOD	n>LOQ	AM	Range	Steigen	Smøla	(pg/g)	(pg/g)
6:2FTS	0	0	-	-	-	-	30.0	90.0
PFNS	0	0	-	-	-	-	30.0	90.0
PFOSA[b]	13	13	577.9	234.7 - 1109.8	X (7)	X (6)	28.6	85.9
PFBS	0	0	-	-	-	-	497.8	1493.3
PFPS	0	0	-	-	-	-	1.7	5.1
PFHxS[c]	4	4	2903.2	617.8 - 5168.7	X (4)	-	1.7	5.1
PFHpS	0	0	-	-	-	-	1.7	5.1
brPFOS	0	0	-	-	-	-	28.6	85.9
linPFOS[b]	5	5	891.2	222.3 - 1824.4	X (4)	X (1)	28.6	85.9
PFDcS	0	0	-	-	-	-	28.6	85.9
PFBA	0	0	-	-	-	-	497.8	1493.3
PFPA	0	0	-	-	-	-	200.0	600.0
PFHxA[b]	3	3	44.0	17.2 - 73.7	X (3)	-	1.7	5.1
PFHpA	0	0	-	-	-	-	1.7	5.1
PFOA	1	1	105.4	105.4 - 105.4	X (1)	-	28.6	85.9
PFNA	3	2	230.7	178.1 - 283.3	X (3)	-	28.6	85.9
PFDcDA	1	0	68.2	68.2 - 68.2	-	X (1)	28.6	85.9
PFUnDA[b]	19	16	448.9	89.3 - 602.2	X (9)	X (10)	28.6	85.9
PFDoDA	6	5	130.3	105.5 - 197.6	X (3)	X (3)	28.6	85.9
PFTrDA[b]	11	11	297.7	107.6 - 455.7	X (4)	X (4)	28.6	85.9
PFTeDA	0	0	-	-	-	-	28.6	85.9

a Calculations of concentrations above LOQ.
b AM of quantified concentrations more than 10 times above LOD.
c AM of detected concentrations more than 1000 times above LOD.

Table C3:

Mean percentage recovery for plasma and feather samples of WTE nestlings (n = 27)

Compound	Plasma Mean (%)	Feather Mean (%)
PFBA	88.6	54.8
PFPA	96.6	52.9
PFHxA	89.7	51.2
PFOA	89.0	49.3
PFNA	99.1	48.5
PFDA	78.1	50.7
PFUnDA	68.0	47.7
PFDoDA	56.2	49.2
PFHxS	86.1	49.0
PFOS	80.0	47.3
PFOSA	81.1	48.2
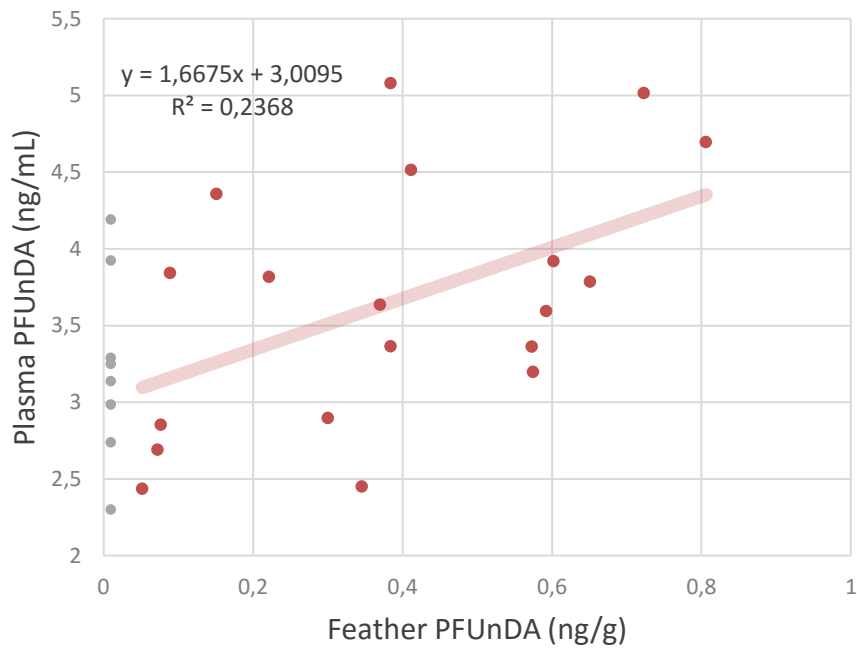
Figure C1: Relationship between feather (ng/g) and plasma (ng/mL) concentrations of PFUnDA for all individuals. The red dots are levels above LOD in feather samples and grey dots are feather samples below LOD. The regression line is based on all nestlings (n = 19) with feather levels above LOD

Appendix D

Individual concentrations of PFASs, proteins and leukocyte profiles

Table D1
Individual PFASs and ∑PFASs concentrations (ng/mL) in plasma of WTE nestlings (n = 27) from Smøla (SM, n = 13) and Steigen (ST, n = 14).

ID	PFHpS	brPFOS	linPFOS	PFOA	PFNA	PFDA	PFUnDA	∑PFAS
ST 1.1	0.09	9.55	23.26	1.27	5.73	2.21	3.20	45.32
ST 2.1	0.08	2.52	10.05	0.53	1.74	1.02	3.25	19.19
ST 2.2	0.08	1.85	9.55	0.14	1.56	1.05	2.98	17.21
ST 3.1	0.14	3.27	15.50	0.58	2.91	1.38	3.63	27.42
ST 4.1	0.01	6.27	25.63	0.00	6.48	1.56	4.70	44.65
ST 4.2	0.01	2.66	15.41	0.40	2.88	0.99	2.74	25.08
ST 5.1	0.15	6.02	12.14	0.83	4.11	0.91	2.30	26.46
ST 6.1	0.31	6.21	22.08	0.45	4.21	1.57	3.78	38.62
ST 6.2	0.00	8.74	22.37	0.53	4.78	0.98	3.36	40.76
ST 7.1	0.00	6.21	23.89	0.22	3.05	1.55	4.51	39.44
ST 7.2	0.16	11.70	27.07	0.67	4.16	2.52	5.08	51.37
ST 8.1	0.01	4.74	13.24	0.38	2.54	1.50	3.36	25.76
ST 8.2	0.00	2.01	9.79	0.21	2.43	1.28	3.29	19.01
ST 9.1	0.15	4.28	17.59	0.96	4.97	1.58	5.02	34.54
SM 1.1	0.00	2.70	18.16	0.36	3.03	1.76	3.59	29.60
SM 1.2	0.01	3.93	23.41	0.57	2.70	2.30	3.92	36.84
SM 2.1	0.06	2.23	18.12	0.51	1.79	1.15	3.82	27.68
SM 2.2	0.01	1.85	12.99	0.31	1.17	0.82	2.69	19.85
SM 3.1	0.00	1.59	10.60	0.12	1.82	0.97	2.43	17.53
SM 4.1	0.01	1.30	7.35	0.22	1.14	0.81	2.85	13.69
SM 5.1	0.05	2.28	9.35	0.34	1.59	0.98	3.92	18.51
SM 6.1	0.02	0.55	6.04	0.20	0.57	0.66	2.45	10.49
SM 7.1	0.01	1.93	12.27	0.44	1.62	1.22	3.14	20.64
SM 7.2	0.11	4.20	20.54	0.08	3.02	1.81	4.36	34.11
SM 8.1	0.26	2.63	15.45	0.56	4.86	1.31	3.84	28.92
SM 9.1	0.16	2.08	14.12	0.33	3.05	1.24	2.90	23.88
SM 10.1	0.13	3.39	31.85	0.55	2.82	1.45	4.19	44.39
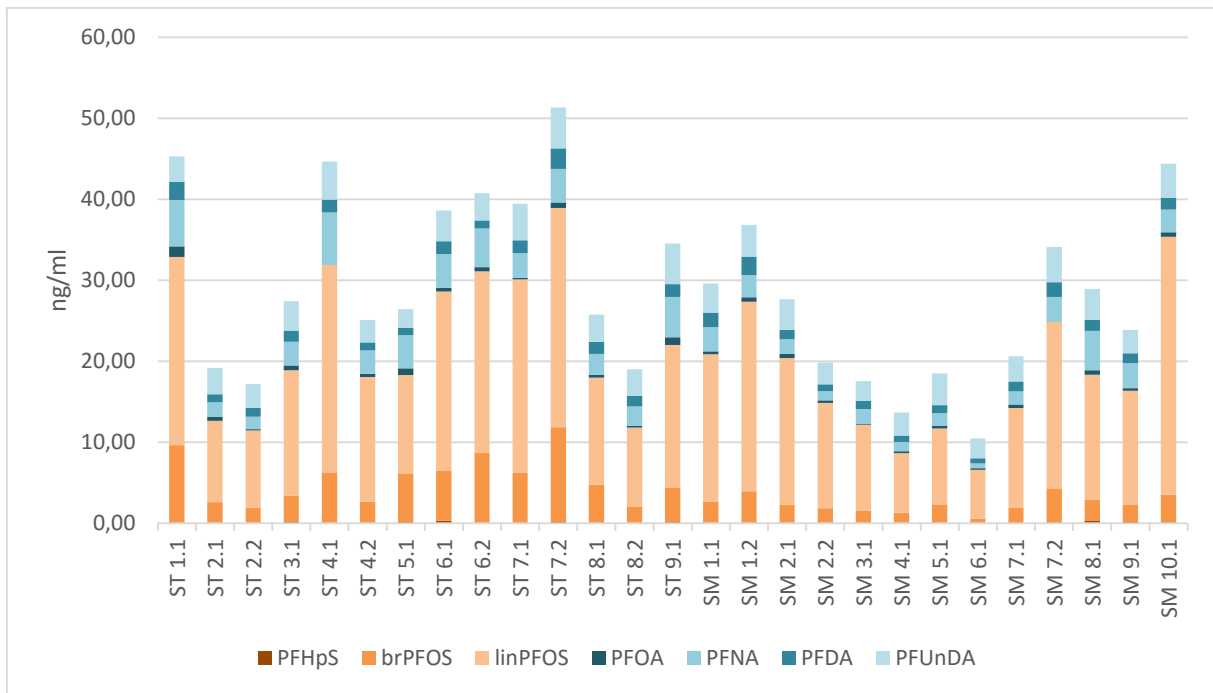
Figure D1: Histogram showing individual contaminant concentrations (ng/mL) in plasma samples from WTE nestlings (n = 27) from Smøla (SM, n = 13) and Steigen (ST, n = 14).
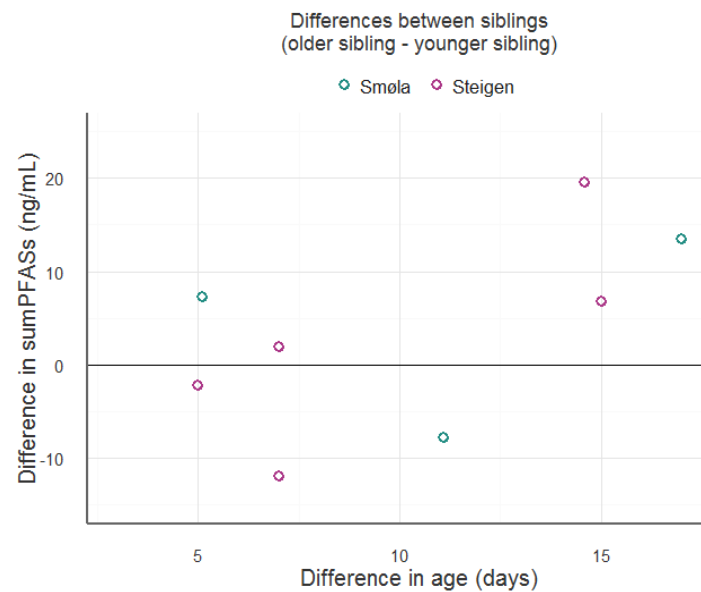
Figure D2: The difference in ∑PFASs levels in plasma and age between older sibling and younger sibling. Not all the older siblings had higher concentrations of PFASs (below the line).

Table D2.

Individual leukocyte profiles in percentages (%), heterophil/lymphocyte ratio (H:L), and relative count of leukocytes (LEU10), heterophils (HET10) and lymphocytes (LYM10) per 10 000 red blood cells (RBC). Multiple blood smears were made for each individual, but some smears were lost due to quality (described in 2.4.2). 7 WTEs from Steigen and 12 WTEs from Smøla were quantified.

ID	n	Het	Eos	Bas	Lym	Mon	H:L	LEU10	HET10	LYM10
Steigen (7/14)										
ST 1.1	1	36	25	0	34	5	1.06	103.9	37.4	35.3
ST 2.1	2	41.5	22	1	31.5	4	1.32	85.3	35.4	26.9
ST 6.1	1	45	16	0	37	2	1.22	102.8	46.2	38.0
ST 6.2	2	49.5	13.5	1	32	4	1.55	103.5	51.2	33.1
ST 7.1	1	53	14	0	31	2	1.71	71.2	37.7	22.1
ST 8.2	1	54	8	1	35	2	1.54	96.5	52.1	33.8
ST 9.1	2	44	15.5	1	38	1.5	1.16	168.7	74.2	64.1
Smøla (12/13)										
SM 1.1	2	62	10	0	23.5	4.5	2.64	109.3	67.8	25.7
SM 1.2	1	49	8	0	42	1	1.17	63.0	30.9	26.5
SM 2.1	2	49	8.5	0.5	36.5	5.5	1.34	134.1	65.7	48.9
SM 2.2	2	43	9.5	0	41	6.5	1.05	114.6	49.3	47.0
SM 3.1	2	57	18	0	21	4	2.71	156.2	89.0	32.8
SM 4.1	2	42	20	1.5	33.5	3	1.25	73.7	31.0	24.7
SM 5.1	1	57	22	0	19	2	3.00	89.4	50.9	17.0
SM 6.1	1	48	15	0	33	4	1.45	126.2	60.6	41.6
SM 7.1	1	47	21	1	25	6	1.88	46.9	22.1	11.7
SM 7.2	1	58	21	0	19	2	3.05	64.9	37.7	12.3
SM 8.1	2	42.5	14.5	0	37.5	5.5	1.13	108.3	46.0	40.6
SM 9.1	1	41	28	1	27	3	1.52	75.5	30.9	20.4

n = smears analysed, Het = heterophils (%), Eos = eosinophils (%), Bas = basophils (%), Lym = lymphocytes (%), Mon = monocytes (%).
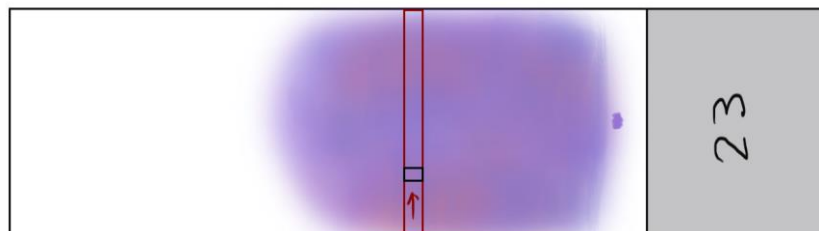
Figure D2: A blood smear. The differential count was started in the monolayer (preferably a place with few broken cells) and proceeded upwards. The red blood cells were counted inside a rectangle four times throughout the count.

Table D3.

Individual protein fractions in plasma of nestling WTEs, analysed by capillary electrophoresis and quantified on total protein concentrations

ID	PreAlb	Alb	α1	α2	β	γ	TP
ST 1.1	4.83	12.84	0.75	3.18	4.47	3.93	30
ST 2.1	3.76	13.96	1.16	3.63	5.25	5.25	33
ST 2.2	4.50	13.70	0.99	3.57	4.71	3.53	31
ST 3.1	4.96	14.48	0.81	3.32	5.05	2.39	31
ST 4.1	4.21	11.99	0.70	3.19	4.10	2.81	27
ST 4.2	4.40	10.60	0.45	2.95	4.05	2.55	25
ST 5.1	3.60	13.98	1.18	3.88	5.30	3.07	31
ST 6.1	3.90	14.72	0.77	3.68	5.18	3.74	32
ST 6.2	1.24	14.58	0.70	3.59	4.67	2.21	27
ST 7.1	2.29	16.46	0.68	3.57	5.15	2.85	31
ST 7.2	2.58	15.27	0.75	3.45	4.74	3.21	30
ST 8.1	1.46	16.55	0.71	4.00	4.50	3.78	31
ST 8.2	2.38	16.30	1.09	4.22	4.92	4.09	33
ST 9.1	4.32	15.27	1.39	4.18	5.71	3.13	34
SM 1.1	7.89	11.87	0.65	3.13	7.68	2.79	34
SM 1.2	5.58	14.20	0.43	2.79	5.77	2.23	31
SM 2.1	6.30	16.07	0.95	3.89	5.22	2.59	35
SM 2.2	4.49	15.81	0.95	4.01	5.37	3.37	34
SM 3.1	6.53	13.27	0.73	3.43	5.68	3.37	33
SM 4.1	4.93	13.13	0.64	2.97	4.12	2.21	28
SM 5.1	4.41	13.50	1.02	3.54	4.86	2.67	30
SM 6.1	3.91	17.27	0.68	3.81	5.37	2.96	34
SM 7.1	4.77	14.73	0.62	3.22	4.68	2.98	31
SM 7.2	7.41	13.49	0.65	3.01	4.12	2.33	31
SM 8.1	2.70	16.80	0.62	3.63	4.59	2.67	31
SM 9.1	3.46	16.48	0.45	4.03	4.83	2.75	32
SM 10.1	5.61	12.56	0.62	3.75	4.93	3.53	31

PreAlb= prealbumin, Alb = albumin, α1 = α_1-globulins, α2 = α_2-globulins, β = β-globulins, γ-globulins

Appendix E

Individual and sex-dependent biometrics

Table E1.
Biometrics of white-tailed eagle nestlings from Smøla and Steigen. Norway.

ID	Sex M/F	Body mass (g)	Bill length (mm)	Bill height (mm)	Tarsus width (mm)	Tarsus depth (mm)	Hallux length (mm)	Tail length (mm)	Wing length (mm)	Crop (g)
ST 1.1	M	4950	54.2	38.3	14.4	15.0	41.6	271	476	0
ST 2.1	F	4150	49.7	30.8	13.8	16.2	35.5	120	355	0
ST 2.2	M	3650	44.8	29.2	13.8	15.7	32.6	85	277	0
ST 3.1	F	4950	48.0	33.0	15.6	17.0	37.0	168	392	150
ST 4.1	F	5100	49.8	33.2	15.3	16.3	37.8	183	432	300
ST 4.2	F	4800	48.9	34.8	16.0	18.2	45.5	111	355	300
ST 5.1	M	4050	45.6	30.8	13.5	15.1	34.7	105	311	150
ST 6.1	F	5950	53.1	35.7	17.2	19.1	41.7	200	486	0
ST 6.2	M	-	47.3	31.5	13.2	14.2	15.7	175	434	150
ST 7.1	M	4650	50.8	32.9	14.2	16.4	29.5	265	500	50
ST 7.2	M	4350	50.0	34.0	14.3	16.7	39.7	230	485	0
ST 8.1	F	5100	51.2	35.4	15.6	18.0	40.4	145	365	50
ST 8.2	F	4700	49.7	34.5	16.0	17.1	38.9	71	307	0
ST 9.1	F	5200	52.0	39.8	16.1	18.0	43.4	185	455	50
SM 1.1	F	6650	53.1	36.8	16.0	20.5	41.4	215	505	50
SM 1.2	M	5200	50.3	33.9	13.7	16.7	37.9	240	505	40
SM 2.1	F	6600	54.9	40.0	17.6	20.6	14.4	209	503	0
SM 2.2	M	5100	49.2	33.5	15.0	17.6	37.8	264	544	0
SM 3.1	F	6600	52.6	36.5	16.5	19.5	41.1	241	464	0
SM 4.1	M	4950	50.0	33.4	14.5	18.1	39.4	263	510	50
SM 5.1	F	6000	54.9	38.0	17.8	20.4	43.0	284	565	0
SM 6.1	F	5100	50.9	34.2	16.6	17.4	41.6	172	388	0
SM 7.1	M	4200	48.8	31.5	14.2	17.1	35.8	190	440	170
SM 7.2	F	6000	56.8	36.7	17.7	19.7	41.1	274	536	0
SM 8.1	M	4500	48.8	33.6	15.1	17.0	38.2	258	490	0
SM 9.1	F	5800	56.8	36.5	16.4	18.8	42.7	268	535	0
SM 10.1	M	5000	51.9	33.5	14.9	18.8	39.1	250	521	150

Table E2.

Biometric measurements of WTE nestlings separated by sex, given as arithmetic mean (AM), standard error (SE) and range. Significant p values for estimates are given as bold font and asterisks (*), where $p < 0.001$ is indicated by ***, $p < 0.01$ by **, and $p < 0.05$ by * (Mann-Whitney U test).

Biometric	Males (n = 12)		Females (n = 15)		
	AM ± SE	Range	AM ± SE	Range	p
Body mass[a] (g)	4600 ± 143	3650 ± 5200	5513 ± 200	4150 ± 6650	**0.005** **
Bill length (mm)	49.3 ± 0.7	44.8 ± 54.2	52.2 ± 0.7	48.0 ± 56.8	**0.02** *
Bill height (mm)	33.0 ± 0.6	29.2 ± 38.3	35.7 ± 0.6	30.8 ± 40.0	**0.007** **
Tarsus width (mm)	14.2 ± 0.2	13.2 ± 15.1	16.3 ± 0.3	13.8 ± 17.8	**<0.001** ***
Tarsus depth (mm)	16.5 ± 0.4	14.2 ± 18.8	18.4 ± 0.4	16.2 ± 20.6	**0.005** ***
Hallux length (mm)	35.2 ± 2.0	15.7 ± 41.6	39.0 ± 1.9	14.4 ± 45.5	**0.02** *
Tail length (mm)	216 ± 19	85 ± 271	190 ± 16	71 ± 284	0.323
Wing length (mm)	458 ± 24	277 ± 544	443 ± 20	307 ± 565	0.558

a n = 11 for males

Table E3.

Biometric measurements of white-tailed eagle nestlings separated by population, given as arithmetic mean (AM), standard error (SE) and range. Significant p values for estimates are given as bold font and asterisks (*), where $p < 0.001$ is indicated by ***, $p < 0.01$ by **, and $p < 0.05$ by * (Mann-Whitney U test).

Biometric	Steigen (n = 14)		Smøla (n = 13)		
	AM ± SE	Range	AM ± SE	Range	p
Body mass[a] (g)	4738 ± 164	3650 ± 5950	5515 ± 226	4200 ± 6650	**0.015** *
Bill length (mm)	49.7 ± 0.7	44.8 ± 54.2	52.2 ± 0.8	48.8 ± 56.8	**0.049** *
Bill height (mm)	33.9 ± 0.8	29.2 ± 39.8	35.2 ± 0.7	31.5 ± 40.0	0.159
Tarsus width (mm)	14.9 ± 0.3	13.2 ± 17.2	15.8 ± 0.4	13.7 ± 17.8	0.089
Tarsus depth (mm)	16.6 ± 0.4	14.2 ± 19.1	18.6 ± 0.4	16.7 ± 20.6	**0.003** **
Hallux length (mm)	36.7 ± 2.0	15.7 ± 45.5	38.0 ± 2.1	14.4 ± 43.0	0.481
Tail length (mm)	165 ± 16.9	71 ± 271	241 ± 9.5	172 ± 284	**0.002** **
Wing length (mm)	402 ± 20.0	277 ± 500	500 ± 13.1	388 ± 565	**0.0004** **

a n = 13 for the Steigen population

Appendix F

Internal Standard (ISTD)

Table F4

Internal standard (ISTD) for plasma and feather samples provided by NILU.

Compound	Abbreviation	Concentration (ng/µL)
Perfluorobutanoic acid	PFBA	0.1
Perfluoropentanoic acids	PFPA	0.1
Perfluorohexanoic acid	PFHxA	0.1
Perfluoroheptanoic acid	PFHpA	0.1
Perfluorooctanoic acid	PFOA	0.1
Perfluorononanoic acid	PFNA	0.1
Perfluorodecanoic acid	PFDA	0.1
Perfluoroundecanoic acid	PFUnDA	0.1
Perfluorododecanoic acid	PFDoDA	0.1
Perfluorotetradecanoic acid	PFTeDA	0.1
Perfluorohexane sulfonate	PFHxS	0.0946
Perfluorooctane sulfonate	PFOS	0.0956
Perfluorooctane sulfonamide	PFOSA	0.1
Chloro-Perfluorohexyl phosphonic acid	Cl-PFHxPA	0.3
6:2 Fluorotelomer sulfonate	6:2 FTS	0.095

Appendix G

Haematology: Cell identification

1a
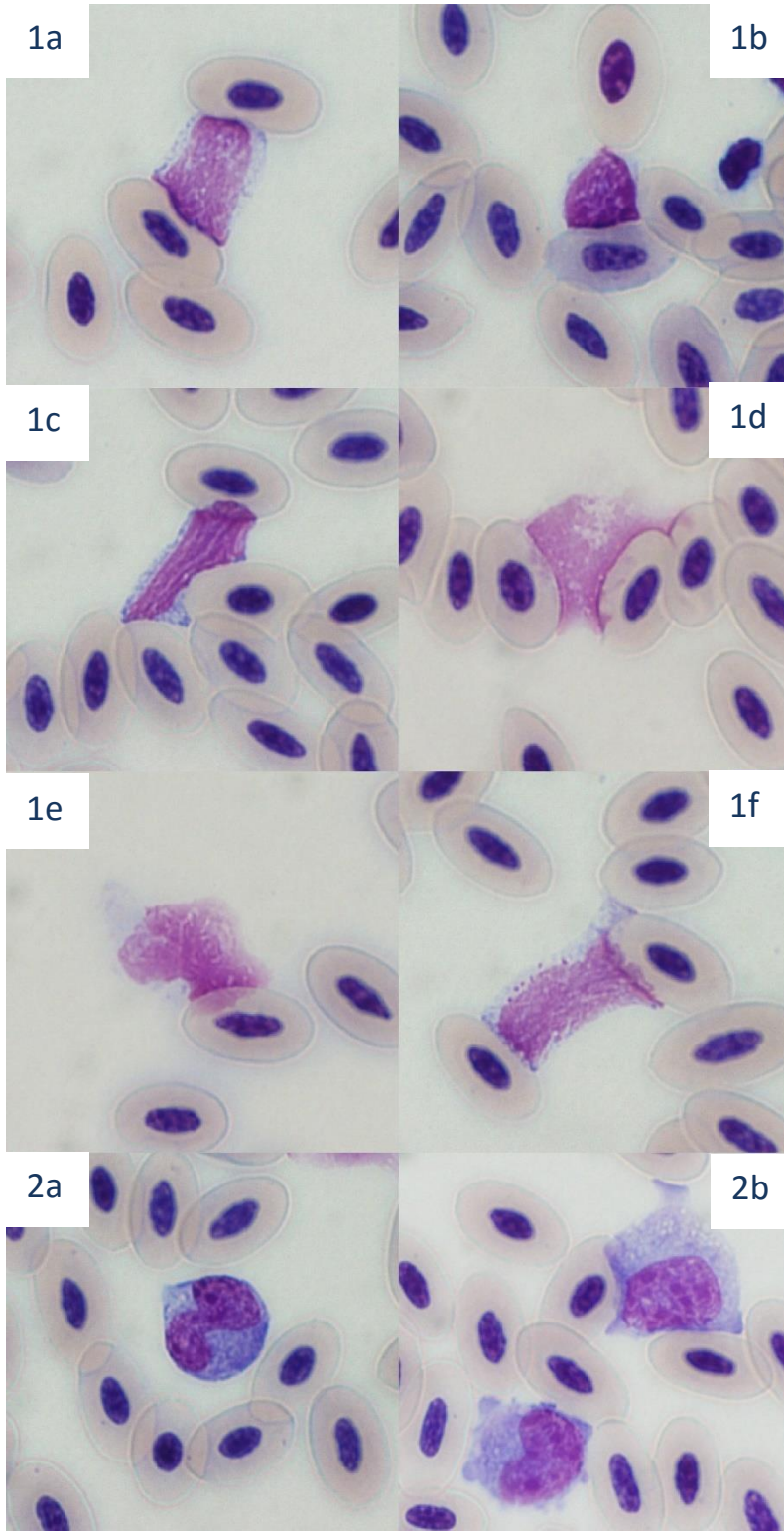
1b

Lymphocytes

Very pleumorphic in shape and size. Did not particularly resemble cells of other species in literature. Usually medium – large with irregular shape and pale cytoplasm.

1a) A typical lymphocyte encountered, with moderate to pale incomplete rim of cytoplasm, and moderate colored nucleus.

1c

1d

1b) A small/medium lymphocyte, with a more "regular" shape.

1c) Another typical lymphocyte, shape often formed by surrounding erythrocytes.

1d) A possible lymphocyte, broken with no visible cytoplasm, and therefore not identifiable.

1e) A broken lymphocyte with clearly visible cytoplasm and a resembling patterned nucleus, therefore counted. In some of the individuals, it seemed that lymphocytes more easily lysed than other cells.

1e

1f

1f) A large granulated lymphocyte. Not often encountered, but more evident in some of the individuals.

Monocytes

Mostly large cells with round to irregular shape. Large to moderate cytoplasm with a distinct basophilic colour. Nucleus round - ovoid or horseshoe shaped with distinct patterns/reticular chromatin and a clear edge.

2a

2b

2a) A typical round monocyte encountered. Easiest differentiated from lymphocytes by amount of cytoplasm and strong coloration.

2b) Many monocytes had a more irregular shape. Lower cell with cytoplasmic pseudopodia.

Heterophils

Round in shape with a violet lobed nucleus. Cells encountered had often small "round" granules with moderate density and a pale basophilic-colourless cytoplasm.

3a) A typical heterophil encountered, with a basophilic nucleus, usually paler than in eosinophils.
3b) A broken heterophil.

Eosinophils

Round cells with a high density of acidophilic granules, large and pearl-looking. Nucleus lobed with moderate to darkly stained chromatin.

4a) A typical eosinophil encountered, with high density of granules and a dark many-lobed nucleus.
4b) Another typical eosinophil, with basophilic cytoplasm visible at the edge or in between round granules.

Basophils

Not often encountered, although a few individuals seemed to have relatively many basophils. These had darkly basophilic large granules and pale basophilic cytoplasm.

5a) A typical basophil with dark cytoplasmic granules and irregular shaped cytoplasm.
5b) Basophil with visible nucleus and less density of granules.

Thrombocytes

Thrombocytes were usually smaller than other cells, with darkly stained chromatin. Ovoid in shape with pale basophilic cytoplasm with pseudopodia. However, a wide range of difference was seen between individual birds. Thrombocytes encountered seldom aggregated.

6a) A typical thrombocyte with less round shape and very darkly stained chromatin.
6b) Many individuals had large rounder thrombocytes that could resemble small lymphocytes.
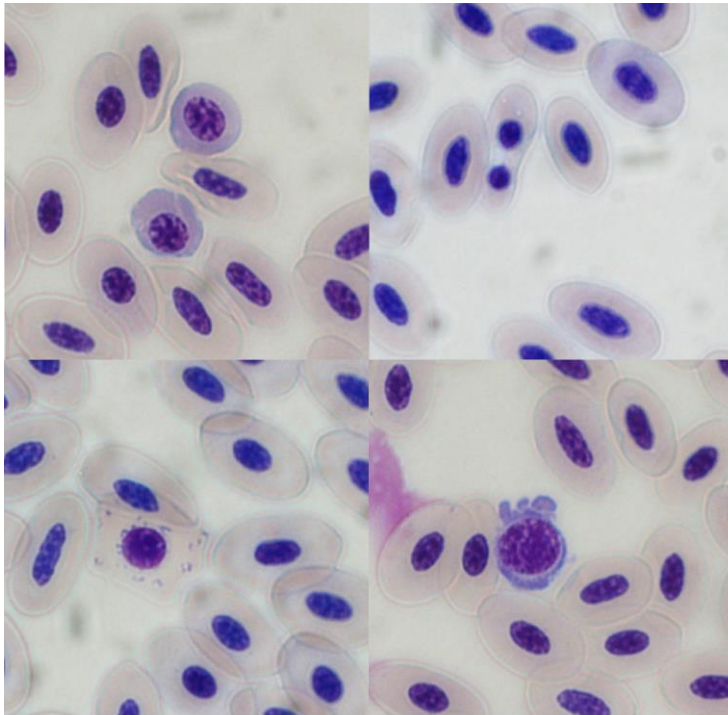
Erythrocytes

Mature cells were ovoid in shape with a darkly stained nucleus and pale eosinophilic cytoplasm.

7a) Mature erythrocytes with round to ovoid shape and two polychromatic thrombocyte with a more basophilic cytoplasm and rounder shape.

7b) An erythrocyte with a segmented nucleus, rarely encountered during the counting.

7c) An erythrocyte with basophilic stippling (sometimes referred to as a reticulocyte), this may be due to aggregation of rRNA in the cytoplasm. Not commonly encountered, while some individuals had a higher proportion of these.

7d) An early stage of erythrocyte (rubricyte or prorubricyte). The continuous maturation process was evident in the variation of developing erythrocytes. This example also show cytoplasmic blebs/pseudopodia.

Table G1

Coefficient of variation (C_V), mean, standard deviation (SD) and range of one recounted blood smear. The smear was counted five times; at the start, after 10, 30 and 40 smears, and at the end. C_V is calculated with eq. G1 and G2, were eq. G2 is unbiased when dealing with a lower sample size (n = 5).

	Mean ± SD	Range	C_V	$\widehat{C_V}$
Heterophils	40.8 ± 4.8	36 - 49	0.117	0.125
Lymphocytes	33.4 ± 7.3	19 - 39	0.219	0.233
Eosinophils	18.6 ± 3.8	15 - 26	0.206	0.219
Basophils	2.0 ± 0.9	1 - 3	0.447	0.475
Monocytes	5.2 ± 2.3	3 - 8	0.445	0.473

$$C_V = \frac{\sigma}{\mu} \qquad (eq.\,G1)$$

$$\widehat{C_V} = \left(1 + \frac{1}{4n}\right) C_V \qquad (eq.\,G2)$$

Appendix H

Principal component analysis 1 (PCA1)

PCA1 3rd and 4th dimension plot, eigenvalues, individual scores (first 5 dimensions), loadings of variables (first 5 dimensions), statistical interpretation. Dimension description helped finding which variables were most correlated to the different components (dim1 – dim5), based on an F-test for variables and a T-test for categories (H1: correlation coefficient is significantly different than zero when $p < 0.05$).
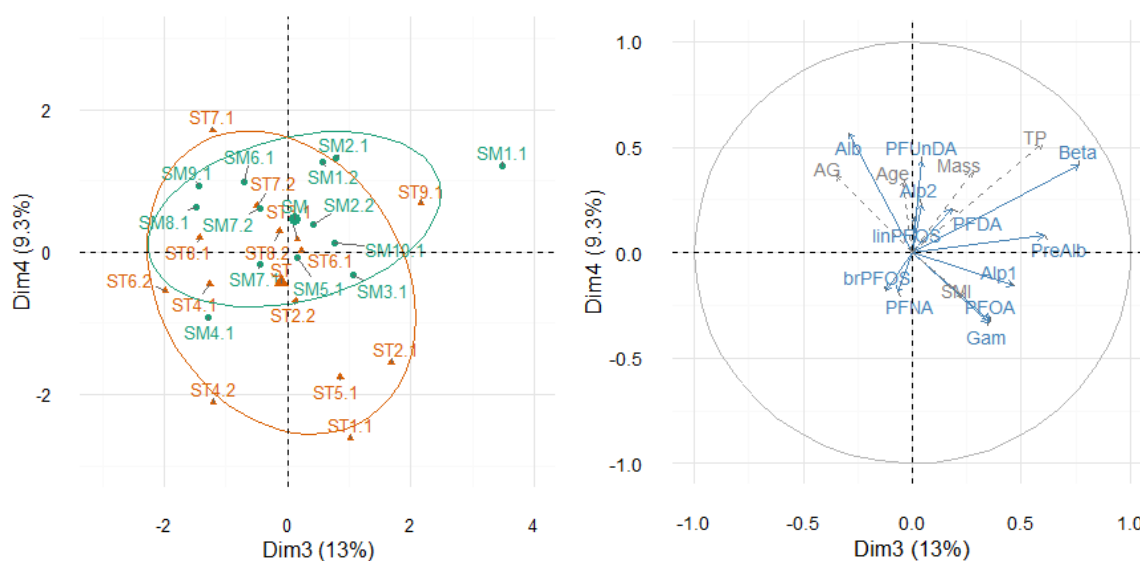
Figure H1: Principal Component Analysis of contaminants and proteins, 3rd and 4th dimension. 3rd dimension explains 13.0 % of the total variation, while 4th dimension explains 9.35 %. Individuals in the score-plot (left) are coloured after population (Steigen/Smøla), while the loading-plot (right) show contributing variables in blue and supplementary variables in grey. SMI = scaled mass index, TP = Total protein, AG = Albumin: Globulin ratio, PreAlb = Prealbumin, Alb = albumin, Alp1 = α_1-globulins, Alp2 = α_2-globulins, Beta = β-globulins, Gam = γ-globulins

Table H1
Eigenvalues of PCA1. The matrix had 12 dimensions, where the first four had 76.29 % of the explained variation and were visualised for interpretation.

Eigenvalues	Dim.1	Dim.2	Dim.3	Dim.4	Dim.5	Dim.6	Dim.7	Dim.8	Dim.9	Dim.10	Dim.11	Dim.12
Variance	3.85	2.63	1.55	1.12	0.79	0.69	0.47	0.35	0.24	0.18	0.08	0.04
% of var.	32.08	21.90	12.95	9.35	6.55	5.76	3.95	2.92	2.03	1.52	0.68	0.29
Cumulative % of var.	32.08	53.99	66.94	76.29	82.84	88.60	92.55	95.47	97.50	99.03	99.71	100.00
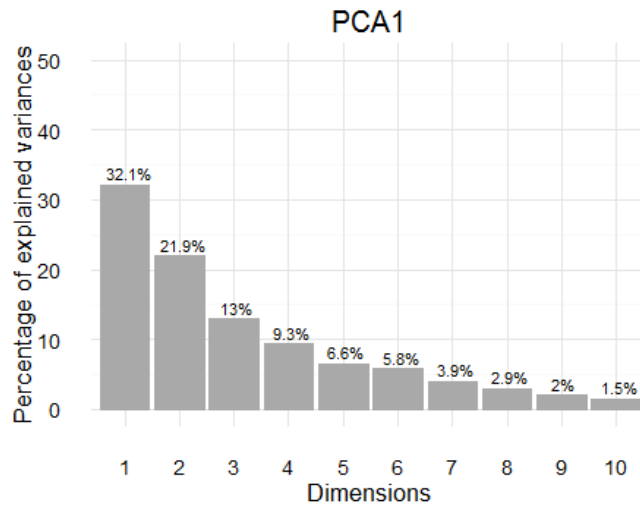
Figure H2: Percentage of variance explained by the first 10 dimensions of PCAm1 given as a boxplot.

Table H2

PCA1 individual scores (vector), contribution (ctr) to the construction and quality of representation (cos2) of the five first dimensions of PCA1. The distance signifies the cumulative vector of all dimension.

ID	Dist	Dim.1	ctr	cos2	Dim.2	ctr	cos2	Dim.3	ctr	cos2	Dim.4	ctr	cos2	Dim.5	ctr	cos2
ST1.1	5.10	3.74	13.43	0.54	0.71	0.72	0.02	1.02	2.49	0.04	-2.62	22.64	0.26	-1.26	7.53	0.06
ST2.1	4.00	-1.84	3.24	0.21	1.79	4.51	0.20	1.69	6.77	0.18	-1.55	7.94	0.15	1.25	7.41	0.10
ST2.2	2.55	-2.11	4.30	0.69	-0.14	0.03	0.00	0.13	0.04	0.00	-0.68	1.55	0.07	1.09	5.58	0.18
ST3.1	1.39	0.14	0.02	0.01	-0.68	0.65	0.24	0.16	0.06	0.01	0.18	0.10	0.02	-0.58	1.56	0.17
ST4.1	4.27	2.85	7.81	0.45	-1.11	1.73	0.07	-1.26	3.79	0.09	-0.46	0.69	0.01	2.06	20.05	0.23
ST4.2	3.75	-0.22	0.05	0.00	-2.70	10.30	0.52	-1.20	3.44	0.10	-2.11	14.67	0.32	-0.16	0.11	0.00
ST5.1	3.38	-0.66	0.42	0.04	1.74	4.24	0.26	0.86	1.77	0.07	-1.76	10.16	0.27	-1.30	7.96	0.15
ST6.1	1.93	1.27	1.54	0.43	0.94	1.26	0.24	0.24	0.13	0.02	0.01	0.00	0.00	0.29	0.40	0.02
ST6.2	3.46	1.48	2.10	0.18	0.91	1.17	0.07	-1.98	9.33	0.33	-0.54	0.97	0.02	-1.07	5.42	0.10
ST7.1	2.81	1.28	1.57	0.21	0.77	0.83	0.07	-1.22	3.53	0.19	1.71	9.62	0.37	0.34	0.54	0.02
ST7.2	4.97	4.37	18.36	0.77	1.47	3.05	0.09	-0.50	0.59	0.01	0.65	1.41	0.02	0.20	0.18	0.00
ST8.1	2.92	-0.56	0.30	0.04	2.07	6.06	0.50	-1.42	4.81	0.24	0.20	0.13	0.01	0.00	0.00	0.00
ST8.2	3.52	-1.99	3.81	0.32	2.53	9.02	0.52	-0.13	0.04	0.00	0.29	0.28	0.01	0.98	4.48	0.08
ST9.1	4.54	1.35	1.75	0.09	2.92	11.99	0.41	2.17	11.21	0.23	0.68	1.53	0.02	0.28	0.37	0.00
SM1.1	4.94	0.48	0.22	0.01	-2.72	10.39	0.30	3.48	28.82	0.50	1.22	4.87	0.06	-0.73	2.49	0.02
SM1.2	3.91	2.12	4.34	0.30	-2.38	7.98	0.37	0.58	0.80	0.02	1.26	5.28	0.11	-1.19	6.67	0.09
SM2.1	2.44	-0.84	0.68	0.12	0.18	0.05	0.01	0.79	1.50	0.11	1.32	5.74	0.29	-0.07	0.02	0.00
SM2.2	2.90	-2.57	6.37	0.79	0.85	1.03	0.09	0.42	0.42	0.02	0.39	0.51	0.02	-0.11	0.06	0.00
SM3.1	3.17	-2.23	4.80	0.50	-1.60	3.61	0.25	1.06	2.66	0.11	-0.32	0.33	0.01	0.09	0.04	0.00
SM4.1	3.72	-2.03	3.96	0.30	-2.43	8.35	0.43	-1.30	4.00	0.12	-0.91	2.75	0.06	-0.03	0.00	0.00
SM5.1	2.32	-1.40	1.88	0.36	-0.29	0.12	0.02	0.16	0.06	0.01	-0.08	0.02	0.00	0.79	2.93	0.12
SM6.1	4.00	-3.64	12.72	0.83	0.18	0.04	0.00	-0.70	1.18	0.03	0.99	3.21	0.06	-0.95	4.27	0.06
SM7.1	1.93	-1.09	1.14	0.32	-1.08	1.63	0.31	-0.44	0.46	0.05	-0.18	0.11	0.01	-0.39	0.71	0.04
SM7.2	3.65	1.33	1.69	0.13	-2.62	9.68	0.52	-0.45	0.48	0.02	0.61	1.24	0.03	1.42	9.49	0.15
SM8.1	2.56	0.41	0.16	0.03	0.85	1.03	0.11	-1.49	5.29	0.34	0.63	1.32	0.06	-0.81	3.08	0.10
SM9.1	2.71	-1.12	1.20	0.17	0.35	0.17	0.02	-1.44	4.92	0.28	0.94	2.89	0.12	-1.03	5.00	0.15
SM10.1	3.12	1.50	2.17	0.23	-0.53	0.39	0.03	0.77	1.42	0.06	0.13	0.06	0.00	0.88	3.66	0.08

Table H3

PCA1 quantitative variable loading (correlation), contribution (ctr) to the construction and quality of representation (cos2) of the five first dimensions. Bold font means that they are significantly correlated to the dimension.

Variables	Dim.1	ctr	cos2	Dim.2	ctr	cos2	Dim.3	ctr	cos2	Dim.4	ctr	cos2	Dim.5	ctr	cos2
brPFOS	**0.84**	18.27	0.70	0.30	3.50	0.09	-0.12	0.95	0.02	-0.18	2.87	0.03	-0.09	1.04	0.01
linPFOS	**0.89**	20.47	0.79	-0.06	0.12	0.00	0.01	0.01	0.00	0.17	2.55	0.03	0.09	0.99	0.01
PFOA	**0.46**	5.55	0.21	**0.40**	6.12	0.16	0.36	8.11	0.13	-0.32	9.28	0.10	**-0.50**	32.36	0.25
PFNA	**0.80**	16.79	0.65	0.23	1.97	0.05	-0.07	0.28	0.00	-0.19	3.19	0.04	-0.04	0.24	0.00
PFDA	**0.85**	18.75	0.72	-0.03	0.03	0.00	0.18	2.08	0.03	0.21	3.89	0.04	-0.01	0.01	0.00
PFUnDA	**0.72**	13.36	0.51	0.11	0.49	0.01	0.04	0.12	0.00	**0.44**	16.99	0.19	**0.43**	23.26	0.18
PreAlb	-0.04	0.05	0.00	**-0.70**	18.61	0.49	**0.60**	23.48	0.37	0.08	0.58	0.01	0.09	0.99	0.01
Alb	-0.25	1.67	0.06	**0.63**	14.95	0.39	-0.29	5.40	0.08	**0.57**	28.74	0.32	-0.23	6.74	0.05
Alp1	-0.22	1.25	0.05	**0.65**	15.92	0.42	**0.47**	14.00	0.22	-0.16	2.19	0.03	0.29	10.40	0.08
Alp2	-0.34	3.00	0.12	**0.83**	26.25	0.69	0.04	0.11	0.00	0.23	4.66	0.05	0.03	0.15	0.00
Beta	-0.11	0.31	0.01	-0.02	0.02	0.00	**0.76**	37.60	0.58	**0.42**	15.33	0.17	-0.29	10.56	0.08
Gam	-0.14	0.53	0.02	**0.56**	12.03	0.32	0.35	7.87	0.12	-0.33	9.73	0.11	0.32	13.27	0.10

'

Table H4

PCA1 supplementary quantitative variable loading (correlation) and quality of representation (cos2) of the five first dimensions. Albumin/ globulin ratio (AG) had a significant negative correlation with the 2nd dimension. Total protein (TP) were best represented in the 3rd and 4th dimensions. The variation of age, mass and SMI does not show very high correlation with any dimensions.

Supp. Variables	Dim.1	cos2	Dim.2	cos2	Dim.3	cos2	Dim.4	cos2	Dim.5	cos2
TP	-0.37	0.13	0.33	0.11	**0.60**	0.36	**0.52**	0.27	-0.07	0.00
AG	0.01	0.00	**-0.59**	0.35	-0.35	0.13	0.37	0.14	-0.12	0.01
Age	0.29	0.08	-0.31	0.10	-0.04	0.00	0.35	0.12	-0.14	0.02
Mass	-0.01	0.00	-0.35	0.12	0.28	0.08	**0.39**	0.15	-0.04	0.00
SMI	-0.29	0.09	-0.04	0.00	0.24	0.06	-0.21	0.05	-0.20	0.04

Table H5

Supplementary categorical variables in PCAm1. Categorical loading (coordinate in dimension), quality of representation (cos2) and v-test value (-2 < x < 2: not significantly related to dimension) of each dimension. Bold font means that they are significantly correlated to the dimension. Note that the two populations are significantly different projected in dim2 (but also show large difference in dim1).

Supp. categories	Dist	Dim.1	cos2	v.test	Dim.2	cos2	v.test	Dim.3	cos2	v.test	Dim.4	cos2	v.test	Dim.5	cos2	v.test
F	0.59	-0.43	0.54	-1.25	-0.05	0.01	-0.18	0.21	0.13	0.96	0.13	0.05	0.69	0.24	0.17	1.57
M	0.73	0.54	0.54	1.25	0.06	0.01	0.18	-0.26	0.13	-0.96	-0.16	0.05	-0.69	-0.30	0.17	-1.57
SM	1.24	-0.70	0.32	-1.75	**-0.86**	0.49	-2.62	0.11	0.01	0.44	**0.46**	0.14	2.14	-0.16	0.02	-0.90
ST	1.15	0.65	0.32	1.75	**0.80**	0.49	2.62	-0.10	0.01	-0.44	**-0.43**	0.14	-2.14	0.15	0.02	0.90
Inland	1.70	-0.12	0.01	-0.13	-1.46	0.73	-1.91	0.24	0.02	0.40	0.06	0.00	0.12	0.50	0.09	1.20
Mixed	1.38	-0.25	0.03	-0.35	-0.48	0.12	-0.80	0.39	0.08	0.85	**0.96**	0.48	2.47	**-0.66**	0.23	-2.02
Sea	0.71	0.12	0.03	0.40	**0.51**	0.52	2.09	-0.19	0.07	-1.03	**-0.35**	0.25	-2.22	0.11	0.03	0.85
Sibling N	0.70	-0.36	0.26	-0.77	0.11	0.03	0.29	0.12	0.03	0.39	-0.20	0.08	-0.78	-0.36	0.26	-1.70
Sibling Y	0.48	0.25	0.26	0.77	-0.08	0.03	-0.29	-0.08	0.03	-0.39	0.13	0.08	0.78	0.25	0.26	1.70
FirstSibling: 0	0.34	0.01	0.00	0.02	-0.19	0.32	-0.39	0.02	0.00	0.05	-0.01	0.00	-0.01	-0.02	0.00	-0.07
FirstSibling: 1	0.14	0.00	0.00	-0.02	0.08	0.32	0.39	-0.01	0.00	-0.05	0.00	0.00	0.01	0.01	0.00	0.07

Principal component analysis 2 (PCA2)

PCA1 3rd and 4th dimension plot, eigenvalues, individual scores (first 5 dimensions), loadings of variables (first 5 dimensions), statistical interpretation. Dimension description helped finding which variables were most correlated to the different components (dim1 – dim5), based on an F-test for variables and a T-test for categories (H1: correlation coefficient is significantly different than zero when p < 0.05).
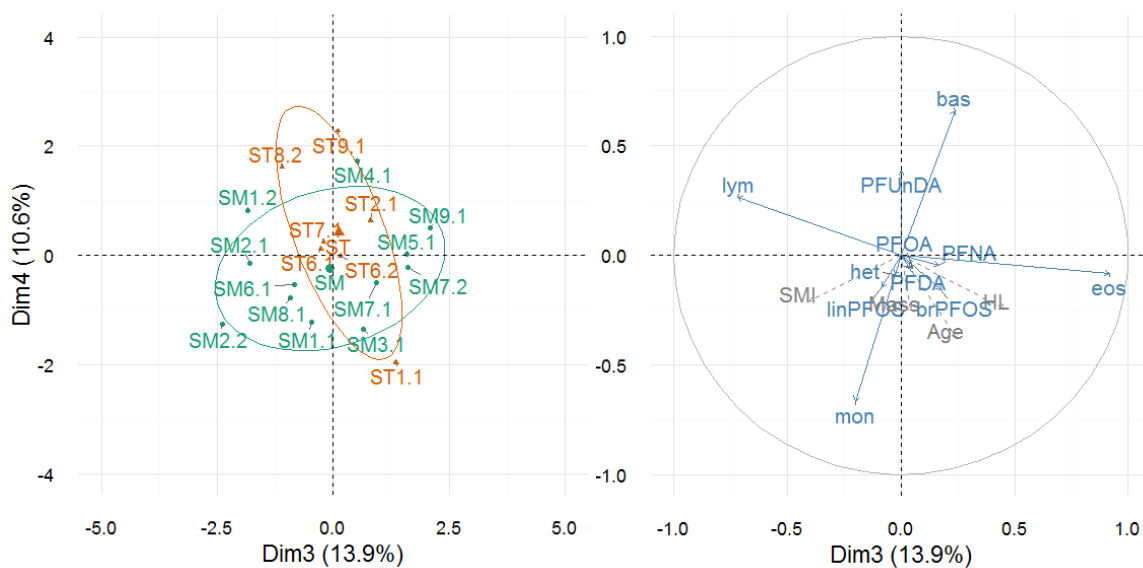
Figure H3: Principal Component Analysis of contaminants and proteins, 3rd and 4th dimension. 3rd dimension explains 13.9 % of the total variation, while 4th dimension explains 10.6 %. Individuals in the score-plot (left) are coloured after population (Steigen/Smøla), while the loading-plot (right) show contributing variables in blue and supplementary variables in grey. SMI = scaled mass index, HL = heterophil/lymphocyte ratio, het = heterophils, lym = lymphocytes, eos = eosinophils, mon = monocytes and bas = basophils.

Table H6:

Eigenvalues of PCAm1. The matrix had 10 dimensions, where the first four gave 82.95 % of explained variation and were visualised for interpretation.

Eigenvalues	Dim.1	Dim.2	Dim.3	Dim.4	Dim.5	Dim.6	Dim.7	Dim.8	Dim.9	Dim.10
Variance	4.17	2.26	1.53	1.17	0.59	0.47	0.34	0.26	0.18	0.04
% of var.	37.88	20.58	13.87	10.61	5.32	4.29	3.12	2.36	1.64	0.32
Cumulative % of var.	37.88	58.47	72.34	82.95	88.27	92.56	95.68	98.05	99.68	100.00

Figure H4: Percentage of variance explained by the 10 dimensions of PCA1 given as a boxplot.

Table H7:

PCA2 individual scores (vector), contribution (ctr) to the construction and quality of representation (cos2) of the five first dimensions. The distance (Dist) signifies a cumulative vector of all dimensions.

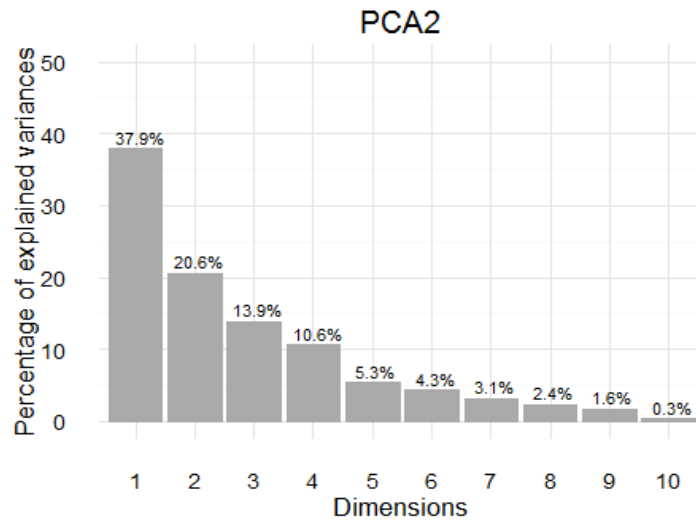| ID	Dist	Dim.1	ctr	cos2	Dim.2	ctr	cos2	Dim.3	ctr	cos2	Dim.4	ctr	cos2
ST1.1	5.67	4.36	23.96	0.59	2.53	14.89	0.20	1.35	6.30	0.06	-1.97	17.44	0.12
ST2.1	2.39	-1.26	2.01	0.28	1.64	6.29	0.48	0.81	2.27	0.12	0.64	1.83	0.07
ST6.1	2.53	2.15	5.82	0.72	-0.23	0.13	0.01	-0.26	0.24	0.01	0.11	0.06	0.00
ST6.2	3.19	1.59	3.17	0.25	0.64	0.95	0.04	0.16	0.09	0.00	-0.01	0.00	0.00
ST7.1	2.94	1.72	3.72	0.34	-2.01	9.42	0.47	-0.20	0.14	0.01	0.25	0.28	0.01
ST8.2	2.72	-1.18	1.77	0.19	-0.67	1.04	0.06	-1.10	4.18	0.16	1.62	11.86	0.36
ST9.1	3.94	2.79	9.80	0.50	0.66	1.00	0.03	0.09	0.03	0.00	2.28	23.39	0.33
SM1.1	2.98	0.10	0.01	0.00	-2.23	11.58	0.56	-0.47	0.78	0.03	-1.22	6.74	0.17
SM1.2	3.84	2.46	7.63	0.41	-1.16	3.11	0.09	-1.84	11.66	0.23	0.83	3.09	0.05
SM2.1	2.29	-0.26	0.09	0.01	0.28	0.19	0.02	-1.80	11.13	0.61	-0.15	0.10	0.00
SM2.2	3.57	-1.75	3.87	0.24	1.39	4.50	0.15	-2.38	19.58	0.45	-1.26	7.11	0.12
SM3.1	3.30	-2.55	8.20	0.60	-1.20	3.32	0.13	0.65	1.45	0.04	-1.35	8.21	0.17
SM4.1	3.58	-2.58	8.39	0.52	1.59	5.84	0.20	0.52	0.93	0.02	1.73	13.44	0.23
SM5.1	3.27	-1.52	2.91	0.22	-1.88	8.24	0.33	1.60	8.81	0.24	0.02	0.00	0.00
SM6.1	3.57	-3.17	12.69	0.79	0.34	0.27	0.01	-0.85	2.48	0.06	-0.54	1.33	0.02
SM7.1	2.62	-1.60	3.24	0.37	1.01	2.37	0.15	0.94	3.04	0.13	-0.50	1.10	0.04
SM7.2	3.56	0.69	0.61	0.04	-2.99	20.75	0.70	1.60	8.86	0.20	-0.22	0.21	0.00
SM8.1	2.52	0.93	1.09	0.14	1.06	2.61	0.18	-0.92	2.89	0.13	-0.77	2.68	0.09
SM9.1	2.90	-0.90	1.02	0.10	1.23	3.52	0.18	2.10	15.15	0.52	0.51	1.15	0.03

Table H8

PCA2 quantitative variable loading (correlation), contribution (ctr) to the construction and quality of representation (cos2) of the for first dimensions. Bold font means that they are significantly correlated to the dimension ($p < 0.05$).

Variables	Dim.1	ctr	cos2	Dim.2	ctr	cos2	Dim.3	ctr	cos2	Dim.4	ctr	cos2
brPFOS	**0.85**	17.17	0.72	0.07	0.22	0.01	0.18	2.06	0.03	-0.16	2.07	0.02
linPFOS	**0.89**	19.14	0.80	-0.21	1.98	0.05	-0.08	0.46	0.01	-0.15	1.80	0.02
PFOA	**0.71**	12.17	0.51	**0.54**	2.91	0.29	0.05	0.15	0.00	-0.06	0.29	0.00
PFNA	**0.88**	18.48	0.77	0.13	0.78	0.02	0.17	1.83	0.03	-0.05	0.17	0.00
PFDA	**0.82**	16.03	0.67	-0.26	2.89	0.07	0.04	0.10	0.00	-0.06	0.32	0.00
PFUnDA	**0.65**	10.11	0.42	-0.42	7.87	0.18	0.00	0.00	0.00	0.39	12.67	0.15
lym	0.34	2.75	0.12	**0.51**	1.31	0.26	**-0.72**	33.68	0.51	0.26	5.94	0.07
het	-0.22	1.12	0.05	**-0.92**	7.13	0.84	-0.03	0.05	0.00	-0.09	0.69	0.01
bas	-0.23	1.23	0.05	**0.47**	9.89	0.22	0.24	3.65	0.06	**0.66**	37.41	0.44
eos	-0.06	0.08	0.00	0.28	3.56	0.08	**0.92**	55.35	0.85	-0.08	0.59	0.01
mon	-0.27	1.72	0.07	**0.51**	1.48	0.26	-0.20	2.67	0.04	**-0.67**	38.07	0.44

Table H9

PCA2 supplementary quantitative variable loading (correlation) and quality of representation (cos2) of the five first dimensions. Bold font means that they are significantly correlated to the dimension ($p < 0.05$).

Supp. variables	Dim.1	cos2	Dim.2	cos2	Dim.3	cos2	Dim.4	cos2
HL	-0.29	0.08	**-0.76**	0.58	**0.46**	0.21	-0.24	0.06
Age	0.15	0.02	-0.14	0.02	0.25	0.06	-0.38	0.14
Mass	-0.04	0.00	**-0.50**	0.25	0.04	0.00	-0.25	0.06
SMI	-0.08	0.01	-0.20	0.04	-0.41	0.16	-0.21	0.05

Table H10

Supplementary categorical variables in PCA2. Categorical loading (coordinate in dimension), quality of representation (cos2) and v-test value (-2 < x < 2: not significantly related to dimension) of each dimension. Note that the two populations are significantly different projected in dim1.

Supp. Cat.	Dist	Dim.1	cos2	v.test	Dim.2	cos2	v.test	Dim.3	cos2	v.test	Dim.4	cos2	v.test
F	0.73	-0.47	0.41	-1.13	-0.46	0.40	-1.52	0.22	0.09	0.87	0.15	0.05	0.71
M	1.00	0.64	0.41	1.13	0.63	0.40	1.52	-0.30	0.09	-0.87	-0.21	0.05	-0.71
SM	0.94	**-0.85**	0.81	-2.30	-0.21	0.05	-0.79	-0.07	0.01	-0.32	-0.24	0.07	-1.25
ST	1.61	**1.45**	0.81	2.30	0.37	0.05	0.79	0.12	0.01	0.32	0.42	0.07	1.25
Inland	2.07	-1.15	0.31	-1.04	-1.06	0.26	-1.29	1.06	0.27	1.58	-0.69	0.11	-1.17
Mixed	1.06	0.10	0.01	0.14	0.10	0.01	0.18	**-0.89**	0.69	-2.07	-0.34	0.11	-0.92
Sea	0.71	0.29	0.16	0.63	0.26	0.13	0.77	0.21	0.09	0.77	0.41	0.33	1.71
Sibling N	0.98	-0.33	0.11	-0.58	0.54	0.31	1.30	0.57	0.34	1.66	-0.01	0.00	-0.04
Sibling Y	0.71	0.24	0.11	0.58	-0.39	0.31	-1.30	-0.41	0.34	-1.66	0.01	0.00	0.04
FirstSibling 0	1.21	-0.27	0.05	-0.34	-0.19	0.03	-0.33	-0.46	0.14	-0.93	-0.05	0.00	-0.12
FirstSibling 1	0.43	0.10	0.05	0.34	0.07	0.03	0.33	0.16	0.14	0.93	0.02	0.00	0.12

Appendix I

Model selection and description predicting protein levels

Table I1

Model selection of different variables predicting variation in prealbumin and albumin:globulin ratio (A:G) by AICc. Models with ΔAICc<2 are further described in Table I2 and I3.

Response variable	ID	Predictor variable	AICc	ΔAICc	AICc weight
Prealbumin	1	Mass	86.09	0.00	0.34
	2	Mass:Pop	87.26	1.17	0.19
	3	Mass + Sex	87.69	1.60	0.15
	4	Mass:Sex	88.27	2.18	0.11
	5	Mass + Pop	88.28	2.19	0.11
	6	Mass:Sex + Sex	89.66	3.57	0.06
	7	Mass + Sex + Pop	90.91	4.82	0.03
	8	Pop	101.54	15.45	0.00
	9	Age + Pop	104.56	18.47	0.00
	10	Age	106.53	20.44	0.00
Albumin: Globulin (ratio)	1	Pop	-14.96	0.00	0.44
	2	Age+Pop	-13.37	1.58	0.20
	3	Age:Pop	-13.09	1.87	0.17
	4	Age	-11.30	3.66	0.07
	5	Age:Pop + Pop	-10.12	4.84	0.04
	6	Age + Sex + Pop	-10.05	4.91	0.04
	7	Mass + Pop	-9.88	5.08	0.03
	8	Mass + Pop + Sex	-6.49	8.46	0.01
	9	Mass	-4.73	10.23	0.00

Table I2

Plasma levels of prealbumin predicted by mass (kg) and sex of WTE nestlings by linear regression (19 nests, 27 birds). Significant t values for estimates are given as bold font, and p values were added as asterisks (*), where $p < 0.001$ is indicated by ***, $p < 0.01$ by **, and $p < 0.05$ by *.

	Model 1[a]			Model 2			Model 3[a]		
Variable	Estimate	SE	t value	Estimate	SE	t value	Estimate	SE	t value
Intercept	-1.3652	1.2694	-1.075	-0.6425	1.366	-0.47	-3.4111	2.1698	-1.572
Males							0.6626	0.564	1.175
Mass	1.1231	0.2403	**4.674***				1.4656	0.3807	**3.85***
Mass : Smøla				1.0496	0.2439	**4.303***			
Mass : Steigen				0.9002	0.2902	**3.102**			

a Intercept is females

Table I3

Plasma albumin: globulin ratio predicted by mass (kg) and sex of WTE nestlings by linear regression (19 nests, 27 birds). Significant t values for estimates are given as bold font, and *p* values were added as asterisks (*), where *p* < 0.001 is indicated by ***, *p* < 0.01 by **, and *p* < 0.05 by *.

Variable	Model 1[a]			Model 2[a]			Model 3		
	Estimate	SE	t value	Estimate	SE	t value	Estimate	SE	t value
Intercept	1.64422	0.04413	**37.26*****	1.368189	0.243372	**5.622*****	1.218846	0.205213	**5.939*****
Steigen	-0.22554	0.06129	**-3.68*****	-0.172218	0.076459	**-2.252***			
Age				0.003513	0.003046	1.153			
Age: Smøla							0.005387	0.002652	**2.032***
Age: Steigen							0.003181	0.003189	0.998

a Intercept is the Smøla population

Appendix J

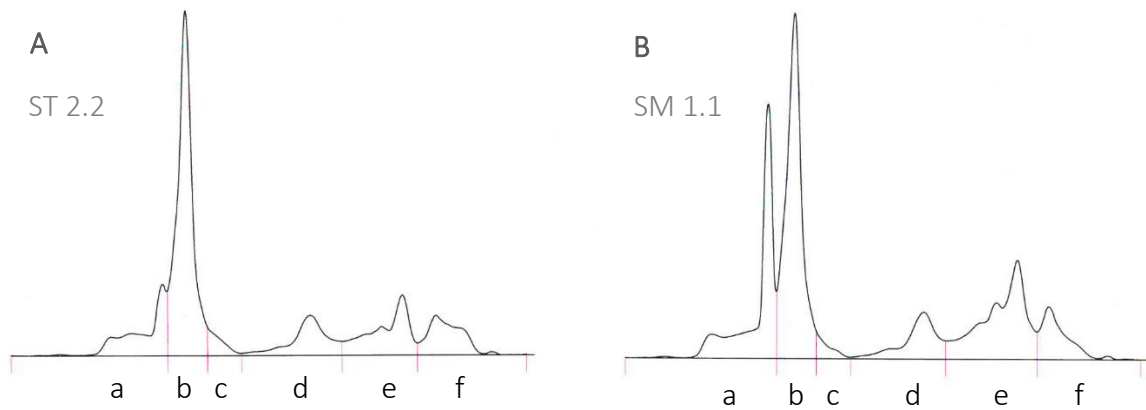## Electrophoretic pattern of plasma proteins

Figure J1: Electrophoretic pattern of WTE (*Haliaeetus albicilla*) nestlings. Protein fractions are (a) prealbumin, (b) albumin, (c) α₁-globulin, (d) α₂-globulin, (e) β-globulin and (f) γ-globulin. The pattern of (A) was typical with a medium prealbumin spike (a smaller ridge in some individuals), and a medium amount of globulins. The pattern of prealbumin was the most variable sometimes parting clearly from the albumin top, shown in (B). No birds had a particularly different pattern compared to the rest, something that can indicate that all nestlings were healthy.

Appendix K

Leukocyte levels by population

Table K1
Leukocyte levels separated by population, no significant differences were found between the two.

Analyte	Steigen (n = 7)			Smøla (n = 12)		
	AM ± SE	Median	Range	AM ± SE	Median	Range
Lymphocytes (%)	34.1 ± 1.0	34.0	31.0 - 38.0	29.8 ± 2.4	30.0	19.0 - 42.0
abs	36.2 ± 5.1	33.8	22.1 - 64.1	29.1 ± 3.8	26.1	11.7 - 48.9
Heterophils (%)	46.1 ± 2.5	45.0	36.0 - 54.0	49.6 ± 2.1	48.5	41.0 - 62.0
abs	47.8 ± 5.1	46.2	35.4 - 74.2	48.5 ± 5.7	47.6	22.1 - 89.0
Eosinophils (%)	16.3 ± 2.1	15.5	8.0 - 25.0	16.3 ± 1.7	15.5	8.0 - 28.0
Basophiles (%)	0.6 ± 0.2	1.0	0.0 - 1.0	0.3 ± 0.1	0.0	0.0 - 1.5
Monocytes (%)	2.9 ± 0.5	2.0	1.5 - 5.0	3.9 ± 0.5	4.0	1.0 - 6.5
Leukocytes abs	104.6 ± 11.6	102.8	71.2 - 168.7	96.8 ± 9.1	102.8	46.9 - 168.7
H:L ratio	1.4 ± 0.1	1.3	1.1 - 1.7	1.9 ± 0.2	1.5	1.0 3.1

Appendix L

Model estimating maternal load, equations and description

Equation L1 was considered to measure the effect of growth dilution, as this was believed to be the biggest contributor to depuration, instead, this was used to control for estimates calculated by equation L2, which combines elimination and growth dilution.

$$C_t V_t = C_0 V_0 \qquad (eq.L1)$$

Where: C_t = Concentration at a given time, V_t = Volume at given time (substituted by mass), C_0 = Concentration at a given time, V_0 = Volume at given time (substituted by mass).

$$C_t = C_0 * e^{-k*t} \qquad (eq.L2)$$

Where: C_t = Concentration at a given time (d^{-1}), C_0 = Concentration at a given time (d^{-1}), k = overall depuration rate constant and t = time (d^{-1}).

Equation L2 calculates internal concentrations of ∑PFASs deriving from maternal transfer, assuming a one-compartment model with concentration in eggs used as C_0. The overall elimination rate constant (k) was found by equation L3.

$$k = k_e + k_g \qquad (eq.L3)$$

Where: k = overall depuration rate constant, k_e = first-order elimination constant and k_g = growth rate constant

The elimination constant where found by equation L4, with depuration half-life of PFOS set as the depuration half-life of ∑PFASs. Half-life of PFOS was acquired with estimates by Yoo et al., (2009), set to 125 days which give k_e = 0.00555.

$$k_e = \frac{\log_e(2)}{t_{1/2}} \qquad (eq.L4)$$

Where: k_e = first-order elimination constant, $t_{1/2}$ = depuration half-life

To obtain the k_g an alternative method was used described by Crookes and Brooke, (2011). The method is appropriate when k_g is expected to dominate the overall depuration constant

(k). Since males and females are growing at a different rate, the two were separated when obtaining k_g. As described in the example 1 (5.7.1) by Crookes and Brooke, (2011), it is possible to use the negative slope between $1/\log_e(\text{mass(kg)})$ and age (days). Figure X show k_g obtained through regression between the egg-weight and actual mass of males and females sampled.
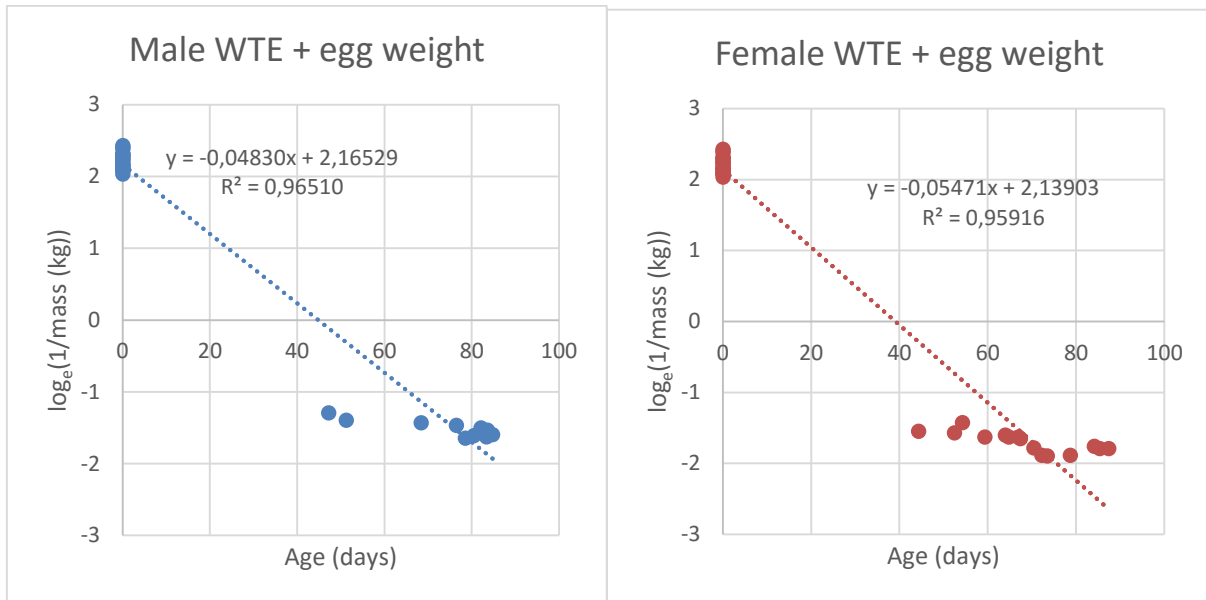

Figure L1: Obtaining k_g through regression. $k_{g\ Males}$ = 0.04830 and $k_{g\ Females}$ = 0.05471.

The overall depuration constant was then calculated: k_M = 0.00555 + 0.04830 = 0.05385, k_F = 0.00555 + 0.05471 = 0.06026 for males and females respectively.

Data from WTE eggs were given by Torgeir Nygård (NINA). A total of 23 eggs was analysed over the period 1990 – 2010, giving concentrations of PFASs (given as ∑PFASs (ng/g ww)) and egg weight (g), 7 of the eggs were omitted from analyses. The mean concentration was used, as well as the egg with highest amount (g) and lowest amount (g) to give an upper-lower range. Caution should be taken when interpreting these estimates, as these are highly simplified models with a large uncertainty. A longer list of assumptions taken when calculating the estimates is given in Table L1, although there is probably more that could be mentioned.

Table L1

Assumptions for estimating the internal concentrations of ∑PFASs deriving from maternal transfer. The arrows signify if the true concentration from internal transfer would be higher or lower than the estimate from the model

Assumptions	Actual concentration would Increase (↑) or decreases (↓)	Note
One-compartment model for the internal concentration which follows a first-order kinetic model	unknown, possibly ↑	Different compartments accumulate different concentrations of PFASs. Clearance of toxicants is also dependent on compartment, while half-life is based on PFOS in plasma
Half-life based on PFOS, while estimations are of ∑PFASs	unknown, possibly ↓	By example, the half-life of PFOA are generally considered lower, t1/2 = 4.6 days (Yoo et al., 2009).
Egg-shell weight is included in the measurement of egg-weight, and all PFASs in eggs is assumed to be absorbed	↓	In the kinetic model it is assumed that all of the weight and PFASs is taken up into the nestling, but the weight of the egg-shell was not known and not subtracted. The model is based on concentration, while the growth dilution constant is based on weight.
PFOS half-life are based on an exposure study on chicken	unknown	Different species
Modelled concentrations will grow exponentially with decreasing age. Variation of growth in the period between egg and fledgling are not accounted for	↓ in younger nestlings	The model error will increase with decreasing age. It is assumed that most of the growth dilution will occur early after hatching. By eq. L1, concentrations are halved three times before a nestling reach 1 kg.
Egg concentrations are not from the same nestlings in the study (growth dilution constant based on the relationship between egg weight and nestling weight) and the origin (location etc.) are not known for the eggs	unknown	Concentrations in eggs ranged from 57-210 ng/g ww, which will have big consequence for modelled concentration. It is possible that some of the eggs are taken from highly polluted or less polluted areas. The concentration of PFASs in WTE eggs from Smøla and Steigen is not known.
Plasma concentrations are assumed to represent internal concentrations and the blood volume is assumed to maintain a constant fraction of body weight over time after hatching	-	This is only assumed when comparing plasma concentrations with estimated internal PFASs levels from maternal transfer